UNIVERSITY OF CALIFORNIA,
IRVINE

Development of bioorthogonal chemical reporters for studying host-pathogen interactions

DISSERTATION

submitted in partial satisfaction of the requirements
for the degree of

DOCTOR OF PHILOSOPHY

in Chemistry

by

Lidia Nazarova

Dissertation Committee:
Assistant Professor Jennifer A. Prescher, Chair
Assistant Professor Aaron P. Esser-Kahn
Professor Shiou-Chuan (Sheryl) Tsai

2015

DEDICATION

This dissertation is dedicated to my mother, Natalia Nazarova.

TABLE OF CONTENTS

LIST OF FIGURES

LIST OF TABLES

LIST OF SCHEMES

ACKNOWLEDGMENTS

I would like to express my deepest gratefulness to my committee chair, Professor Jennifer Prescher, who has taught me so many things it would not be possible to list them all here. Thank you for your everlasting patience, support throughout the darkest days of graduate school, and for presenting me with all the wonderful opportunities that I have been exposed to. It truly has been the honor and privilege to be a part of your very first class of graduate students.

I would like to thank my committee members Dr. Sheryl Tsai and Dr. Aaron Esser-Kahn. I greatly appreciate Dr. Tsai's insightful comments on my research project in its earliest stages. I appreciate continuous feedback that I have been receiving from Dr. Esser-Kahn after my advancement to candidacy.

I am thankful to the UCI faculty and personnel for making this graduate program such an intellectually engaging and exciting place to be at. In particular, I would like to thank Dr. Chris Vanderwal for being an excellent advisor on any academic matters a graduate student might have. I will remember my interactions with Drs. Suzan Blum and Liz Jarvo and how they challenged me on my scientific proposals. A special thank you goes to the chemistry department staff, especially Tenley Dunn and Kerry Kick for being a tremendous help in so many situations.

I would like to acknowledge wonderful collaborators that I had a pleasure to work with in the last five years. I have learned so much about parasitology and immunology from joint lab meetings with Drs. Naomi Morrissette and Melissa Lodoen and their graduate students and postdocs. I was very lucky to have an opportunity to closely work with Roxanna Ochoa. This work would not be possible without her. I greatly appreciate all the help I have gotten from Dr. Nori Ueno and Dr. Lanny Gov. You were always ready to give me a hand when I was struggling with a reagent, experimental technique or data analysis.

The last five years have been an exciting journey for me and this all would not have been possible if it were not for my wonderful labmates in the Prescher lab. It was not always easy to be the first graduate students in the lab, but I am happy that there were five of us together: Dave McCutcheon, Dr. Miranda Paley, Dave Patterson, Rachel Steinhardt. I am very grateful for being baymates with Dr. Hui-Wen Shih. I greatly value all the philosophical conversations and experience sharing that we had over the last two years. I was very lucky to have been working side by side with Krysten Jones and Joanna Laird. It was so wonderful to have an ability to ask your opinion and experience on so many biological experiments. A special thanks goes to Jeffrey Briggs, who was an undergraduate researcher in our lab, for being patient during our teaching-learning experience. I have quickly realized that when you mentor someone you learn a great deal from them. I have also enjoyed working with Dave Kamber on a few cyclopropene projects and I appreciate how efficient our collaborations always were. I am confident that my last project is staying in good hands. All other past and present members of the

Prescher lab, especially Dave Row, William Porterfield, Colin Rathbun, and Brendan Zhang.

I would like to acknowledge all my previous research mentors and teachers for their help for the last many years. Without you I would not have become a scientist. I especially appreciate all the mentoring that I received from Dr. Asya Shpirt and Dr. Leonid Kononov, who took me on as an undergraduate student under their guidance and patiently supervised all my baby steps in the lab. Thanks to Nikolay Kondakov for his support and sense of humor inside and outside the lab. I am grateful to Dr. Leslie Wo-Mei Fung and Dr. Michael Famulok for providing me with the opportunities to intern in their labs during my undergraduate career and see how research is being done in different countries. Dr. Shelli McAlpine has taught me many important details of scientific research and collaborative process.

I am very grateful for all the wonderful people I met when I first came to the US for graduate school. It was a huge transition for me, but Dimitri Rodionov, Tatiana Abramihina, Alexander Noskov, Olga Lyssanova, Erin Singh, and Josie Armstead made it such an exciting and enriching experience. Nora Rachtman was my classmate from day one and we went through many new experiences while getting used to the new teaching style.

Thanks to all my wonderful friends both in the US and back at home who always believed in me and cheered me on. We had many insightful and philosophical conversations with Dr. Dmitry Shabashov, Dr. Alex Prokofjevs, and Dr. Dmitry Usanov. I have enjoyed exploring southern California with my friends Lucy Ulanova, Denis Ulanov, Ildar Absalyamov, and Anastasia Kadina. William Leibzon, Dr. Andrey Solovyev, and Dr. Diana Aleksanyan will always hold a special place in my heart. Thanks to all my friends at UCI who I met in classes and running around the department it attempts to make my experiments work, especially Kritika Mohan.

My mother, Natalia Nazarova, is always my biggest supporter in all my undertakings. Thanks to my family, especially Valentina Filichkina, Nina Safonova, Olga Politova, and Alexander Politov.

A very special acknowledgement goes to Max Katsev, for all his love and support, especially during the last stages of my graduate school.

Financial support for this dissertation was provided by the University of California-Irvine.

CURRICULUM VITAE

Lidia Nazarova

EDUCATION AND TRAINING
University of California, Irvine, Irvine, CA
Doctor of Philosophy in Chemistry
June, 2015

Higher Chemical College of the Russian Academy of Sciences, Moscow, Russia
Specialist diploma in Chemistry, with Honors
June, 2008

RESEARCH EXPERIENCE
University of California-Irvine, Irvine, CA
Graduate Student
Department of Chemistry
Advisor: Dr. Jennifer A. Prescher
Thesis Topic: Development of bioorthogonal chemical reporters for studying host-pathogen interactions

San Diego State University, San Diego, CA
Research Assistant
Advisor: Dr. Shelli R. McAlpine
Research Topic: Design and synthesis of cyclic peptide derivatives as potential anticancer agents

University of Illinois, Chicago, Chicago, IL
Research Assistant
Advisor: Dr. Leslie Wo-Mei Fung
Research Topic: Investigating interactions of different isoforms of spectrin protein with Calcium-dependent cysteine proteases calpain I and caspase-3 using in vitro activity assays

Bonn University, Bonn, Germany
Research Assistant
Advisor: Dr. Michael Famulok
Research Topic: Synthesis of small molecule enzyme inhibitors based on the 1,2,4-triazole core

N. D. Zelinsky Institute of Organic Chemistry of the RAS, Moscow, Russia
Research Assistant
Advisor: Dr. Leonid O. Kononov
Diploma Topic: Synthesis of dibenzyl glycosyl phosphates using ion-exchange resin

TEACHING EXPERIENCE

Graduate Teaching Assistant,
Department of Chemistry,
University of California-Irvine
Chemical Biology, Spring 2012, Winter 2013, Winter 2014, Winter 2015 (head TA)
General Chemistry Discussions, Spring 2011, Fall 2012, Winter 2012
General Chemistry Lab, Winter 2011
Organic Chemistry Labs, Fall 2010, Fall 2013

Graduate Teaching Assistant,
Department of Chemistry,
University of California, San Diego
Organic Chemistry Discussion, Winter 2010

Graduate Teaching Assistant,
Department of Chemistry,
San Diego State University
General Chemistry Labs and Discussions, Fall 2008, Spring 2009, Fall 2009

HONORS AND AWARDS

Second place in Associated Graduate Students Symposium (UCI)
Harry E. Hamber Memorial Scholarship (SDSU)

PUBLICATIONS

9. Nazarova, L. A.*; Ochoa, R.*; Jones, K. A.; Morrissette, N. S.; Prescher, J. A. Extracellular Toxoplasma gondii tachyzoites metabolize and incorporate unnatural sugars into cellular glycoproteins. *In preparation*. * *equal contribution*

8. Nazarova, L. A.; Shpirt, A. M.; Orlova, A. V.; Kononov, L. O. Glycosylation by nucleophiles on ion-exchange resin: novel synthesis of dibenzyl glycosyl phosphates. *Izv. Akad. Nauk Ser. Khim.* **2015,** *5*, 1202-1204. (in Russian)

7. Patterson, D. M.*; Nazarova, L. A.*; Prescher, J. A. Finding the right (bioorthogonal) chemistry. *ACS Chem. Biol.* **2014**, *9*, 592-605. * *equal contribution*

6. Kamber, D. N.; Nazarova, L. A.; Liang, Y.; Lopez, S. A.; Patterson, D. M.; Shih, H.-W.; Houk, K. N.; Prescher, J. A. Isomeric cyclopropenes exhibit unique bioorthogonal reactivities. *J. Am. Chem. Soc.* **2013**, *135*, 13680-13683.

5. Patterson, D. M.; Nazarova, L. A.; Xie, B. J.; Kamber, D. N.; Prescher, J. A. Functionalized cyclopropenes as bioorthogonal chemical reporters. *J. Am. Chem. Soc.* **2012**, *134*, 18638-18643.

4. Davis, M. R.; Singh, E. K.; Wahyudi, H.; Alexander, L. D.; Kunicki, J. B.; Nazarova, L. A.; Fairweather, K. A.; Giltrap, A. M.; Jolliffe, K. A.; McAlpine, S. R.

Synthesis of Sansalvamide A peptidomimetics: triazole, oxazole, thiazole, and pseudoproline containing compounds. *Tetrahedron* **2012**, *68*, 1029-1051.

3. Johnson, V. A.; Singh, E. K.; Nazarova, L. A.; Alexander, L. D.; and McAlpine, S. R. Macrocyclic inhibitors of Hsp90. *Curr. Top. Med. Chem.* **2010**, *10*, 1380-1402.

2. Singh, E. K.; Nazarova, L. A.; Lapera, S. A.; Alexander, L. D.; McAlpine, S. R. Histone deacetylase inhibitors: synthesis of cyclic tetrapeptides and their triazole analogs. *Tetrahedron Lett.* **2010**, *51*, 33, 4357-4360.

1. Rolius, R.; Antoniou, C.; Nazarova, L. A.; Kim, S. H.; Cobb, G.; Gala, P.; Rajaram, P.; Li, Q.; Fung, L. W.-M. Inhibition of calpain but not caspase activity by spectrin fragments. *Cell. Mol. Biol. Lett.* **2010**, *15*, 3, 395-405.

PRESENTATIONS

9. Nazarova, L. A.; Ochoa, R.; Morrissette, N. S.; Prescher, J. A. 2nd Southern California Eukaryotic Pathogen Symposium, Riverside, CA, November 16, 2012. (**oral presentation**)

8. Ochoa, R.; Nazarova, L. A.; Prescher, J. A.; Morrissette, N. S. Detecting complex carbohydrate modification in *Toxoplasma gondii* with unnatural sugars. AAAS, Vancouver, Canada, February 16–20, 2012. Abstract #7919.

7. Nazarova, L. A.; Shpirt, A. M.; Kononov, L. O. An efficient synthesis of glycosyl dibenzyl phosphates by glycosylation of dibenzyl phosphate polymer with glycosyl halides. 25th International Carbohydrate Symposium, Tokyo (Chiba), Japan, August 1-6, 2010.

6. Nazarova, L. A.; Singh, E. K.; Lapera, S.; McAlpine, S. R. Novel macrocyclic histone deacetylase inhibitors. 239th ACS National Meeting, San Francisco, CA, March 21-25, 2010. Abstracts of Papers, MEDI-252. (**This paper was selected for the sci-mix poster session.**)

5. Singh, E. K.; Lapera, S.; Nazarova, L. A.; Vasko, R. C.; McAlpine, S. R. Synthesis and biological evaluation of cyclic tetrapeptides serving as histone deacetylase inhibitors. 238th ACS National Meeting, Washington, DC, August 16-20, 2009. Abstracts of Papers, MEDI-053.

4. Nazarova, L. A.; Shpirt, A. M.; Kononov, L. O. Synthesis of glycosyl phosphates using an ion exchange resin. XV International Conference on the Chemistry of Phosphorus compounds, Saint-Petersburg, Russia, May 25-30, 2008. Book of Abstracts, p. 188.

3. Nazarova, L. A.; Shpirt, A. M.; Kononov, L. O. Application of a new phosphate reagent to dibenzyl glycosyl phosphate synthesis. XV International Scientific

Conference for Undergraduate and Graduate Students, and Young Scientists "Lomonosov - 2008", Moscow, Russia, April 11-14, 2008. Book of Abstracts, p. 486.

2. Nazarova, L. A.; Shpirt, A. M.; Malysheva, N. N.; Kononov, L. O. Synthesis of O-benzylated sialic acid derivatives with various substituents at N(5) as potential glycosyl donors. IX Science School-Conference on Organic Chemistry, Zvenigorod, Russia, December 11-15, 2006. Book of Abstracts, p. 255.

1. Nazarova, L. A.; Shpirt, A. M.; Malysheva, N. N.; Kononov, L. O. Synthesis of O-benzylated sialic acid derivatives with various substituents at N(5) as potential glycosyl donors. 2nd Baltic Meeting on Microbial Carbohydrates, Rostock, Germany, October 4-8, 2006. Book of Abstracts, p. 11. (**oral presentation)**.

ABSTRACT OF THE DISSERTATION

Development of bioorthogonal chemical reporters for studying host-pathogen interactions

By

Lidia Nazarova

Doctor of Philosophy in Chemistry

University of California, Irvine, 2015

Professor Jennifer Prescher, Chair

Bioorthogonal chemical reporters are small functional groups that can be metabolically incorporated into biomolecules by the cell's native metabolic machinery. In a second step, these moieties can be covalently modified with probes for detection or isolation. I applied this strategy to profile glycoproteins in *Toxoplasma gondii*, a prevalent intracellular parasite that infects nearly one-third of the world's population and may cause life-threatening conditions in immunocompromised patients. Using the bioorthogonal chemical reporter strategy, I identified a large, diverse set of glycosylated proteins in *T. gondii* including some previously unannotated proteins likely involved in modulating host-parasite interactions.

In addition to glycosylated structures, parasites and host cells exchange numerous other metabolites. Simultaneous monitoring of these communication pathways requires multiple cell-compatible reactions that can be used concurrently, or "mutually orthogonal" bioorthogonal chemistries. Unfortunately, the existing toolbox of bioorthogonal chemistries is rather sparse, limiting our ability to look at multiple

biomolecules in tandem. I contributed to the development of novel chemical reporters for simultaneous profiling of host-pathogen crosstalk. My labmates and I established a new bioorthogonal chemical reaction—a cycloaddition between 1,3-disubstituted cyclopropenes and tetrazines—that can be used in living systems. Excitingly, this reaction can be used in tandem with common azide-alkyne chemistries for multi-component imaging. We also demonstrated that 1,3-disubstituted cyclopropenes can be used concurrently with isomeric cyclopropenes—3,3-cyclopropenes—in biological labeling applications. Both of these molecules harbor unique reaction preferences, enabling them to be used simultaneously. This was noteworthy result, since the structures of these cyclopropenes only differ by the placement of a single methyl group. I also developed another orthogonal chemical reporter for use in multi-component applications: methylene cyclopropane. This molecule exhibits unique cycoaddition reactivities and is poised to join the ranks of useful chemical reporters.

CHAPTER 1: Bioorthogonal chemical reporters for studying biological processes

1.1 Introduction

Cellular processes are driven by the coordinated actions of numerous biopolymers and small molecule metabolites. A complete understanding of cell and organismal biology thus requires methods to probe these diverse classes of biomolecules in real time. GFP and other genetically encoded reporters are available for tracking protein products in live cells and organisms. While powerful, such genetic tagging tools are not amenable to monitoring glycans, lipids, and other critical cellular components [1]. To address this need, the chemical biology community has developed a general platform to target cellular molecules with visual tags and other probes. This strategy relies on the installation of unique functional groups into target biomolecules and their selective reaction with covalent probes (Figure 1-1A). The chemistries employed in this approach must be selective and non-perturbing to biological systems. For these reasons, they have been collectively termed bioorthogonal [2].

The earliest work in bioorthogonal reaction development—nearly two decades ago—focused on methods to covalently target unique amino acid sequences with small molecule probes [3,4]. Since then, dozens more unique transformations have been added to the bioorthogonal toolkit. The majority of these chemistries are applicable not only to

protein tagging, but also to studies with glycans, lipids, and numerous other biomolecules. The reactions differ widely, though, in terms of their selectivities, rates, and other attributes, and choosing among them can be difficult.

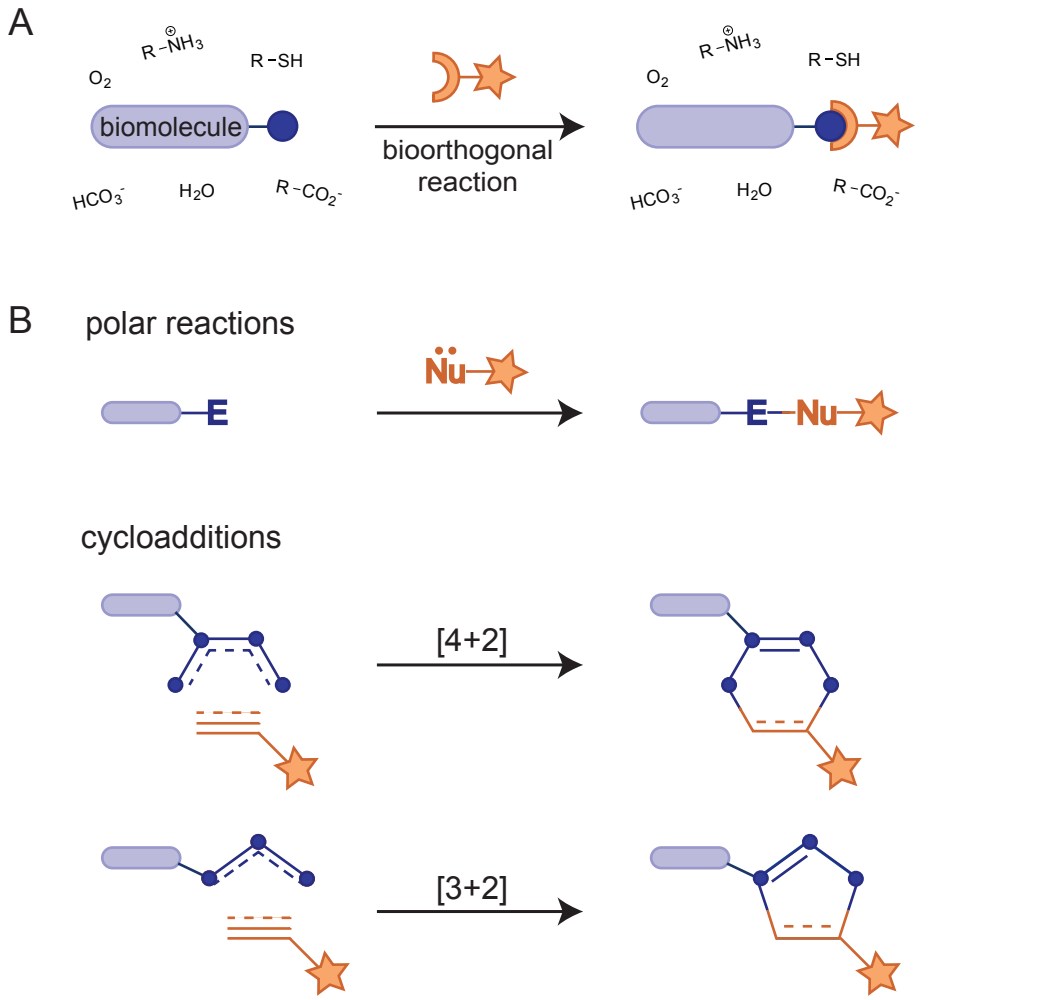

Figure 1-1 A bioorthogonal chemical reaction. (A) A unique functional group (blue circle) appended to a target biomolecule is covalently ligated with a complementary probe (orange arc). The two reagents must react selectively with one another and be inert to the biological surroundings (i.e., bioorthogonal). Depending on the choice of probe (star), this method enables the selective visualization or identification of biomolecules in complex environments. (B) Two types of transformations are predominant in the bioorthogonal toolkit: polar reactions between nucleophiles and electrophiles and cycloaddition chemistries.

This chapter deconstructs the major classes of bioorthogonal chemistries and draws relevant comparisons and contrasts between them. My focus is on those reactions that are applicable to tagging diverse types of molecules in complex environments. I first introduce the common bioorthogonal transformations and highlight their utility in various experiments. I then provide a general set of considerations for selecting a suitable reaction for a given application. Last, I highlight existing challenges to the development and implementation of bioorthogonal reactions.

1.2 Common bioorthogonal transformations

The selective, covalent tagging of biomolecules—especially in live cells and tissues—is no easy task. For one, the biological milieu is replete with functional groups that can interfere with the desired labeling reaction. The bioorthogonal probes must also be stable in aqueous environments, yet readily reactive with one another. Furthermore, the chemistries must be nontoxic. The challenges involved in designing such reactions have captured the imagination of several chemists, and over the past decade, transformations have emerged that meet most or all of the criteria for bioorthogonality. The majority can be classified as either polar reactions or cycloadditions, although notable exceptions exist (Figure 1-1B). The chemistries differ in terms of the functional groups employed, reaction rates, and overall selectivities, but all are suitable for use in aqueous environments and, in some cases, live cells and animals (Table 1-1).

1.2a Polar reactions

Reactions between nucleophiles and electrophiles (i.e., polar reactions) are

omnipresent in organic synthesis, but only a handful are suitable for use in biological settings. Among the most well established for biomolecule labeling are aldehyde and ketone condensations [5,6]. Aldehydes and ketones—as electrophiles—are rare commodities on proteins and other biopolymers, and they can be selectively ligated with alpha-effect nucleophiles (e.g., hydrazides and aminooxy compounds) to form relatively stable Schiff bases [7-12]. Ketones and aldehydes have been appended to a variety of biomolecules, including proteins [13,14] and glycans [15,16], and ultimately targeted with functionalized hydrazides or aminooxy compounds for visualization or retrieval.

While versatile, these chemistries have some liabilities with regard to biomolecule labeling. For example, the reaction products—hydrazones, in particular—are susceptible to hydrolysis in cellular environments [17]. To generate more stable adducts, Bertozzi and colleagues recently developed an aldehyde condensation that exploits aminoxy-tryptamines [18,19]. This transformation is a variant of the classic Pictet-Spengler reaction: the aldehyde and tryptamine initially react to form an oxyiminium ion; this intermediate is subject to further indole attack and ultimately C-C bond formation. Ketone and aldehyde condensations are also not 'bioorthogonal' in the truest sense of the word. Aldehydes are present in glucose and other abundant intracellular metabolites; ketones are found in mammalian hormones and microbial natural products. These endogenous molecules can be inadvertently labeled when cells are exposed to aminooxy or hydrazide probes.

To avoid cross-reactivity altogether, reactions that employ non-natural functional groups are highly prized. The quintessential example of this sort is the Staudinger ligation of organic azides and triaryl phosphines [20]. Organic azides are mild electrophiles and

have yet to be found in eukaryotes. Similarly, triaryl phosphines—as soft nucleophiles—are virtually absent in living systems [21,22]. While tolerant of biological functionality, azides and phosphines react readily with one another [23,24]. In the case of the Staudinger ligation, the reaction forges stable amide linkages between the two reactants. This transformation is slower than most bioorthogonal chemistries, but remains a popular choice for in vivo work, owing to its remarkable selectivity and compatibility with cells, tissues, and even live animals [25-29].

1.2b Cycloadditions

Nearly all recent additions to the bioorthogonal toolkit comprise cycloadditions. Two classes, in particular—dipolar cycloadditions and Diels-Alder chemistries—have emerged as excellent options for derivatizing biomolecules with visual tags and other probes.

The most popular bioorthogonal cycloadditions also capitalize on the unique features of azides [30]. In addition to being mild electrophiles, organic azides are 1,3-dipoles capable of reacting with terminal alkynes [31-33]. To proceed at a reasonable rate, though, this reaction requires a Cu(I) catalyst. The copper-catalyzed azide-alkyne cycloaddition (CuAAC)—or "click" chemistry—occurs readily in aqueous environments and provides chemically robust triazoles [34-36]. The speed and relative simplicity of this transformation has been widely exploited for biomolecule visualization (mostly in fixed cells) [37-39] and biomolecule retrieval in various "-omics" studies [40-43]. Azides and alkynes also rank among the smallest bioorthogonal motifs and are non-perturbing to most biomolecules. For this reason, CuAAC has been the "go-to" choice for monitoring

the activities and targets of numerous small molecules, including enzyme inhibitors and therapeutic drugs [44-47].

Table 1-1 Bioorthogonal chemistries.

Reaction type	Reactant 1 ●	Reactant 2	Approximate rate constant ($M^{-1}s^{-1}$)	Comments	References
Aldehyde/ketone condensation	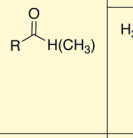	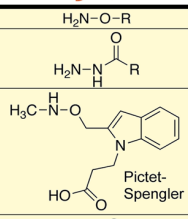	0.001 (H_2O) 0.26 (100 mM sodium phosphate)	adducts prone to hydrolysis; aniline catalyst can be used reaction provides more stable C-C linkages	Jencks **1959** Agarwal **2013**
Staudinger ligation		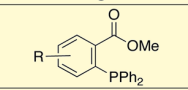	0.003 (PBS)	phosphines susceptible to oxidation	Saxon **2000**
Cyanobenzothiazole condensation		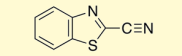	9.19 (PBS)	side reactivity with free thiols	Rao **2009**
CuAAC	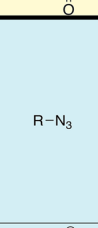	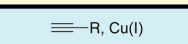	k_{obs} 10-100 (10-100 μM Cu)	copper catalyst required	Tornoe **2002**
Strain-promoted azide-alkyne cycloadditions (SPAAC)		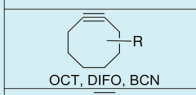	0.0012-0.14 (ACN)	no metal catalyst; some octynes susceptible to thiol attack	Agard **2004**
		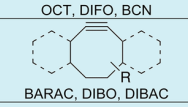	0.17-0.96 (ACN)		Jewett **2010**
Alternative 1,3-dipolar cycloadditions		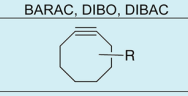	0.013-3.9 (ACN/H_2O)	some nitrones susceptible to hydrolysis	McKay **2010**
	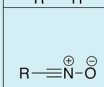	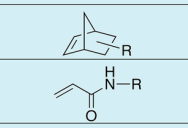	30 (H_2O)	nitrile oxide generated *in situ* (photolysis)	Gutsmiedl **2009**
	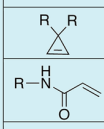	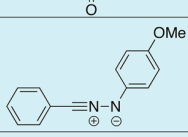	0.15-58 (1:1 ACN:PBS)	nitrile imine generated in situ (photolysis)	Yu **2012**
	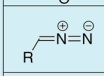	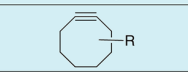	13.5 (ACN/H_2O)	diazo generated from azide precursor	McGrath **2012**
	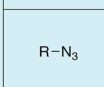	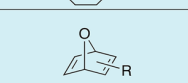	70,000-106,000 (H_2O)	oxanorbornadiene susceptible to reactivity with basic amino acids	van Berkel **2007**
Inverse Electron-Demand Diels-Alder (IED-DA)		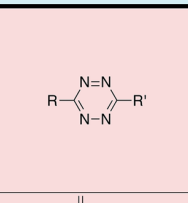	210-2,800,000 (PBS, 37°C)	TCO can isomerize over time	Blackman **2008**
	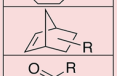		0.12-9.46 (95:5 H_2O:MeOH)	norbornene and functionalized cyclopropenes are shelf stable	Devaraj **2008**
			0.03-13 (12-15% DMSO in PBS)		Yang **2012** Patterson **2012**
Hetero-Diels-Alder		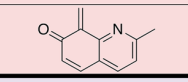	0.0015 (5:1 H_2O:MeOH)	quinone methide generated *in situ*	Li **2013**
Miscellaneous ligations		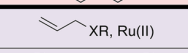	0.03-0.3 (PBS/tBuOH)	ruthenium catalyst required	Lin **2013**
		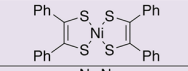	0.25 (PBS/EtOH)	requires nickel-stabilization of pi-electrons	Sletten **2011**
	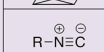	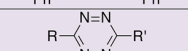	0.12-0.57 (THF/H_2O)	products can hydrolyze in water	Stockmann **2011**
	Ar-X	R-B(OH)$_2$, [Pd]	N/A	palladium catalyst required; boronic acids are moderately cytotoxic	Chalker **2009**
	Ar-X	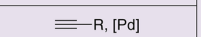 R, [Pd]		palladium catalyst required	Kodama **2007**

While routinely applied in vitro, CuAAC has been slower to transition in vivo. This is due, in part, to the tri-component nature of the reaction and its requirement for a cytotoxic metal catalyst. To obviate the need for Cu(I), Bertozzi and colleagues exploited an alternative mechanism to drive azide-alkyne cycloaddition: ring strain [48,49]. They initially designed a cyclooctyne scaffold (OCT) comprising C≡C-C bonds that were "bent" from the preferred linear geometry by 17 degrees [50]. The free energy from such bond deformation was sufficient to promote azide-alkyne reaction under ambient conditions and without metal catalyst. This strain-promoted azide-alkyne cycloaddition (SPAAC) has been widely used to tag azido proteins and other biomolecules on live cells [51,52] and in living organisms [53-55].

Iterative modifications to OCT have been reported over the past five years, and there are now over 10 different cyclooctynes suitable for bioorthogonal labeling [56]. Notable examples include DIBO [52] and BARAC [57] (Table 1-1). These reagents comprise cyclooctyne cores fused to benzene rings. The pendant rings provide increased strain energy and ultimately accelerate the cycloaddition reaction with azides [58]. While DIBO and BARAC provide among the fastest SPAAC rates, their increased hydrophobicity can result in non-specific "sticking" to other biomolecules and insertion into cell membranes [59].

Cyclooctynes are also reactive partners for 1,3-dipoles other than azides. Nitrones [60,61], nitrile oxides [62,63], and diazo groups [64,65] have all been appended to various proteins and selectively ligated with strained alkynes. Most of these cycloadditions are quite fast, with second order rate constants ranging from 1-50 $M^{-1}s^{-1}$ [60,66]. However, the rapid reactivity afforded by these strong dipoles often comes at the

expense of their poor stability in aqueous media. Nitrile oxides are particularly prone to hydrolysis and must be generated in situ—near the site of intended reactivity—for efficient ligation.

In addition to alkynes, strained alkenes are good candidates for bioorthogonal dipolar cycloadditions. Lin and coworkers recently reported that cyclopropene—a highly strained alkene—reacts readily with nitrile imines to form pyrazoline adducts [67]. Nitrile imines, like other strong dipoles, are prone to rapid hydrolysis and must be generated in situ. Fortunately, these motifs can be generated from relatively stable precursors, including tetrazoles and chlorooximes, using fairly mild conditions (short pulses of UV light and mild base, respectively) [67-69]. These conditions are compatible with a variety of biomolecules and, in some cases, live cells.

Strained molecules also play lead roles in the second major class of bioorthogonal cycloadditions: Diels–Alder ligations. In 2008, Fox and coworkers demonstrated that the strained molecule trans-cyclooctene (TCO) reacts efficiently with electron-deficient tetrazines in aqueous solution and in the presence of model proteins [70]. These inverse electron-demand Diels–Alder (IED-DA) reactions are the fastest bioorthogonal transformations on record, with rate constants ranging from 10^3-10^6 $M^{-1}s^{-1}$ in some cases [71,72]. Due to their rapid reactivity, TCO-tetrazine ligations have found immediate application in a variety of biological pursuits, most notably live animal imaging [73-76]. Covalent tagging reactions in rodents and other organisms demand ultra-fast reactions as only small amounts of reagent can typically be used. Unreacted/unbound probe (which cannot be simply rinsed away) is thus kept to a minimum, resulting in high signal-to-noise ratios [77]. A variety of sterically and electronically modified tetrazines have also

been developed that exhibit different IED-DA rates, enabling relatively facile "tuning" of the reaction [71,78,79].

Tetrazine reactivity with other strained alkenes has also been exploited for bioorthogonal ligation [76,80,81]. Coinciding with the initial report on TCO, Hilderbrand and coworkers demonstrated IED-DA reactivity with norbornene (NB) and electron-deficient tetrazines. NB reacts more sluggishly than TCO, but is far more stable in solution and upon storage. The embedded trans-double bond in TCO can isomerize to the cis configuration over time, resulting in the accumulation of a non-reactive scaffold [73]. We and others have also shown that another strained alkene—cyclopropene—is amenable to reactions with various tetrazines. Cyclopropenes possess a distinct advantage over TCO owing to their smaller size and broad compatibility with cellular enzymes [67,81,82]. However, the IED-DA reactions between these small microcycles and tetrazine are considerably slower than those with TCO. Further modifications to the cyclopropene core may improve these rates.

1.3 Considerations for selecting an appropriate bioorthogonal chemistry

With over 20 bioorthogonal transformations now reported in the literature, and new ones being discovered at a rapid pace, selecting the "best fit" for a given application is non-trivial. The chemistries vary widely in terms of their selectivities and biocompatibilities, and many of their perceived strengths and weaknesses remain anecdotal. Below, we outline some general considerations for the end user of bioorthogonal chemistries and offer some guidelines for selecting among the options

(Figure 1-2). In general, experiments with live cells or tissues demand the most selective reactions, with little tolerance for off-target labeling. Experiments with fixed cells or isolated biomolecules, by contrast, are typically less demanding in terms of reagent selectivity. Thus, they can interface with a larger number of chemistries.

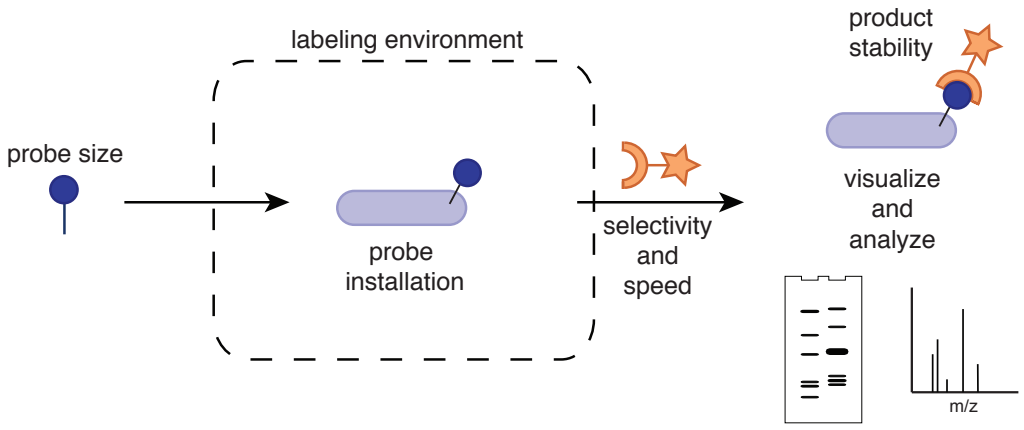

Figure 1-2 Selecting an appropriate bioorthogonal chemistry. Considerations include the target biomolecule and mode of functional group installation, the size of the labeling agents, and the stability of the covalent adduct. Bioorthogonal reaction selectivity and speed are also important parameters.

1.3a Selectivity of bioconjugation

The selective tagging of any biomolecule requires that one of the chemical motifs (e.g., aldehyde, azide, alkyne) is directly attached to the target of interest. Several options exist for installing bioorthogonal functionality onto protein targets (Figure 1-3A). These biopolymers can be readily derivatized at their N- or C-termini using mild chemistries [83-85]. A variety of bioconjugation reactions can also be employed to affix bioorthogonal motifs to Lys and Cys residues [86], as well as to aromatic amino acids [87-90]. For example, Van Hest and colleagues reported a facile method to install azido groups onto Lys side chains via diazo transfer [91]. While efficient, these approaches are inherently non-specific and typically result in more than one modification to the protein backbone.

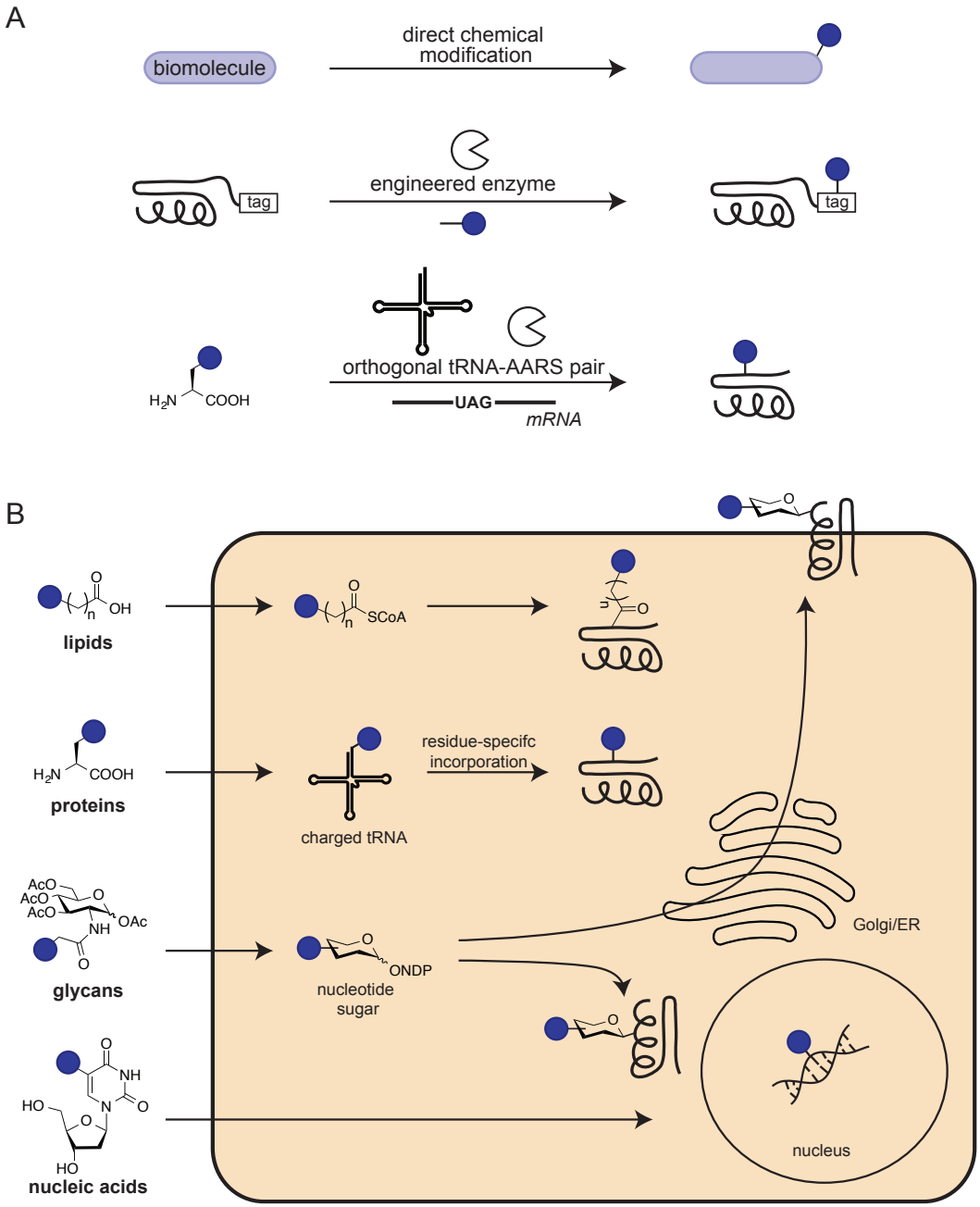

Figure 1-3 Installing bioorthogonal functionality into target biomolecules. (A) Several strategies exist to introduce bioorthogonal motifs (blue circles) into protein targets. These include direct chemical functionalization (top), enzymatic ligation of the requisite motifs onto defined acceptor peptides (tags, middle), and unnatural amino acid mutagenesis with functionalized amino acids and orthogonal tRNA/AARS pairs (bottom). (B) Unique chemical handles can be metabolically introduced into proteins and non-proteinaceous biomolecules alike via cellular biosynthesis. In this approach, metabolic precursors (left) outfitted with bioorthogonal functional groups (blue circles) are supplied to cells and ultimately incorporated into target biomolecules via the cell's own enzymatic machinery.

For site-specific installation of bioorthogonal motifs, enzymatic tagging platforms are available. Most of these strategies exploit ligases that have been engineered to append modified substrates (bearing ketones, cyclooctynes and other reactive motifs) to defined acceptor peptides [92-98]. In a recent example, Ting and coworkers generated a lipoic acid ligase variant (LplA) capable of appending small molecule azides to lysine residues within a 13-residue consensus sequence [99-102]. Once installed, the azido motifs were subsequently ligated with a variety of functionalized cyclooctynes and visualized over time. This two-step, enzyme-mediated tagging strategy can be used to tag protein targets in vitro and in a variety of cellular compartments. Additionally, the LplA acceptor peptide, similar to those for other engineered enzymes, is highly modular and can be grafted into multiple proteins.

Bioorthogonal motifs can also be introduced site-specifically into proteins using unnatural amino acid mutagenesis [103,104]. This strategy exploits unique amino-acyl tRNA synthetase (AARS)/tRNA pairs to deliver non-natural amino acids into growing polypeptide chains in repsonse to unique codons. Keto, azido, and alkynyl versions of Phe have all been introduced into protein targets (at defined positions) via this approach [105,106]. Amino acids outfitted with larger motifs—including TCO and various cyclooctynes—have been similarly incorporated into protein targets using newly engineered AARS/tRNA pairs [67,107-113]. Continued advancements in this field will enable multiple bioorthogonal units to be selectively installed in protein targets both in vitro and in vivo [114,115]. It is also possible to incorporate bioorthogonal amino acids into target proteins relying on the cell's own endogenous machinery, without the need for unique AARS/tRNA pairs [116,117]. These residue-specific replacement strategies are

inherently non-selective, but are nonetheless attractive for generating functionalized proteins owing to their high yields and relative simplicity. Since these methods rely on native biosynthetic pathways—and enzymes with stringent substrate specificities—they are only compatible with non-natural amino acids bearing small chemical appendages (e.g. ketones, azides, alkynes).

For non-proteinaceous biomolecules, fewer methods exist for installing bioorthogonal functional groups. Direct chemical modification is possible, although impractical for most applications [9,118]. Mutant enzymes are also available to append reactive motifs to glycans, but most are not generalizable and confined to in vitro work [119]. For experiments in cells and tissues, the majority of non-proteinaceous biomolecules can be outfitted with bioorthogonal probes via cellular biosynthesis (Figure 1-3B). This approach relies on metabolic precursors that are supplied to cells and ultimately installed into target biomolecules using the cell's own enzymatic machinery [2]. Similar to the residue-specific tagging of proteins mentioned above, only small bioorthogonal motifs are broadly compatible with native cellular enzymes and thus good candidates for this approach. Upon installation, the bioorthogonal motifs can be covalently ligated with probes for visualization or enrichment.

1.3b Biocompatibility of common bioorthogonal chemistries

A primary consideration in choosing chemistries for biological use is the biocompatibility of the reagents. Comprehensive toxicity profiles have not been generated for most of the common bioorthogonal transformations. However, most can be safely used (with milli- to micromolar concentrations of reagents) without detriment to

biological systems. One exception is the copper-catalyzed azide-alkyne cycloaddition (CuAAC). Copper ions are readily chelated by native amino acids and can induce the formation of reactive oxygen species, resulting in damage to cells and tissues. Concerns about copper cytotoxicity have largely relegated CuAAC to experiments with isolated biomolecules and fixed cells/tissues over the past decade. In recent years, though, Finn, Wu and others have identified ligands that sequester copper from unintended targets and offer improved cell compatability [120-124]. Ting and coworkers also devised a strategy to reduce the overall amount of copper required for efficient CuAAC [125]. Their approach features picolyl azide, a chelating scaffold that pre-organizes the copper and azido reactants. This arrangement promotes cycloaddition at exceedingly low—and biocompatible—concentrations of metal [126,127]. The picolyl azide unit can also be appended to numerous proteins of interest using the engineered LplA ligase [100]. Collectively, these advancements will facilitate the wider adoption of CuAAC in live cell labeling applications.

A second consideration relevant to biocompatibility involves the selectivity of the reactants. For the majority of the transformations in Table 1-1, some degree of non-specific labeling has been observed. Cyclooctynes, for example, are prone to attack by cysteine and other biological nucleophiles [58,128,129]. This side reactivity has stymied their use in some intracellular labeling applications, but can largely be avoided in environments devoid of free thiols (e.g., extracellular spaces or where thiols have been capped with acylating agents). Non-specific reactivity has also been observed in CuAAC reactions when excess alkyne is used [130,131]. These conditions promote the formation of reactive copper acetylides. Fortunately, such side reactivity can be mitigated by simply

"reversing" the reactants—using low concentrations of alkyne and excess azide to drive the reaction. Cravatt and Speers were among the first to note improved signal-to-noise ratios with these conditions in protein profiling experiments [131].

A final point to consider with regard to reagent biocompatibility is the overall solution stability of the reactants and their covalent adducts. Azides, alkynes, and their triazole products are remarkably stable in aqueous buffers and a variety of cellular environments. Many bioorthogonal reagents, though, are prone to hydrolysis. For example, the most electron- deficient tetrazines used for rapid IED-DA reactions hydrolyze readily in water and only tolerate incubation times on the minutes-to-hours time scale. Additionally, some 1,3-dipoles readily dimerize in water and must be generated in situ for covalent tagging experiments.

On the basis of toxicity and selectivity considerations, the Staudinger ligation of azides and triaryl phosphines ranks among the best reactions for biological labeling applications. Minimal-to-no background labeling has been observed with these reagents under a variety of conditions. Indeed, this reaction has been employed in proteomics studies where the analytes of interest are in low abundance and sensitive detection is required [132,133]. It should be noted, though, that phosphine reagents are prone to non-specific oxidation over time [20]. While these reactivities do not contribute to back-ground signal per se, they do reduce the effective concentration of the probe available for labeling.

1.3c Steric considerations

Small bioorthogonal motifs are generally desired in any application to avoid

perturbing the biological system under study. For experiments requiring the metabolic installation of chemical probes, reagent size can be the deciding factor as native cellular enzymes often do not tolerate substrates with large appendages. On the basis of size considerations alone, azides and terminal alkynes have emerged as preferred scaffolds in bioorthogonal labeling [134]. Both of these moieties are remarkably compact, comprising just a few atoms, and are innocuous to most (but not all) biosynthetic pathways [135]. Azido metabolites have been used to target proteins [117,136], glycans [137-139], and lipids [140,141] among other biomolecules [142]. In all cases, the azido species were readily detected via covalent reaction with a complementary alkyne, cyclooctyne, or phosphine reagent. Alkynyl metabolites have been similarly employed in biological experiments [38,143-148]. A suite of alkyne-selective reactions does not yet exist; therefore, these probes are typically detected using CuAAC. Ketones and aldehydes are similar in size to azides and alkynes. However, their somewhat sluggish reactivities at neutral pH have limited their broad utilization in cellulo.

Identifying alternatives to the azide and alkyne that rival these motifs in terms of size and selective reactivity is an ongoing challenge. Linear alkenes are options, though these small motifs are not as robustly reactive with complementary probes [149]. Nitrile imines and other 1,3-dipoles are also candidates, though most must be generated in situ [62,69,150-154]. Cyclopropene, a recently reported bioorthogonal reagent, appears to strike a balance between robust reactivity and shelf stability. We and others have shown that these microcycles can be appended to discrete monosaccharides and metabolically incorporated into cellular glycans and proteins [80-82,149]. More work must be done, though, to assess the long-range biological compatibility and versatility of these motifs.

1.3d Kinetic profiles of bioorthogonal reactions

Reaction rate is another important parameter to assess when selecting suitable bioorthogonal chemistries. For slow reactions, a large amount of one reagent must typically be used to drive the labeling event. Large amounts of any of reagent can be prohibitively expensive or potentially toxic. Fast reactions largely avoid these issues, as only minimal quantities are required. When the need for speed is paramount, the IED-DA reaction between tetrazine and TCO is unrivaled. The rates of these reactions range from 10^3-10^6 $M^{-1}s^{-1}$, making them appropriate for biological processes that occur on the minutes-to-seconds time scale or that involve biomolecule targets in low abundance (e.g., in vivo imaging) [71,155]. In a recent example, Weissleder and coworkers utilized the TCO-tetrazine reaction to image tumor cells in whole animals. TCO was appended to a tumor-targeting antibody (α-A33) that localized to colon cancer grafts upon injection [74]. Following clearance of unbound antibody, the cancer cells could be readily visualized using as little as 2 μM of a tetrazine-^{18}F conjugate to tag the tumor-bound TCOs. Similar imaging experiments with Staudinger ligation and SPAAC chemistries failed to provide adequate signal-to-noise ratios, owing to the slower kinetics of these transformations and the need for large boluses of reagent [156-158].

Activatable probes can be considered when using large amounts of labeling reagent is unavoidable. These reagents produce detectable signal only upon covalent reaction. Thus, the probe can be added in excess to drive the reaction without the need for extensive rinsing. Fluorogenic cyclooctynes have been developed for this purpose; these scaffolds "turn on" fluorescence only upon reaction with azides [159-161]. In a recent example, Boons and coworkers reported an activatable version of DIBO that exhibits a

1000-fold increase in fluorescence upon azide ligation [160]. Activatable tetrazines [159,162] and azides [163,164] are also available.

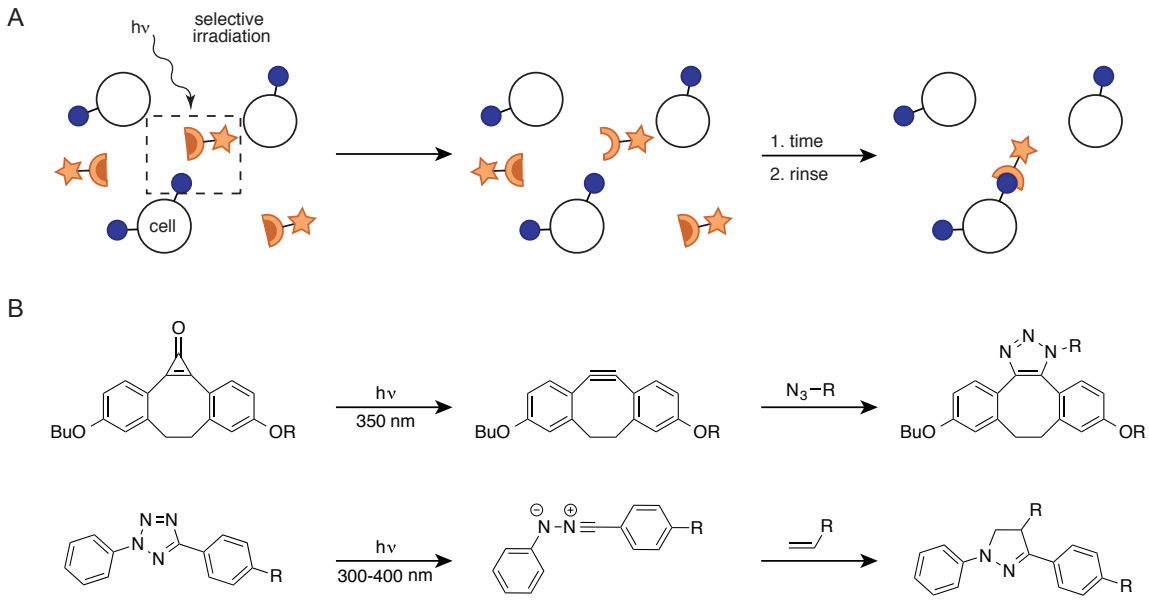

Figure 1-4 "On-demand" bioorthogonal reactivity. (A) Bioorthogonal functionality can be revealed in situ in live cells using pulsed light. Selective irradiation liberates the desired functionality only in the region of interest, conferring both spatial and temporal resolution on the labeling reaction. (B) Two examples of "photo-click" reactions. Irradiation of the cyclopropenone scaffold releases a functional cyclooctyne capable of reacting with azides (top). Similarly, irradiation of the tetrazole scaffold generates a nitrile imine (bottom). This 1,3-dipole can covalently label nearby alkenes.

1.3e Tweaking the reagents for bioorthogonal reactions

Like most experiments, the application of any bioorthogonal chemistry often requires some degree of optimization. Thus, it is helpful to have access to a variety of scaffolds that operate via a similar mechanism, but differ in such parameters as rate, solubility, and lipophilicity. As mentioned above, a panel of cyclooctynes that differ in their electronic and solubility properties is now available; these reagents can be "matched" to a given application involving azide ligation. Similarly, a wide variety of

tetrazine probes for IED-DA cycloadditions have been reported [78,165]. Mehl and colleagues recently capitalized on tetrazine "tunability" to install these non-natural motifs into recombinant proteins [108]. Tetrazines exploited for rapid IED-DA reactivity comprise electron-withdrawing groups, making them susceptible to hydrolysis and reactivity with endogenous thiols. This instability is not detrimental in most applications where short labeling times are employed. In the case of recombinant protein production, though, long incubation times are necessary to biosynthetically introduce amino acids into growing polypeptide chains. The authors identified a tetrazine with electron-donating groups that harbored the requisite stability and compatibility for long-term in vivo use and incorporation into recombinant proteins [53,166].

The Staudinger ligation is also quite "tunable," although most methods to boost reactivity also accelerate phosphine oxidation [167,168]. Phosphine probes can be manipulated to produce "turn-on" fluorescence in response to azide ligation, similar to their octyne counterparts [169]. Raines and others have also developed phosphine scaffolds that can be cleaved from the product post-ligation, leaving behind native amide bonds [170,171]. These latter reagents participate in "traceless" Staudinger ligations and have been particularly useful in protein semi-synthesis [172], installing photo-crosslinking groups on cellular metabolites [173], and templating biomaterials *in vivo* [174].

1.3f Commercial availability of the reagents for bioorthogonal reactions

The accessibility of required reactants can also be a deciding factor when selecting a bioorthogonal chemistry. Based on reagent availability and ease of use,

CuAAC ranks among the most accessible reactions to date. A variety of alkyne- and azide-modified substrates can be purchased from commercial sources, and many can be used directly in metabolic labeling experiments. Several additional azide and alkyne precursors are available that can be readily appended to biomolecules using straightforward chemistries. The availability of reagents, coupled with the relatively user-friendly features of the reaction, have enabled the rapid adoption of CuAAC in diverse disciplines. This chemistry has been used to monitor oligonucleotide production [38,136], construct organotypic hydrogels [175,176], and even visualize temporal changes in glycosylation relevant to development [138,177].

Other bioorthogonal transformations have been slower to transition to the wider biological community, mostly owing to their more challenging syntheses and lack of commercial suppliers. However, a number of reagent precursors (based on BCN, TCO, tetrazine, and phosphine scaffolds) have been recently made available. We anticipate that these probes will bolster new discoveries in a wide variety of fields.

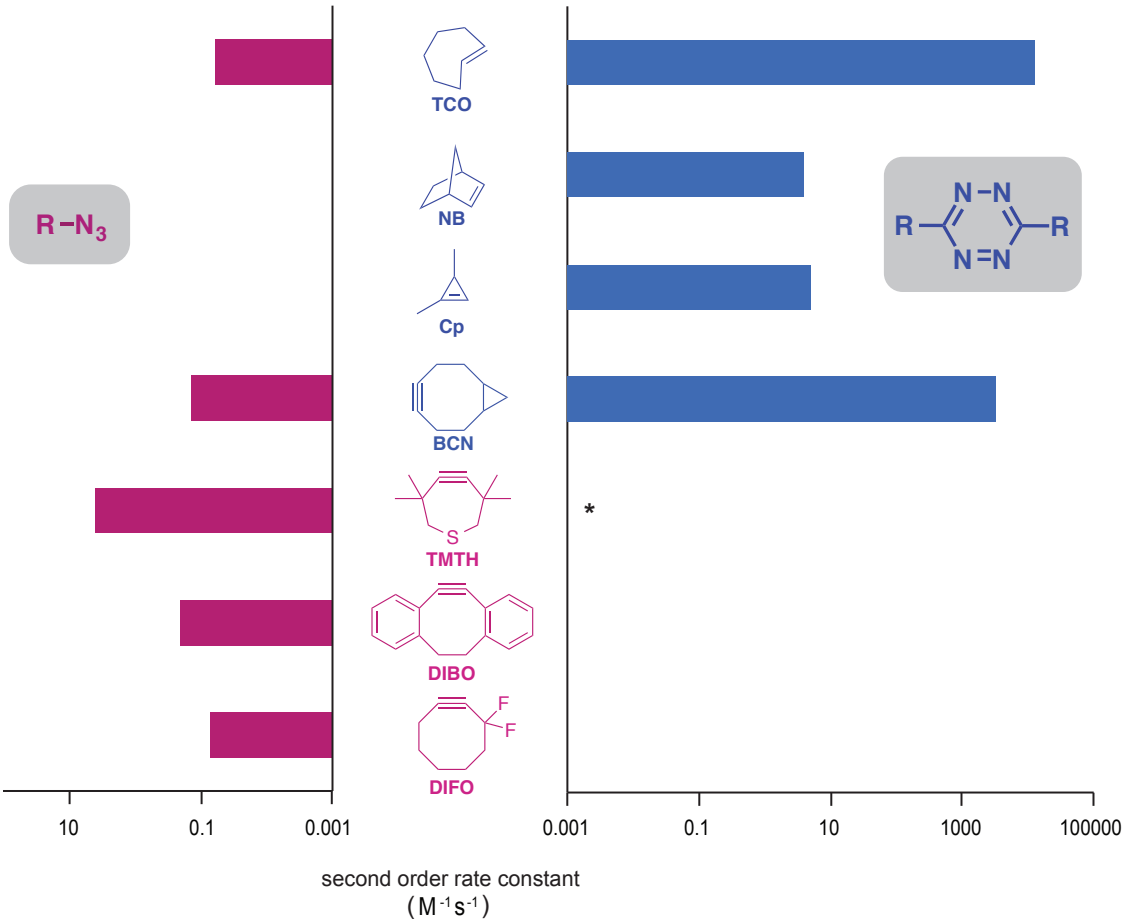

Figure 1-5 Identifying mutually orthogonal transformations. Strained alkenes and alkynes possess dramatically different reactivities with azido (left) and tetrazine (right) probes. The alkenes in blue react rapidly with tetrazine via IED-DA chemistries, while the alkynes in red exhibit rapid reactivity with azides. Bicyclononyne (BCN, black) does not significantly favor tetrazines or azides in terms of reaction rate. With judicious selection, some of these reagents can be used concurrently in bioorthogonal labeling applications. *Predicted rate constant from DFT calculations [203].

1.4 Future directions for development of bioorthogonal transformations

Identifying chemistries for efficient biomolecule tagging in increasingly complex environments—cells, animal models, and even humans—is an ongoing challenge [155]. The search for ever faster and more selective reactions will be aided by explorations into new realms of chemical space. Already, Rao, Chin and others have discovered that cyanobenzothiazole condensations exhibit both rapid and specific reactivity with

aminothiols [178,179]. Similar advances are being made in the realm of bioorthogonal organometallic transformations. In seminal work, the Davis group reported ruthenium-catalyzed cross-metathesis reactions for efficient protein tagging [180-183], along with palladium-catalyzed cross-couplings amenable to targeting proteins, glycans, and nucleotides [184-189].

A corollary challenge to identifying new transformations is elucidating methods to control bioorthogonality (i.e., turning functional groups "on" and "off"). Such "on-demand" reactivity is especially critical for reagents that are only semi-stable in biological environments. Photochemical activation is a particularly attractive mechanism for generating reactivity "on demand" [68,69,190-195]. Pulsed light can be controlled both spatially and temporally, and thus offers a method to release bioorthogonal reagents and localize reactivity [196,197] (Figure 1-4). Popik and coworkers exploited the photo-triggered release of cyclooctyne reagents to control azide-alkyne reactivity [195,198]. In related work, Lin and colleagues utilized "photo-click" chemistry to tag alkene-modified proteins [68]. The derivatized proteins were incubated with tetrazole probes. Upon UV illumination, tetrazoles photolyze to generate nitrile imines that can ligate terminal alkenes. The spatial resolution of these and other photo-click reactions is dependent on the lifetime of the liberated reagent. For nitrile imine, the lifetime is relatively short, as the 1,3-dipole is subject to rapid water quenching [67]. This "react" or "self-destruct" scenario enables more focal labeling and thus excellent spatial resolution. Continued development of mild methods to release bioorthogonal reagents "on-demand," including two-photon absorption and selective chemical reactions, are important pursuits [192,193,199-201].

As new bioorthogonal reagents continue to be explored and validated, another major challenge looms: identifying transformations that not only work well in vivo, but also work well with existing bioorthogonal chemistries. Many of the most common bioorthogonal reactions are incompatible with one another in live cells. For example, certain cycloalkynes have been shown to be highly reactive with tetrazine and therefore do not lend themselves to multi-component studies (Figure 1-5) [202,203]. However, careful selection of bioorthogonal reagents can enable simultaneous and selective labeling [110,202]. Recently, we and others demonstrated the mutual orthogonality of the alkene-tetrazine ligation with variants of SPAAC [81,109,149,204,205]. In one example, Hilderbrand and coworkers utilized Herceptin-TCO and cetuximab-DBCO antibody conjugates to target A431 and SKBR3 cells, respectively [204]. Upon co-administration of the complementary azido- and tetrazine-fluorophores, both cell populations were selectively labeled and visualized.

The identification of mutually orthogonal transformations is being aided by computational studies. Houk and colleagues developed a distortion-interaction model that has proven effective at predicting reactivity of strained molecules with 1,3-dipoles and dienes [58,206,207]. Steric clashes between many of the large, strained molecules can be exploited to disfavor certain cycloadditions, while promoting others [203]. In recent work, we utilized this model to identify two sets of cyclopropenes—differing by the presence of a single methyl group—that exhibit unique cycloaddition preferences.208 These unique reactivities were employed to append unique fluorophores to model proteins. We anticipate that computational algorithms will continue to have a major impact in identifying combinations of mutually orthogonal transformations or those that

can be used sequentially [203,209]. Assays to rapidly identify candidate classes of probes will also be helpful in this regard [210].

1.5 Considerations for the development of novel bioorthogonal chemistries

The past decade has seen a marked expansion of the bioorthogonal toolkit, with a variety of polar reactions and cycloaddition chemistries demonstrating utility for biomolecule labeling in complex environments. As the number of bioorthogonal reactions continues to grow, selecting an appropriate chemistry for a given application is increasingly challenging. The reactions differ in a number of key attributes, including selectivities and rates, and understanding the "personalities" of each transformation is key to their successful implementation.

1.6 Objectives of this study

I was interested in applying chemical reporters and bioorthogonal chemistries to probe host-pathogen interactions. I chose *Toxoplasma gondii* (*T. gondii*) as a model organism for these studies. *T. gondii* is a prevalent intracellular parasite that infects nearly one-third of the world's population and may cause life-threatening conditions in immunocompromised patients. Understanding how *T. gondii* communicates with host cells to remain undetected by the immune system is key to understanding and treating parasitic infections. One class of biomolecules that may modulate these communication networks comprises glycoproteins. *Toxoplasma* is known to secrete glycoproteins and other glycoconjugates into host cells via a number of special organelles: rhoptries, dense granules, and micronemes. Surprisingly, despite their abundance, the roles and downstream effects of such biomolecules are not widely known.

Although the chemical reporter stratergy has been recently applied for studying biological systems, it has not yet been utilized in *T. gondii*. A number of hurdles for successful application exist, including the fact that the parasite resides inside of mammalian cells and is likely blocked from obtaining the requisite reporter metabolites. *T. gondii* has a set of glycosyltransferases distinct from that of most mammalian organisms. These glycosyltransferases might not be promiscuous enough to accept reporter sugars. To address these issues, I established suitable conditions for metabolic labeling of the parasite. Once incorporated into biomolecules, the metabolic labels must be easily detected. Evaluating the interactions between the parasite and its host cells

requires an ability to simultaneously tag and visualize *T. gondii's* and its host signaling biomolecules. This task is highly dependent on accessing mutually orthogonal bioorthogonal chemistries. Towards this end, I focused on finding bioorthogonal transformations suitable for use with existing biocompartible reactions.

In summary, the goals of this thesis work were to:

1. Establish the optimal conditions for metabolic labeling of *T. gondii* with unnatural sugars and identify targeted glycopropetins via mass spectrometry. (Chapter 2)
2. Identify the type of glycans that are being labeled by using unnatural sugars in *T. gondii* by biochemical and enzymatic assays. (Chapter 2)
3. Synthesize methyl cyclopropene sialic acid derivatives for metabolic targeting of mammalian cell glycans. (Chapter 3)
4. Perform sequential labeling of model proteins with isomeric cyclopropenes to establish orthogonal bioorthogonal chemical labeling probes for visualization of host-pathogen interactions. (Chapter 3)
5. Develop a novel bioorthogonal transformation based on methylene cyclopropane for examining of host-pathogen interactions. (Chapter 4)

This thesis reports the successful completion of aims 1-4 and the progress, to date, towards aim 5. In the subsequent chapters, I demonstrate the strategy for successful

metabolic labeling of *T. gondii* with unnatural sugars and establish the targets of this labeling as both proteins carrying the modification and type of modification.

In later chapters, I show the development of novel mutually orthogonal reactions based on isomeric three-membered microcycles (cyclopropenes and methylene cyclopropane) and showcase their utility for concurrent labeling applications.

References

(1) Chang, P. V.; Bertozzi, C. R. Imaging beyond the proteome. *Chem. Commun.* **2012**, *48*, 8864-8879.

(2) Prescher, J. A.; Bertozzi, C. R. Chemistry in living systems. *Nat. Chem. Biol.* **2005**, *1*, 13-21.

(3) Giepmans, B. N.; Adams, S. R.; Ellisman, M. H.; Tsien, R. Y. The fluorescent toolbox for assessing protein location and function. *Science* **2006**, *312*, 217-224.

(4) Scheck, R. A.; Schepartz, A. Surveying protein structure and function using bis-arsenical small molecules. *Acc. Chem. Res.* **2011**, *44*, 654-665.

(5) Cornish, V. W.; Hahn, K. M.; Schultz, P. G. Site-specific protein modification using a ketone handle. *J. Am. Chem. Soc.* **1996**, *118*, 8150-8151.

(6) Sletten, E. M.; Bertozzi, C. R. Bioorthogonal Chemistry: Fishing for selectivity in a sea of functionality. *Angew. Chem. Int. Ed.* **2009**, *48*, 6974-6998.

(7) Rideout, D. Self-assembling cytotoxins. *Science* **1986**, *233*, 561-563.

(8) Shao, J.; Tam, J. P. Unprotected peptides as building-blocks for the synthesis of peptide dendrimers with oxime, hydrazone, and thiazolidine linkages. *J. Am. Chem. Soc.* **1995**, *117*, 3893-3899.

(9) Zeng, Y.; Ramya, T. N.; Dirksen, A.; Dawson, P. E.; Paulson, J. C. High-efficiency labeling of sialylated glycoproteins on living cells. *Nat. Methods* **2009**, *6*, 207-209.

(10) Crisalli, P.; Kool, E. T. Water-soluble organocatalysts for hydrazone and oxime formation. *J. Org. Chem.* **2013**, *78*, 1184-1189.

(11) Dirksen, A.; Dawson, P. E. Rapid oxime and hydrazone ligations with aromatic aldehydes for biomolecular labeling. *Bioconjug. Chem.* **2008**, *19*, 2543-2548.

(12) Dutta, D.; Pulsipher, A.; Luo, W.; Yousaf, M. N. Synthetic chemoselective rewiring of cell surfaces: generation of three-dimensional tissue structures. *J. Am. Chem. Soc.* **2011**, *133*, 8704-8713.

(13) Wang, L.; Zhang, Z.; Brock, A.; Schultz, P. G. Addition of the keto functional group to the genetic code of *Escherichia coli*. *Proc. Natl. Acad. Sci. U.S.A*. **2003**, *100*, 56-61.

(14) Wang, L.; Xie, J.; Schultz, P. G. Expanding the genetic code. *Annu. Rev. Biophys. Biomol. Struct.* **2006**, *35*, 225-249.

(15) Mahal, L. K.; Yarema, K. J.; Bertozzi, C. R. Engineering chemical reactivity on cell surfaces through oligosaccharide biosynthesis. *Science* **1997**, *276*, 1125-1128.

(16) Chang, P. V.; Prescher, J. A.; Hangauer, M. J.; Bertozzi, C. R. Imaging cell surface glycans with bioorthogonal chemical reporters. *J. Am. Chem. Soc.* **2007**, *129*, 8400-8401.

(17) Kalia, J.; Raines, R. T. Hydrolytic stability of hydrazones and oximes. *Angew. Chem. Int. Ed.* **2008**, *47*, 7523-7526.

(18) Agarwal, P.; van der Weijden, J.; Sletten, E. M.; Rabuka, D.; Bertozzi, C. R. A Pictet-Spengler ligation for protein chemical modification. *Proc. Natl. Acad. Sci.* **2013**, *110*, 46-51.

(19) Agarwal, P.; Kudirka, R.; Albers, A. E.; Barfield, R. M.; de Hart, G. W.; Drake, P. M.; Jones, L. C.; Rabuka, D. Hydrazino-Pictet-Spengler ligation as a biocompatible method for the generation of stable protein conjugates. *Bioconjug. Chem.* **2013**, *24*, 846-851.

(20) Schilling, C. I.; Jung, N.; Biskup, M.; Schepers, U.; Brase, S. Bioconjugation via azide-Staudinger ligation: an overview. *Chem. Soc. Rev.* **2011**, *40*, 4840-4871.

(21) Griffin, R. J. The medicinal chemistry of the azido group. *Prog. Med. Chem.* **1994**, *31*, 121-232.

(22) Brase, S.; Gil, C.; Knepper, K.; Zimmermann, V. Organic azides: an exploding diversity of a unique class of compounds. *Angew. Chem. Int. Ed.* **2005**, *44*, 5188-5240.

(23) Saxon, E.; Bertozzi, C. R. Cell surface engineering by a modified Staudinger reaction. *Science* **2000**, *287*, 2007-2010.

(24) van Berkel, S. S.; van Eldijk, M. B.; van Hest, J. C. Staudinger ligation as a method for bioconjugation. *Angew. Chem. Int. Ed.* **2011**, *50*, 8806-8827.

(25) Prescher, J. A.; Dube, D. H.; Bertozzi, C. R. Chemical remodelling of cell surfaces in living animals. *Nature* **2004**, *430*, 873-877.

(26) Neves, A. A.; Stockmann, H.; Harmston, R. R.; Pryor, H. J.; Alam, I. S.; Ireland-Zecchini, H.; Lewis, D. Y.; Lyons, S. K.; Leeper, F. J.; Brindle, K. M. Imaging sialylated tumor cell glycans in vivo. *FASEB J.* **2011**, *25*, 2528-2537.

(27) Hang, H. C.; Geutjes, E. J.; Grotenbreg, G.; Pollington, A. M.; Bijlmakers, M. J.; Ploegh, H. L. Chemical probes for the rapid detection of fatty-acylated proteins in mammalian cells. *J. Am. Chem. Soc.* **2007**, *129*, 2744-2745.

(28) Kho, Y.; Kim, S. C.; Jiang, C.; Barma, D.; Kwon, S. W.; Cheng, J.; Jaunbergs, J.; Weinbaum, C.; Tamanoi, F.; Falck, J.; Zhao, Y. A tagging-via-substrate technology for

detection and proteomics of farnesylated proteins. *Proc. Natl. Acad. Sci. U.S.A.* **2004**, *101*, 12479-12484.

(29) Kaewsapsak, P.; Esonu, O.; Dube, D. H. Recruiting the host's immune system to target *Helicobacter pylori*'s surface glycans. *ChemBioChem* **2013**, *14*, 721-726.

(30) Debets, M. F.; van der Doelen, C. W.; Rutjes, F. P.; van Delft, F. L. Azide: a unique dipole for metal-free bioorthogonal ligations. *ChemBioChem* **2010**, *11*, 1168-1184.

(31) Kolb, H. C.; Finn, M. G.; Sharpless, K. B. Click chemistry: diverse chemical function from a few good reactions. *Angew. Chem. Int. Ed.* **2001**, *40*, 2004-2021.

(32) Hein, J. E.; Fokin, V. V. Copper-catalyzed azide-alkyne cycloaddition (CuAAC) and beyond: new reactivity of copper(I) acetylides. *Chem. Soc. Rev.* **2010**, *39*, 1302-1315.

(33) Huisgen, R. 1,3-Dipolar cycloadditions. Past and future. *Angew. Chem. Int. Ed.* **1963**, *2*, 565-598.

(34) Rostovtsev, V. V.; Green, L. G.; Fokin, V. V.; Sharpless, K. B. A stepwise Huisgen cycloaddition process: copper(I)-catalyzed regioselective "ligation" of azides and terminal alkynes. *Angew. Chem. Int. Ed.* **2002**, *41*, 2596-2599.

(35) Tornoe, C. W.; Christensen, C.; Meldal, M. Peptidotriazoles on solid phase: [1,2,3]-triazoles by regiospecific copper(I)-catalyzed 1,3-dipolar cycloadditions of terminal alkynes to azides. *J. Org. Chem.* **2002**, *67*, 3057-3064.

(36) Worrell, B. T.; Malik, J. A.; Fokin, V. V. Direct evidence of a dinuclear copper intermediate in Cu(I)-catalyzed azide-alkyne cycloadditions. *Science* **2013**, *340*, 457-460.

(37) Gramlich, P. M.; Wirges, C. T.; Manetto, A.; Carell, T. Postsynthetic DNA modification through the copper-catalyzed azide-alkyne cycloaddition reaction. *Angew. Chem. Int. Ed.* **2008**, *47*, 8350-8358.

(38) Salic, A.; Mitchison, T. J. A chemical method for fast and sensitive detection of DNA synthesis in vivo. *Proc. Natl. Acad. Sci. U.S.A.* **2008**, *105*, 2415-2420.

(39) Dieterich, D. C.; Lee, J. J.; Link, A. J.; Graumann, J.; Tirrell, D. A.; Schuman, E. M. Labeling, detection and identification of newly synthesized proteomes with bioorthogonal non-canonical amino-acid tagging. *Nat. Protoc.* **2007**, *2*, 532-540.

(40) Salisbury, C. M.; Cravatt, B. F. Click chemistry-led advances in high content functional proteomics. *QSAR Comb. Sci.* **2007**, *26*, 1229-1238.

(41) Nessen, M. A., Kramer, G., Back, J., Baskin, J. M., Smeenk, L. E., de Koning, L. J., van Maarseveen, J. H., de Jong, L., Bertozzi, C. R., Hiemstra, H., de Koster, C. G.

Selective enrichment of azide-containing peptides from complex mixtures. *J. Proteome Res.* **2009**, *8*, 3702-3711.

(42) Zaro, B. W.; Hang, H. C.; Pratt, M. R. Incorporation of unnatural sugars for the identification of glycoproteins. *Methods Mol. Biol.* **2013**, *951*, 57-67.

(43) Leonard, S. E.; Carroll, K. S. Chemical 'omics' approaches for understanding protein cysteine oxidation in biology. *Curr. Opin. Chem. Biol.* **2011**, *15*, 88-102.

(44) Speers, A. E.; Adam, G. C.; Cravatt, B. F. Activity-based protein profiling in vivo using a copper(I)-catalyzed azide-alkyne [3 + 2] cycloaddition. *J. Am. Chem. Soc.* **2003**, *125*, 4686-4687.

(45) Willems, L. I.; van der Linden, W. A.; Li, N.; Li, K. Y.; Liu, N.; Hoogendoorn, S.; van der Marel, G. A.; Florea, B. I.; Overkleeft, H. S. Bioorthogonal chemistry: applications in activity-based protein profiling. *Acc. Chem. Res.* **2011**, *44*, 718-729.

(46) Cravatt, B. F.; Wright, A. T.; Kozarich, J. W. Activity-based protein profiling: from enzyme chemistry to proteomic chemistry. *Annu. Rev. Biochem.* **2008**, *77*, 383-414.

(47) Bateman, L. A.; Zaro, B. W.; Miller, S. M.; Pratt, M. R. An alkyne-aspirin chemical reporter for the detection of aspirin-dependent protein modification in living cells. *J. Am. Chem. Soc.* **2013**, *135*, 14568-73.

(48) Sletten, E. M.; Bertozzi, C. R. From mechanism to mouse: a tale of two bioorthogonal reactions. *Acc. Chem. Res.* **2011**, *44*, 666-676.

(49) Jewett, J. C.; Bertozzi, C. R. Cu-free click cycloaddition reactions in chemical biology. *Chem. Soc. Rev.* **2010**, *39*, 1272-1279.

(50) Agard, N. J.; Prescher, J. A.; Bertozzi, C. R. A strain-promoted [3 + 2] azide-alkyne cycloaddition for covalent modification of biomolecules in living systems. *J. Am. Chem. Soc.* **2004**, *126*, 15046-15047.

(51) Baskin, J. M.; Prescher, J. A.; Laughlin, S. T.; Agard, N. J.; Chang, P. V.; Miller, I. A.; Lo, A.; Codelli, J. A.; Bertozzi, C. R. Copper-free click chemistry for dynamic in vivo imaging. *Proc. Natl. Acad. Sci. U.S.A.* **2007**, *104*, 16793-16797.

(52) Ning, X.; Guo, J.; Wolfert, M. A.; Boons, G. J. Visualizing metabolically labeled glycoconjugates of living cells by copper-free and fast Huisgen cycloadditions. *Angew. Chem. Int. Ed.* **2008**, *47*, 2253-2255.

(53) Chang, P. V.; Prescher, J. A.; Sletten, E. M.; Baskin, J. M.; Miller, I. A.; Agard, N. J.; Lo, A.; Bertozzi, C. R. Copper-free click chemistry in living animals. *Proc. Natl. Acad. Sci. U.S.A.* **2010**, *107*, 1821-1826.

(54) van den Bosch, S. M.; Rossin, R.; Renart Verkerk, P.; Ten Hoeve, W.; Janssen, H. M.; Lub, J.; Robillard, M. S. Evaluation of strained alkynes for Cu-free click reaction in live mice. *Nucl. Med. Biol.* **2013**, *40*, 415-423.

(55) Baskin, J. M.; Dehnert, K. W.; Laughlin, S. T.; Amacher, S. L.; Bertozzi, C. R. Visualizing enveloping layer glycans during zebrafish early embryogenesis. *Proc. Natl. Acad. Sci. U.S.A.* **2010**, *107*, 10360-10365.

(56) Ramil, C. P.; Lin, Q. Bioorthogonal chemistry: strategies and recent developments. *Chem. Commun.* **2013**, *49*, 11007-11022.

(57) Jewett, J. C.; Sletten, E. M.; Bertozzi, C. R. Rapid Cu-free click chemistry with readily synthesized biarylazacyclooctynones. *J. Am. Chem. Soc.* **2010**, *132*, 3688-3690.

(58) Gordon, C. G.; Mackey, J. L.; Jewett, J. C.; Sletten, E. M.; Houk, K. N.; Bertozzi, C. R. Reactivity of biarylazacyclooctynones in copper-free click chemistry. *J. Am. Chem. Soc.* **2012**, *134*, 9199-9208.

(59) Debets, M. F.; van Berkel, S. S.; Dommerholt, J., Dirks; A. T., Rutjes, F. P.; van Delft, F. L. Bioconjugation with strained alkenes and alkynes. *Acc. Chem. Res.* **2011**, *44*, 805-815.

(60) Ning, X.; Temming, R. P.; Dommerholt, J.; Guo, J.; Ania, D. B.; Debets, M. F.; Wolfert, M. A.; Boons, G. J.; van Delft, F. L. Protein modification by strain-promoted alkyne-nitrone cycloaddition. *Angew. Chem. Int. Ed.* **2010**, *49*, 3065-3068.

(61) McKay, C. S.; Blake, J. A.; Cheng, J.; Danielson, D. C.; Pezacki, J. P. Strain-promoted cycloadditions of cyclic nitrones with cyclooctynes for labeling human cancer cells. *Chem. Commun*. **2011**, *47*, 10040-10042.

(62) Sanders, B. C.; Friscourt, F.; Ledin, P. A.; Mbua, N. E.; Arumugam, S.; Guo, J.; Boltje, T. J.; Popik, V. V.; Boons, G. J. Metal-free sequential [3 + 2]-dipolar cycloadditions using cyclooctynes and 1,3-dipoles of different reactivity. *J. Am. Chem. Soc.* **2011**, *133*, 949-957.

(63) Wendeln, C.; Singh, I.; Rinnen, S.; Schulz, C.; Arlinghaus, H. F.; Burley, G. A.; Ravoo, B. J. Orthogonal, metal-free surface modification by strain-promoted azide-alkyne and nitrile oxide-alkene/alkyne cycloadditions. *Chem. Sci.* **2012**, *3*, 2479-2484.

(64) McGrath, N. A.; Raines, R. T. Diazo compounds as highly tunable reactants in 1,3-dipolar cycloaddition reactions with cycloalkynes. *Chem. Sci.* **2012**, *3*, 3237-3240.

(65) Chou, H. H.; Raines, R. T. Conversion of azides into diazo compounds in water. *J. Am. Chem. Soc.* **2013**, *135*, 14936-14939.

(66) McKay, C. S.; Chigrinova, M.; Blake, J. A.; Pezacki, J. P. Kinetics studies of rapid strain-promoted [3 + 2]-cycloadditions of nitrones with biaryl-aza-cyclooctynone. *Org. Biomol. Chem.* **2012**, *10*, 3066-3070.

(67) Yu, Z.; Pan, Y.; Wang, Z.; Wang, J.; Lin, Q. Genetically encoded cyclopropene directs rapid, photoclick-chemistry-mediated protein labeling in mammalian cells. *Angew. Chem. Int. Ed.* **2012**, *51*, 10600-10604.

(68) Song, W.; Wang, Y.; Yu, Z.; Vera, C. I.; Qu, J.; Lin, Q. A metabolic alkene reporter for spatiotemporally controlled imaging of newly synthesized proteins in Mammalian cells. *ACS Chem. Biol.* **2010**, *5*, 875-885.

(69) Song, W.; Wang, Y.; Qu, J.; Madden, M. M.; Lin, Q. A photoinducible 1,3-dipolar cycloaddition reaction for rapid, selective modification of tetrazole-containing proteins. *Angew. Chem. Int. Ed.* **2008**, *47*, 2832-2835.

(70) Blackman, M. L.; Royzen, M.; Fox, J. M. (2008) Tetrazine ligation: fast bioconjugation based on inverse-electron-demand Diels-Alder reactivity. *J. Am. Chem. Soc.* 130, 13518-13519.

(71) Selvaraj, R.; Fox, J. M. trans-Cyclooctene-a stable, voracious dienophile for bioorthogonal labeling. *Curr. Opin Chem Biol.* **2013**, *17*, 753–760.

(72) Bach, R. D. Ring strain energy in the cyclooctyl system. The effect of strain energy on [3 + 2] cycloaddition reactions with azides. *J. Am. Chem. Soc.* **2009**, *131*, 5233-5243.

(73) Rossin, R.; van den Bosch, S. M.; Ten Hoeve, W.; Carvelli, M.; Versteegen, R. M.; Lub, J.; Robillard, M. S. Highly reactive trans-cyclooctene tags with improved stability for Diels-Alder chemistry in living systems. *Bioconjug. Chem.* **2013**, *24*, 1210-1217.

(74) Devaraj, N. K.; Thurber, G. M.; Keliher, E. J.; Marinelli, B.; Weissleder, R. Reactive polymer enables efficient in vivo bioorthogonal chemistry. *Proc. Natl. Acad. Sci. U.S.A.* **2012**, *109*, 4762-4767.

(75) Rossin, R.; Verkerk, P. R.; van den Bosch, S. M.; Vulders, R. C.; Verel, I.; Lub, J.; Robillard, M. S. In vivo chemistry for pretargeted tumor imaging in live mice. *Angew. Chem. Int. Ed.* **2010**, *49*, 3375-3378.

(76) Devaraj, N. K.; Weissleder, R.; Hilderbrand, S. A. Tetrazine-based cycloadditions: application to pretargeted live cell imaging. *Bioconjug. Chem.* **2008***, 19*, 2297-2299.

(77) Budin, G.; Chung, H. J.; Lee, H.; Weissleder, R. A Magnetic gram stain for bacterial detection. *Angew. Chem. Int. Ed.* **2012**, *51*, 7752-7755.

(78) Karver, M. R.; Weissleder, R.; Hilderbrand, S. A. Synthesis and evaluation of a series of 1,2,4,5-tetrazines for bioorthogonal conjugation. *Bioconjug. Chem.* **2011**, *22*, 2263-2270.

(79) Seckute, J.; Devaraj, N. K. Expanding room for tetrazine ligations in the in vivo chemistry toolbox. *Curr. Opin. Chem. Biol.* **2013**, *17*, 761-767.

(80) Yang, J.; Seckute, J.; Cole, C. M.; Devaraj, N. K. Live-cell imaging of cyclopropene tags with fluorogenic tetrazine cycloadditions. *Angew. Chem. Int. Ed.* **2012**, *51*, 7476-7479.

(81) Patterson, D. M.; Nazarova, L. A.; Xie, B.; Kamber, D. N.; Prescher, J. A. Functionalized cyclopropenes as bioorthogonal chemical reporters. *J. Am. Chem. Soc.* **2012**, *134*, 18638-18643.

(82) Cole, C. M.; Yang, J.; Seckute, J.; Devaraj, N. K. Fluorescent live-cell imaging of metabolically incorporated unnatural cyclopropene-mannosamine derivatives. *ChemBioChem* **2013**, *14*, 205-208.

(83) Yi, L.; Sun, H.; Wu, Y. W.; Triola, G.; Waldmann, H.; Goody, R. S. A highly efficient strategy for modification of proteins at the C terminus. *Angew. Chem. Int. Ed.* **2010**, *49*, 9417-9421.

(84) Gilmore, J. M.; Scheck, R. A.; Esser-Kahn, A. P.; Joshi, N. S.; Francis, M. B. N-terminal protein modification through a biomimetic transamination reaction. *Angew. Chem. Int. Ed.* **2006**, *45*, 5307-5311.

(85) Scheck, R. A.; Francis, M. B. Regioselective labeling of antibodies through N-terminal transamination. *ACS Chem. Biol.* **2007**, *2*, 247-251.

(86) Hermanson, G. T. *Bioconjugate Techniques;* Academic Press: San Diego, 1996.

(87) Stephanopoulos, N.; Francis, M. B. Choosing an effective protein bioconjugation strategy. *Nat. Chem. Biol.* **2011**, *7*, 876-884.

(88) Antos, J. M.; Francis, M. B. Transition metal catalyzed methods for site-selective protein modification. *Curr. Opin. Chem. Biol.* **2006**, *10*, 253-262.

(89) Popp, B. V.; Ball, Z. T. Structure-selective modification of aromatic side chains with dirhodium metallopeptide catalysts. *J. Am. Chem. Soc.* **2010**, *132*, 6660-6662.

(90) Antos, J. M.; McFarland, J. M.; Iavarone, A. T.; Francis, M. B. Chemoselective tryptophan labeling with rhodium carbenoids at mild pH. *J. Am. Chem. Soc.* **2009**, *131*, 6301-6308.

(91) van Dongen, S. F. M.; Teeuwen, R. L. M.; Nallani, M.; van Berkel, S. S.; Cornelissen, J. J. L. M.; Nolte, R. J. M.; van Hest, J. C. M. Single-step azide introduction in proteins via an aqueous diazo transfer. *Bioconjug. Chem.* **2009**, *20*, 20-23.

(92) Chen, I.; Howarth, M.; Lin, W.; Ting, A. Y. Site-specific labeling of cell surface proteins with biophysical probes using biotin ligase. *Nat. Methods* **2005**, *2*, 99-104.

(93) Fernandez-Suarez, M.; Baruah, H.; Martinez-Hernandez, L.; Xie, K. T.; Baskin, J. M.; Bertozzi, C. R.; Ting, A. Y. Redirecting lipoic acid ligase for cell surface protein labeling with small-molecule probes. *Nat. Biotechnol.* **2007**, *25*, 1483-1487.

(94) Carrico, I. S.; Carlson, B. L.; Bertozzi, C. R. Introducing genetically encoded aldehydes into proteins. *Nat. Chem. Biol.* **2007***, 3*, 321-322.

(95) Popp, M. W.; Ploegh, H. L. Making and breaking peptide bonds: protein engineering using sortase. *Angew. Chem. Int. Ed.* **2011**, *50*, 5024-5032.

(96) Los, G. V.; Encell, L. P.; McDougall, M. G.; Hartzell, D. D.; Karassina, N.; Zimprich, C.; Wood, M. G.; Learish, R.; Ohana, R. F.; Urh, M.; Simpson, D.; Mendez, J.; Zimmerman, K.; Otto, P.; Vidugiris, G.; Zhu, J.; Darzins, A.; Klaubert, D. H.; Bulleit, R. F.; Wood, K. V. HaloTag: a novel protein labeling technology for cell imaging and protein analysis. *ACS Chem. Biol.* **2008**, *3*, 373-382.

(97) Wu, P.; Shui, W.; Carlson, B. L.; Hu, N.; Rabuka, D.; Lee, J.; Bertozzi, C. R. Site-specific chemical modification of recombinant proteins produced in mammalian cells by using the genetically encoded aldehyde tag. *Proc. Natl. Acad. Sci. U.S.A.* **2009**, *106*, 3000-3005.

(98) Rashidian, M.; Kumarapperuma, S. C.; Gabrielse, K.; Fegan, A.; Wagner, C. R.; Distefano, M. D. Simultaneous dual protein labeling using a triorthogonal reagent. *J. Am. Chem. Soc.* **2013**, *135*, 16388-16396.

(99) Puthenveetil, S.; Liu, D. S.; White, K. A.; Thompson, S.; Ting, A. Y. Yeast display evolution of a kinetically efficient 13-amino acid substrate for lipoic acid ligase. *J. Am. Chem. Soc.* **2009**, *131*, 16430-16438.

(100) Uttamapinant, C.; Sanchez, M. I.; Liu, D. S.; Yao, J. Z.; Ting, A. Y. Site-specific protein labeling using PRIME and chelation-assisted click chemistry. *Nat. Protoc.* **2013**, *8*, 1620-1634.

(101) Liu, D. S.; Tangpeerachaikul, A.; Selvaraj, R.; Taylor, M. T.; Fox, J. M.; Ting, A. Y. Diels-Alder cycloaddition for fluorophore targeting to specific proteins inside living cells. *J. Am. Chem. Soc.* **2012**, *134*, 792-795.

(102) Cohen, J. D.; Zou, P.; Ting, A. Y. Site-specific protein modification using lipoic acid ligase and bis-aryl hydrazone formation. *ChemBioChem* **2012**, *13*, 888-894.

(103) Davis, L.; Chin, J. W. Designer proteins: applications of genetic code expansion in cell biology. *Nat. Rev. Mol. Cell Biol.* **2012**, *13*, 168-182.

(104) Liu, C. C.; Schultz, P. G. Adding new chemistries to the genetic code. *Annu. Rev. Biochem.* **2010**, *79*, 413-444.

(105) Zhang, Z.; Smith, B. A.; Wang, L.; Brock, A.; Cho, C.; Schultz, P. G. A new strategy for the site-specific modification of proteins in vivo. *Biochemistry* **2003**, *42*, 6735-6746.

(106) Deiters, A.; Cropp, T. A.; Mukherji, M.; Chin, J. W.; Anderson, J. C.; Schultz, P. G. Adding amino acids with novel reactivity to the genetic code of *Saccharomyces cerevisiae*. *J. Am. Chem. Soc.* **2003**, *125*, 11782-11783.

(107) Lee, Y. J.; Wu, B.; Raymond, J. E.; Zeng, Y.; Fang, X.; Wooley, K. L.; Liu, W. R. A genetically encoded acrylamide functionality. *ACS Chem. Biol.* **2013**, *8*, 1664-1670.

(108) Seitchik, J. L.; Peeler, J. C.; Taylor, M. T.; Blackman, M. L.; Rhoads, T. W.; Cooley, R. B.; Refakis, C.; Fox, J. M.; Mehl, R. A. Genetically encoded tetrazine amino acid directs rapid site-specific in vivo bioorthogonal ligation with trans-cyclooctenes. *J. Am. Chem. Soc.* **2012**, *134*, 2898-2901.

(109) Plass, T.; Milles, S.; Koehler, C.; Szymanski, J.; Mueller, R.; Wiessler, M.; Schultz, C.; Lemke, E. A. Amino acids for Diels-Alder reactions in living cells. *Angew. Chem. Int. Ed.* **2012**, *51*, 4166-4170.

(110) Lang, K.; Davis, L.; Wallace, S.; Mahesh, M.; Cox, D. J.; Blackman, M. L.; Fox, J. M.; Chin, J. W. Genetic encoding of bicyclononynes and trans-cyclooctenes for site-specific protein labeling in vitro and in live mammalian cells via rapid fluorogenic Diels-Alder reactions. *J. Am. Chem. Soc.* **2012**, *134*, 10317-10320.

(111) Lang, K.; Davis, L.; Torres-Kolbus, J.; Chou, C.; Deiters, A.; Chin, J. W. Genetically encoded norbornene directs site-specific cellular protein labelling via a rapid bioorthogonal reaction. *Nat. Chem.* **2012**, *4*, 298-304.

(112) Li, F.; Zhang, H.; Sun, Y.; Pan, Y.; Zhou, J.; Wang, J. Expanding the genetic code for photoclick chemistry in *E. coli*, mammalian cells, and *A. thaliana*. *Angew. Chem. Int. Ed.* **2013**, *52*, 9700-9704.

(113) Bianco, A.; Townsley, F. M.; Greiss, S.; Lang, K.; Chin, J. W. Expanding the genetic code of *Drosophila melanogaster*. *Nat. Chem. Biol.* **2012**, *8*, 748-750.

(114) Neumann, H.; Wang, K.; Davis, L.; Garcia-Alai, M.; Chin, J. W. Encoding multiple unnatural amino acids via evolution of a quadruplet-decoding ribosome. *Nature* **2010**, *464*, 441-444.

(115) Wan, W.; Huang, Y.; Wang, Z.; Russell, W. K.; Pai, P. J.; Russell, D. H.; Liu, W. R. A facile system for genetic incorporation of two different noncanonical amino acids into one protein in *Escherichia coli*. *Angew. Chem. Int. Ed.* **2010**, *49*, 3211-3214.

(116) Dieterich, D. C.; Link, A. J.; Graumann, J.; Tirrell, D. A.; Schuman, E. M. Selective identification of newly synthesized proteins in mammalian cells using

bioorthogonal noncanonical amino acid tagging (BONCAT). *Proc. Natl. Acad. Sci. U.S.A.* **2006**, *103*, 9482-9487.

(117) Ngo, J. T.; Tirrell, D. A. Noncanonical amino acids in the interrogation of cellular protein synthesis. *Acc. Chem. Res.* **2011**, *44*, 677-685.

(118) Geoghegan, K. F.; Stroh, J. G. Site-directed conjugation of nonpeptide groups to peptides and proteins via periodate oxidation of a 2-amino alcohol. Application to modification at N-terminal serine. *Bioconjug. Chem.* **1992**, *3*, 138-146.

(119) Clark, P. M.; Dweck, J. F.; Mason, D. E.; Hart, C. R.; Buck, S. B.; Peters, E. C.; Agnew, B. J.; Hsieh-Wilson, L. C. Direct in-gel fluorescence detection and cellular imaging of O-GlcNAc-modified proteins. *J. Am. Chem. Soc.* **2008**, *130*, 11576-11577.

(120) Soriano Del Amo, D.; Wang, W.; Jiang, H.; Besanceney, C.; Yan, A. C.; Levy, M.; Liu, Y.; Marlow, F. L.; Wu, P. Biocompatible copper(I) catalysts for *in vivo* imaging of glycans. *J. Am. Chem. Soc.* **2010**, *132*, 16893-16899.

(121) Besanceney-Webler, C.; Jiang, H.; Zheng, T.; Feng, L.; Soriano del Amo, D.; Wang, W.; Klivansky, L. M.; Marlow, F. L.; Liu, Y.; Wu, P. Increasing the efficacy of bioorthogonal click reactions for bioconjugation: a comparative study. *Angew. Chem. Int. Ed.* **2011**, *50*, 8051-8056.

(122) Hong, V.; Presolski, S. I.; Ma, C.; Finn, M. G. Analysis and optimization of copper-catalyzed azide-alkyne cycloaddition for bioconjugation. *Angew. Chem. Int. Ed.* **2009**, *48*, 9879-9883.

(123) Hong, V.; Steinmetz, N. F.; Manchester, M.; Finn, M. G. Labeling live cells by copper-catalyzed alkyne--azide click chemistry. *Bioconjug. Chem.* **2010**, *21*, 1912-1916.

(124) Kennedy, D. C.; McKay, C. S.; Legault, M. C.; Danielson, D. C.; Blake, J. A.; Pegoraro, A. F.; Stolow, A.; Mester, Z.; Pezacki, J. P. Cellular consequences of copper complexes used to catalyze bioorthogonal click reactions. *J. Am. Chem. Soc.* **2011**, *133*, 17993-18001.

(125) Uttamapinant, C.; Tangpeerachaikul, A.; Grecian, S.; Clarke, S.; Singh, U.; Slade, P.; Gee, K. R.; Ting, A. Y. Fast, cell-compatible click chemistry with copper-chelating azides for biomolecular labeling. *Angew. Chem. Int. Ed.* **2012**, *51*, 5852-5856.

(126) Brotherton, W. S.; Michaels, H. A.; Simmons, J. T.; Clark, R. J.; Dalal, N. S.; Zhu, L. Apparent copper(II)-accelerated azide-alkyne cycloaddition. *Org. Lett.* **2009**, *11*, 4954-4957.

(127) Kuang, G. C.; Guha, P. M.; Brotherton, W. S.; Simmons, J. T.; Stankee, L. A.; Nguyen, B. T.; Clark, R. J.; Zhu, L. Experimental investigation on the mechanism of chelation-assisted, copper(II) acetate-accelerated azide-alkyne cycloaddition. *J. Am. Chem. Soc.* **2011**, *133*, 13984-14001.

(128) Yao, J. Z.; Uttamapinant, C.; Poloukhtine, A.; Baskin, J. M.; Codelli, J. A.; Sletten, E. M.; Bertozzi, C. R.; Popik, V. V.; Ting, A. Y. Fluorophore targeting to cellular proteins via enzyme-mediated azide ligation and strain-promoted cycloaddition. *J. Am. Chem. Soc.* **2012**, *134*, 3720-3728.

(129) Kim, E. J.; Kang, D. W.; Leucke, H. F.; Bond, M. R.; Ghosh, S.; Love, D. C.; Ahn, J. S.; Kang, D. O.; Hanover, J. A. Optimizing the selectivity of DIFO-based reagents for intracellular bioorthogonal applications. *Carbohydr. Res.* **2013**, *377*, 18-27.

(130) Mackinnon, A. L.; Taunton, J. Target Identification by diazirine photo-cross-linking and click chemistry. *Curr. Protoc. Chem. Biol.* **2009**, *1*, 55-73.

(131) Speers, A. E.; Cravatt, B. F. Profiling enzyme activities *in vivo* using click chemistry methods. *Chem. Biol*. **2004**, *11*, 535-546.

(132) Boyce, M.; Carrico, I. S.; Ganguli, A. S.; Yu, S. H.; Hangauer, M. J.; Hubbard, S. C.; Kohler, J. J.; Bertozzi, C. R. Metabolic cross-talk allows labeling of O-linked beta-N-acetylglucosamine-modified proteins via the N-acetylgalactosamine salvage pathway. *Proc. Natl. Acad. Sci. U.S.A.* **2011**, *108*, 3141-3146.

(133) Agard, N. J.; Baskin, J. M.; Prescher, J. A.; Lo, A.; Bertozzi, C. R. A comparative study of bioorthogonal reactions with azides. *ACS Chem. Biol.* **2006**, *1*, 644-648.

(134) Grammel, M.; Hang, H. C. Chemical reporters for biological discovery. *Nat. Chem. Biol.* **2013**, *9*, 475-484.

(135) Ekkebus, R.; van Kasteren, S. I.; Kulathu, Y.; Scholten, A.; Berlin, I.; Geurink, P. P.; de Jong, A.; Goerdayal, S.; Neefjes, J.; Heck, A. J.; Komander, D.; Ovaa, H. On terminal alkynes that can react with active-site cysteine nucleophiles in proteases. *J. Am. Chem. Soc.* **2013**, *135*, 2867-2870.

(136) Dieterich, D. C.; Hodas, J. J.; Gouzer, G.; Shadrin, I. Y.; Ngo, J. T.; Triller, A.; Tirrell, D. A.; Schuman, E. M. In situ visualization and dynamics of newly synthesized proteins in rat hippocampal neurons. *Nat. Neurosci.* **2010**, *13*, 897-905.

(137) Agard, N. J.; Bertozzi, C. R. Chemical approaches to perturb, profile, and perceive glycans. *Acc. Chem. Res.* **2009**, *42*, 788-797.

(138) Laughlin, S. T.; Baskin, J. M.; Amacher, S. L.; Bertozzi, C. R. In vivo imaging of membrane-associated glycans in developing zebrafish. *Science* **2008**, *320*, 664-667.

(139) Mbua, N. E.; Flanagan-Steet, H.; Johnson, S.; Wolfert, M. A.; Boons, G. J.; Steet, R. Abnormal accumulation and recycling of glycoproteins visualized in Niemann-Pick type C cells using the chemical reporter strategy. *Proc. Natl. Acad. Sci. U.S.A.* **2013**, *110*, 10207-10212.

(140) Hang, H. C.; Wilson, J. P.; Charron, G. Bioorthogonal chemical reporters for analyzing protein lipidation and lipid trafficking. *Acc. Chem. Res.* **2011**, *44*, 699-708.

(141) Kostiuk, M. A.; Corvi, M. M.; Keller, B. O.; Plummer, G.; Prescher, J. A.; Hangauer, M. J.; Bertozzi, C. R.; Rajaiah, G.; Falck, J. R.; Berthiaume, L. G. Identification of palmitoylated mitochondrial proteins using a bio-orthogonal azido-palmitate analogue. *FASEB J.* **2008**, *22*, 721-732.

(142) Heal, W. P.; Jovanovic, B.; Bessin, S.; Wright, M. H.; Magee, A. I.; Tate, E. W. Bioorthogonal chemical tagging of protein cholesterylation in living cells. *Chem. Commun.* **2011**, *47*, 4081-4083.

(143) Hsu, T. L.; Hanson, S. R.; Kishikawa, K.; Wang, S. K.; Sawa, M.; Wong, C. H. Alkynyl sugar analogs for the labeling and visualization of glycoconjugates in cells. *Proc. Natl. Acad. Sci.* **2007**, *104*, 2614-2619.

(144) Huang, H. W.; Chen, C. H.; Lin, C. H.; Wong, C. H.; Lin, K. I. B-cell maturation antigen is modified by a single N-glycan chain that modulates ligand binding and surface retention. *Proc. Natl. Acad. Sci. U.S.A.* **2013**, *110*, 10928-10933.

(145) Anderson, C. T.; Wallace, I. S.; Somerville, C. R. Metabolic click-labeling with a fucose analog reveals pectin delivery, architecture, and dynamics in Arabidopsis cell walls. *Proc. Natl. Acad. Sci. U.S.A.* **2012**, *109*, 1329-1334.

(146) Liu, Y. C.; Yen, H. Y.; Chen, C. Y.; Chen, C. H.; Cheng, P. F.; Juan, Y. H.; Khoo, K. H.; Yu, C. J.; Yang, P. C.; Hsu, T. L.; Wong, C. H. Sialylation and fucosylation of epidermal growth factor receptor suppress its dimerization and activation in lung cancer cells. *Proc. Natl. Acad. Sci. U.S.A.* **2011**, *108*, 11332-11337.

(147) Charron, G.; Li, M. M.; MacDonald, M. R.; Hang, H. C. Prenylome profiling reveals S-farnesylation is crucial for membrane targeting and antiviral activity of ZAP long-isoform. *Proc. Natl. Acad. Sci. U.S.A.* **2013**, *110*, 11085-11090.

(148) Martin, B. R.; Wang, C.; Adibekian, A.; Tully, S. E.; Cravatt, B. F. Global profiling of dynamic protein palmitoylation. *Nat. Methods* **2012**, *9*, 84-89.

(149) Niederwieser, A.; Spate, A. K.; Nguyen, L. D.; Jungst, C.; Reutter, W.; Wittmann, V. Two-color glycan labeling of live cells by a combination of Diels-Alder and click chemistry. *Angew. Chem. Int. Ed.* **2013**, *52*, 4265-4268.

(150) Stockmann, H.; Neves, A. A.; Stairs, S.; Brindle, K. M.; Leeper, F. J. Exploring isonitrile-based click chemistry for ligation with biomolecules. *Org. Biomol. Chem.* **2011**, *9*, 7303-7305.

(151) Wainman, Y. A.; Neves, A. A.; Stairs, S.; Stockmann, H.; Ireland-Zecchini, H.; Brindle, K. M.; Leeper, F. J. Dual-sugar imaging using isonitrile and azido-based click chemistries. *Org. Biomol. Chem.* **2013**, *11*, 7297-7300.

(152) Stairs, S.; Neves, A. A.; Stockmann, H.; Wainman, Y. A.; Ireland-Zecchini, H.; Brindle, K. M.; Leeper, F. J. Metabolic glycan imaging by isonitrile-tetrazine click chemistry. *ChemBioChem* **2013**, *14*, 1063-1067.

(153) Han, M. J.; Xiong, D. C.; Ye, X. S. Enabling Wittig reaction on site-specific protein modification. *Chem. Commun.* **2012**, *48*, 11079-11081.

(154) Lum, K. M.; Xavier, V. J.; Ong, M. J.; Johannes, C. W.; Chan, K. P. Stabilized Wittig olefination for bioconjugation. *Chem. Commun.* **2013**, *49*, 11188-11190.

(155) Rossin, R.; Lappchen, T.; van den Bosch, S. M.; Laforest, R.; Robillard, M. S. Diels-Alder reaction for tumor pretargeting: *in vivo* chemistry can boost tumor radiation dose compared with directly labeled antibody. *J. Nucl. Med.* **2013**, *54*, 1989-1995.

(156) Vugts, D. J.; Vervoort, A.; Stigter-van Walsum, M.; Visser, G. W.; Robillard, M. S.; Versteegen, R. M.; Vulders, R. C.; Herscheid, J. K.; van Dongen, G. A. Synthesis of phosphine and antibody-azide probes for in vivo Staudinger ligation in a pretargeted imaging and therapy approach. *Bioconjug. Chem.* **2011**, *22*, 2072-2081.

(157) Hausner, S. H.; Carpenter, R. D.; Bauer, N.; Sutcliffe, J. L. Evaluation of an integrin αvβ6-specific peptide labeled with [18F]fluorine by copper-free, strain-promoted click chemistry. *Nucl. Med. Biol.* **2013**, *40*, 233-239.

(158) Bouvet, V.; Wuest, M.; Wuest, F. Copper-free click chemistry with the short-lived positron emitter fluorine-18. *Org. Biomol. Chem.* **2011**, *9*, 7393-7399.

(159) Carlson, J. C. T.; Meimetis, L. G.; Hilderbrand, S. A.; Weissleder, R. BODIPY-tetrazine derivatives as superbright bioorthogonal turn-on probes. *Angew. Chem. Int. Ed.* **2013**, *52*, 6917-6920.

(160) Friscourt, F.; Fahrni, C. J.; Boons, G. J. A fluorogenic probe for the catalyst-free detection of azide-tagged molecules. *J. Am. Chem. Soc.* **2012**, *134*, 18809-18815.

(161) Jewett, J. C.; Bertozzi, C. R. Synthesis of a fluorogenic cyclooctyne activated by Cu-free click chemistry. *Org. Lett.* **2011**, *13*, 5937-5939.

(162) Devaraj, N. K.; Hilderbrand, S.; Upadhyay, R.; Mazitschek, R.; Weissleder, R. Bioorthogonal turn-on probes for imaging small molecules inside living cells. *Angew. Chem. Int. Ed.* **2010**, *49*, 2869-2872.

(163) Shieh, P.; Hangauer, M. J.; Bertozzi, C. R. Fluorogenic azidofluoresceins for biological imaging. *J. Am. Chem. Soc.* **2012**, *134*, 17428-17431.

(164) Herner, A.; Nikic, I.; Kallay, M.; Lemke, E. A.; Kele, P. (2013) A new family of bioorthogonally applicable fluorogenic labels. *Org. Biomol. Chem.* **2013**, *11*, 3297-3306.

(165) Yang, J.; Karver, M. R.; Li, W.; Sahu, S.; Devaraj, N. K. Metal-catalyzed one-pot synthesis of tetrazines directly from aliphatic nitriles and hydrazine. *Angew. Chem. Int. Ed.* **2012**, *51*, 5222-5225.

(166) Yao, J. Z.; Uttamapinant, C.; Poloukhtine, A.; Baskin, J. M.; Codelli, J. A.; Sletten, E. M.; Bertozzi, C. R.; Popik, V. V.; Ting, A. Y. Fluorophore targeting to cellular proteins via enzyme-mediated azide ligation and strain-promoted cycloaddition. *J. Am. Chem. Soc.* **2012**, *134*, 3720-3728.

(167) Lin, F. L.; Hoyt, H. M.; van Halbeek, H.; Bergman, R. G.; Bertozzi, C. R. Mechanistic investigation of the Staudinger ligation. *J. Am. Chem. Soc.* **2005**, *127*, 2686-2695.

(168) Majkut, P.; Bohrsch, V.; Serwa, R.; Gerrits, M.; Hackenberger, C. P. Site-specific modification of proteins by the Staudinger-phosphite reaction. *Methods Mol. Biol.* **2012**, *794*, 241-249.

(169) Hangauer, M. J.; Bertozzi, C. R. A FRET-based fluorogenic phosphine for live-cell imaging with the Staudinger ligation. *Angew. Chem. Int. Ed.* **2008**, *47*, 2394-2397.

(170) Saxon, E.; Armstrong, J. I.; Bertozzi, C. R. A "traceless" Staudinger ligation for the chemoselective synthesis of amide bonds. *Org. Lett*. **2000**, *2*, 2141-2143.

(171) Soellner, M. B.; Tam, A.; Raines, R. T. Staudinger ligation of peptides at non-glycyl residues. *J. Org. Chem.* **2006**, *71*, 9824-9830.

(172) Tam, A.; Raines, R. T. Protein engineering with the traceless Staudinger ligation. *Method Enzymol.* **2009**, *462*, 25-44.

(173) Ahad, A. M.; Jensen, S. M.; Jewett, J. C. A traceless Staudinger reagent to deliver diazirines. *Org. Lett.* **2013**, *15*, 5060-5063.

(174) Bertran-Vicente, J.; Hackenberger, C. P. A supramolecular peptide synthesizer. *Angew. Chem. Int. Ed.* **2013**, *52*, 6140-6142.

(175) DeForest, C. A.; Anseth, K. S. Cytocompatible click-based hydrogels with dynamically tunable properties through orthogonal photoconjugation and photocleavage reactions. *Nat. Chem.* **2011**, *3*, 925-931.

(176) Kafri, R.; Levy, J.; Ginzberg, M. B.; Oh, S.; Lahav, G.; Kirschner, M. W. Dynamics extracted from fixed cells reveal feedback linking cell growth to cell cycle. *Nature* **2013**, *494*, 480-483.

(177) Chakraborty, A.; Wang, D.; Ebright, Y. W.; Korlann, Y.; Kortkhonjia, E.; Kim, T.; Chowdhury, S.; Wigneshweraraj, S.; Irschik, H.; Jansen, R.; Nixon, B. T.; Knight, J.; Weiss, S.; Ebright, R. H. Opening and closing of the bacterial RNA polymerase clamp. *Science* **2012**, *337*, 591-595.

(178) Liang, G.; Ren, H.; Rao, J. A biocompatible condensation reaction for controlled assembly of nanostructures in living cells. *Nat. Chem.* **2010**, *2*, 54-60.

(179) Nguyen, D. P.; Elliott, T.; Holt, M.; Muir, T. W.; Chin, J. W. Genetically encoded 1,2-aminothiols facilitate rapid and site-specific protein labeling via a bio-orthogonal cyanobenzothiazole condensation. *J. Am. Chem. Soc.* **2011**, *133*, 11418-11421.

(180) Lin, Y. A.; Boutureira, O.; Lercher, L.; Bhushan, B.; Paton, R. S.; Davis, B. G. Rapid cross-metathesis for reversible protein modifications via chemical access to Se-allyl-selenocysteine in proteins. *J. Am. Chem. Soc.* **2013**, *135*, 12156-12159.

(181) Sletten, E. M.; Bertozzi, C. R. A bioorthogonal quadricyclane ligation. *J. Am. Chem. Soc.* **2011**, *133*, 17570-17573.

(182) Ho, C. M.; Zhang, J. L.; Zhou, C. Y.; Chan, O. Y.; Yan, J. J.; Zhang, F. Y.; Huang, J. S.; Che, C. M. A water-soluble ruthenium glycosylated porphyrin catalyst for carbenoid transfer reactions in aqueous media with applications in bioconjugation reactions. *J. Am. Chem. Soc.* **2010**, *132*, 1886-1894.

(183) Lin, Y. A.; Chalker, J. M.; Davis, B. G. Olefin cross-metathesis on proteins: investigation of allylic chalcogen effects and guiding principles in metathesis partner selection. *J. Am. Chem. Soc.* **2010**, *132*, 16805-16811.

(184) Chalker, J. M.; Wood, C. S.; Davis, B. G. A convenient catalyst for aqueous and protein Suzuki-Miyaura cross-coupling. *J. Am. Chem. Soc.* **2009**, *131*, 16346-16347.

(185) Li, N.; Lim, R. K.; Edwardraja, S.; Lin, Q. Copper-free Sonogashira cross-coupling for functionalization of alkyne-encoded proteins in aqueous medium and in bacterial cells. *J. Am. Chem. Soc.* **2011**, *133*, 15316-15319.

(186) Yusop, R. M.; Unciti-Broceta, A.; Johansson, E. M.; Sanchez-Martin, R. M.; Bradley, M. Palladium-mediated intracellular chemistry. *Nat. Chem.* **2011**, *3*, 239-243.

(187) Spicer, C. D.; Triemer, T.; Davis, B. G. Palladium-mediated cell-surface labeling. *J. Am. Chem. Soc.* **2012**, *134*, 800-803.

(188) Lercher, L.; McGouran, J. F.; Kessler, B. M.; Schofield, C. J.; Davis, B. G. DNA modification under mild conditions by Suzuki-Miyaura cross-coupling for the generation of functional probes. *Angew. Chem. Int. Ed.* **2013**, *52*, 10553-10558.

(189) Li, J.; Lin, S.; Wang, J.; Jia, S.; Yang, M.; Hao, Z.; Zhang, X.; Chen, P. R. Ligand-free palladium-mediated site-specific protein labeling inside gram-negative bacterial pathogens. *J. Am. Chem. Soc.* **2013**, *135*, 7330-7338.

(190) Riggsbee, C. W.; Deiters, A. Recent advances in the photochemical control of protein function. *Trends Biotechnol.* **2010**, *28*, 468-475.

(191) Pauloehrl, T.; Delaittre, G.; Winkler, V.; Welle, A.; Bruns, M.; Borner, H. G.; Greiner, A. M.; Bastmeyer, M.; Barner-Kowollik, C. Adding spatial control to click chemistry: phototriggered Diels-Alder surface (bio)functionalization at ambient temperature. *Angew. Chem. Int. Ed.* **2012**, *51*, 1071-1074.

(192) Arumugam, S.; Popik, V. V. Light-induced hetero-Diels-Alder cycloaddition: a facile and selective photoclick reaction. *J. Am. Chem. Soc.* **2011**, *133*, 5573-5579.

(193) Adzima, B. J.; Tao, Y. H.; Kloxin, C. J.; DeForest, C. A.; Anseth, K. S.; Bowman, C. N. Spatial and temporal control of the alkyne-azide cycloaddition by photoinitiated Cu(II) reduction. *Nat. Chem.* **2011**, *3*, 256-259.

(194) Wang, Y.; Song, W.; Hu, W. J.; Lin, Q. Fast alkene functionalization in vivo by Photoclick chemistry: HOMO lifting of nitrile imine dipoles. *Angew. Chem. Int. Ed.* **2009**, *48*, 5330-5333.

(195) Poloukhtine, A. A.; Mbua, N. E.; Wolfert, M. A.; Boons, G. J.; Popik, V. V. Selective labeling of living cells by a photo-triggered click reaction. *J. Am. Chem. Soc.* **2009**, *131*, 15769-15776.

(196) Deiters, A. Principles and applications of the photochemical control of cellular processes. *ChemBioChem* **2010**, *11*, 47-53.

(197) Lim, R. K.; Lin, Q. Photoinducible bioorthogonal chemistry: a spatiotemporally controllable tool to visualize and perturb proteins in live cells. *Acc. Chem. Res.* **2011**, *44*, 828-839.

(198) McNitt, C. D.; Popik, V. V. Photochemical generation of oxa-dibenzocyclooctyne (ODIBO) for metal-free click ligations. *Org. Biomol. Chem.* **2012**, *10*, 8200-8202.

(199) Yu, Z.; Ohulchanskyy, T. Y.; An, P.; Prasad, P. N.; Lin, Q. Fluorogenic, two-photon triggered photoclick chemistry in live mammalian cells. *J. Am. Chem. Soc.* **2013**, *135*, 16766–16769.

(200) Li, Q.; Dong, T.; Liu, X.; Lei, X. A bioorthogonal ligation enabled by click cycloaddition of o-quinolinone quinone methide and vinyl thioether. *J. Am. Chem. Soc.* **2013**, *135*, 4996–4999.

(201) An, P.; Yu, Z. P.; Lin, Q. Design of oligothiophene-based tetrazoles for laser-triggered photoclick chemistry in living cells. *Chem. Commun.* **2013**, *49*, 9920-9922.

(202) Chen, W. X.; Wang, D. Z.; Dai, C. F.; Hamelberg, D.; Wang, B. H. Clicking 1,2,4,5-tetrazine and cyclooctynes with tunable reaction rates. *Chem. Commun.* **2012**, *48*, 1736-1738.

(203) Liang, Y.; Mackey, J. L.; Lopez, S. A.; Liu, F.; Houk, K. N. Control and design of mutual orthogonality in bioorthogonal cycloadditions. *J. Am. Chem. Soc.* **2012**, *134*, 17904-17907.

(204) Karver, M. R.; Weissleder, R.; Hilderbrand, S. A. Bioorthogonal reaction pairs enable simultaneous, selective, multi-target imaging. *Angew. Chem. Int. Ed.* **2012**, *51*, 920-922.

(205) Willems, L. I.; Li, N.; Florea, B. I.; Ruben, M.; van der Marel, G. A.; Overkleeft, H. S. Triple bioorthogonal ligation strategy for simultaneous labeling of multiple enzymatic activities. *Angew. Chem. Int. Ed.* **2012**, *51*, 4431-4434.

(206) Ess, D. H.; Jones, G. O.; Houk, K. N. Transition states of strain-promoted metal-free click chemistry: 1,3-dipolar cycloadditions of phenyl azide and cyclooctynes. *Org. Lett.* **2008**, *10*, 1633-1636.

(207) Schoenebeck, F.; Ess, D. H.; Jones, G. O.; Houk, K. N. Reactivity and regioselectivity in 1,3-dipolar cycloadditions of azides to strained alkynes and alkenes: a computational study. *J. Am. Chem. Soc.* **2009**, *131*, 8121-8133.

(208) Kamber, D. N.; Nazarova, L. A.; Liang, Y.; Lopez, S. A.; Patterson, D. M.; Shih, H. W.; Houk, K. N.; Prescher, J. A. Isomeric cyclopropenes exhibit unique bioorthogonal reactivities. *J. Am. Chem. Soc.* **2013**, *135*, 13680-13683.

(209) Gold, B.; Dudley, G. B.; Alabugin, I. V. Moderating strain without sacrificing reactivity: design of fast and tunable noncatalyzed alkyne-azide cycloadditions via stereoelectronically controlled transition state stabilization. *J. Am. Chem. Soc.* **2013**, *135*, 1558-1569.

(210) Kolodych, S.; Rasolofonjatovo, E.; Chaumontet, M.; Nevers, M. C.; Creminon, C.; Taran, F. Discovery of Chemoselective and Biocompatible Reactions Using a High-Throughput Immunoassay Screening. *Angew. Chem. Int. Ed.* **2013**, *52*, 12056–12060.

CHAPTER 2: Metabolic labeling of *Toxoplasma gondii* proteins with unnatural sugars

2.1 Introduction

Glycosylation is a ubiquitous post-translational modification that is critically important for diverse cellular functions, including protein folding and sorting, receptor interactions and signal transduction [1,2]. Complex carbohydrates (glycans) are built off polypeptide chains by the actions of numerous glycosyltransferases (enzymes that transfer activated nucleotide sugars to growing glycan chains or underlying protein/lipid units). Glycan structures can be further modified by glycosidases (enzymes that trim sugars from larger structures) or enzymes that add sulfate or acetyl groups to the monosaccharide units. Several proteins synthesized in the rough ER are modified by N-linked glycans (typically attached to asparagine residues), while others are modified via O-linked glycans (attached to serine, threonine, tyrosine, hydroxylysine, or hydroxyproline residues). Some extracellular proteins also comprise glycosylphosphatidylinositol (GPI) anchors, carbohydrate-containing groups that anchor the proteins into the external leaflet of the plasma membrane [3,4]. In recent years, numerous intracellular proteins relevant to cell signaling, metabolism, and gene expression have been discovered to harbor β-O-GlcNAc residues [5,6].

The prevalence and central roles of protein glycosylation are only beginning to be appreciated in apicomplexan pathogens such as *Toxoplasma gondii*. *T. gondii* is an obligate intracellular parasite, capable of infecting all nucleated cell types in diverse

warm-blooded animals and birds [7]. *Toxoplasma* tachyzoites are the rapidly proliferating form of the parasite which cause acute stage infection. This form, as well as other life cycle stages, contains characteristic eukaryotic organelles including a nucleus, endoplasmic reticulum (ER), Golgi apparatus, mitochondrion and plastid as well as specialized membrane-bound secretory organelles termed micronemes, rhoptries and dense granules. Tachyzoites are bounded by a tri-laminar pellicle consisting of a plasma membrane and underlying inner membrane complex (IMC) and the tachyzoite surface is particularly enriched in GPI-linked surface proteins such as TgSAG1 [8]. In order for *Toxoplasma* to survive and replicate, extracellular parasites must actively invade host cells in infected organisms, including humans. Invasion of host cells begins with the initial attachment of GPI-anchored surface antigens on *Toxoplasma* to glycans on the host cell [9]. Secretion from micronemes and rhoptries is required for parasite motility, host cell invasion and establishment of a non-phagosomal membrane-bound parasitophorous vacuole [10,11]. Within the vacuole, tachyzoites undergo an asexual reproduction by endodyogeny, a process in which two daughter cells are produced inside a mother cell. In the absence of a host cell, the parasite is not able to replicate and will not survive. Trafficking of proteins to the parasite surface and to the microneme, rhoptry and dense granule compartments occurs via post-Golgi sorting [12-14] and is likely to require protein glycosylation.

We have an incomplete understanding of glycan modification in apicomplexan parasites due, in part, to a lack of tools for studying these non-templated biopolymers in their native contexts [15]. Lectins (receptor proteins that bind to glycans) [16,17] and glycan-specific antibodies [18] are available to survey parasite glycans, but these reagents

often bind multiple types of structures and thus provide limited information on the types of glycans present. Additionally, many well-known reagents available for studies of mammalian glycosylation (including PNGaseF and other glycosidases) may not recognize unique glycan motifs produced by the parasite. Early reports suggested that GPI anchors are the predominant form of carbohydrate modification of *Toxoplasma* proteins [18-21]. However, there is now ample evidence that *Toxoplasma* proteins can be modified by both N- and O-linked pathways [18,22-27]. Intracellular Toxoplasma proteins decorated with β-O-GlcNAc residues have also been identified [27,28]. Curiously, the predominant glycans in *Toxoplasma* tachyzoites are unusual oligomannosidic ($Man_{5-8}(GlcNAc)_2$) and paucimannosidic ($Man_{3-4}(GlcNAc)_2$) sugars, which are rarely present on mature vertebrate glycoproteins [29]. Significantly, tunicamycin-treated parasites exhibited reduced motility, host cell invasion, and growth, suggesting that parasite glycosylation may represent a significant future drug target [17,27].

Two reports have identified glycosylated proteins in *Toxoplasma* tachyzoites using lectin affinity chromatography and mass spectrometry (MS). In the first study, a Concanavalin A (ConA) column was used to enrich and identify putative glycoproteins, including cytoskeletal proteins (TgMyoA, TgMyoB/C, TgIMC2, actin, tubulin and TgGAP50), secreted proteins (the microneme proteins TgAMA1 and TgPLP1 and several rhoptry proteins) and likely components of the membrane trafficking machinery (putative sortilin and Sec61 orthologs) [17]. More recently, a set of 132 proteins that are likely modified by glycans was identified by serial lectin affinity chromatography (SLAC) and MS [16]. This glycoproteome included surface antigens, microneme, dense granule and

rhoptry components, heat shock proteins, as well as a number of hypothetical proteins. The lectins ConA, wheat germ agglutinin (WGA) and Jacalin were used individually and in serial purification protocols to isolate glycoproteins in this study. While some glycoproteins bound to all three lectins, others were only retained by one or two of the lectins.

As noted above, although lectins can be used to profile some aspects of parasite glycosylation, these reagents do not provide a complete picture of glycan biosynthesis. This complementary information can be captured using the bioorthogonal chemical reporter strategy [30-32]. In this approach, a monosaccharide substrate is modified with a functional group (the reporter) that is chemically inert in biological systems. Upon administration to cells, the modified sugar is processed similarly to its native counterpart and integrated into cellular glycans. Finally, the labeled glycans are reacted with a detectable probe using highly selective, covalent chemistries. Depending on the nature of the probe, this strategy permits both the visualization of glycans and/or their enrichment from complex mixtures for subsequent analyses. In this manuscript, we utilize a bioorthogonal chemical reporter strategy to label and profile glycoproteins in living *Toxoplasma* tachyzoites. This approach identified known and novel glycoproteins in the parasite and, importantly, demonstrated that tachyzoites can metabolize and incorporate sugar derivatives into cellular structures in the absence of host cell machinery. Many of the glycoproteins appear to be modified by O-linked structures, suggesting an important role for these conjugates in the parasite life cycle.

2.2 Extracellular *Toxoplasma* tachyzoites metobilze and incorporate unnatural sugars

We utilized the bioorthogonal chemical reporter strategy to label glycans in living *Toxoplasma* tachyzoites. In this technique, peracetylated azido or alkynyl sugars are metabolized by cells and incorporated into glycan structures (Figure 2-1A). The acetyl groups present on each unnatural sugar facilitate cellular uptake, and the free sugars are liberated by the actions of esterases. Following installation into protein targets, the unique azido or alkynyl groups can be covalently reacted with probes for visualization or purification [30]. Prior to this report, the chemical reporter strategy had not been used to observe glycosylation or other metabolic processes in *Toxoplasma* tachyzoites. Labeling parasites within a host cell presented a challenge, as the unnatural sugars had to traverse both the host cell and parasite plasma membranes in order to reach the tachyzoite cytoplasm. Indeed, we were unable to robustly detect the unnatural sugar labels in intracellular tachyzoites even at high doses of sugar. This was likely due to the action of host cell esterases and competition with the host cell metabolic machinery, preventing the delivery of sugar into the tachyzoite cytoplasm. Since *Toxoplasma* tachyzoites are most metabolically active when they are intracellular, we labeled extracellular *Toxoplasma* tachyzoites in established ionic conditions that mimic intracellular cues (intracellular Endo Buffer) [34].

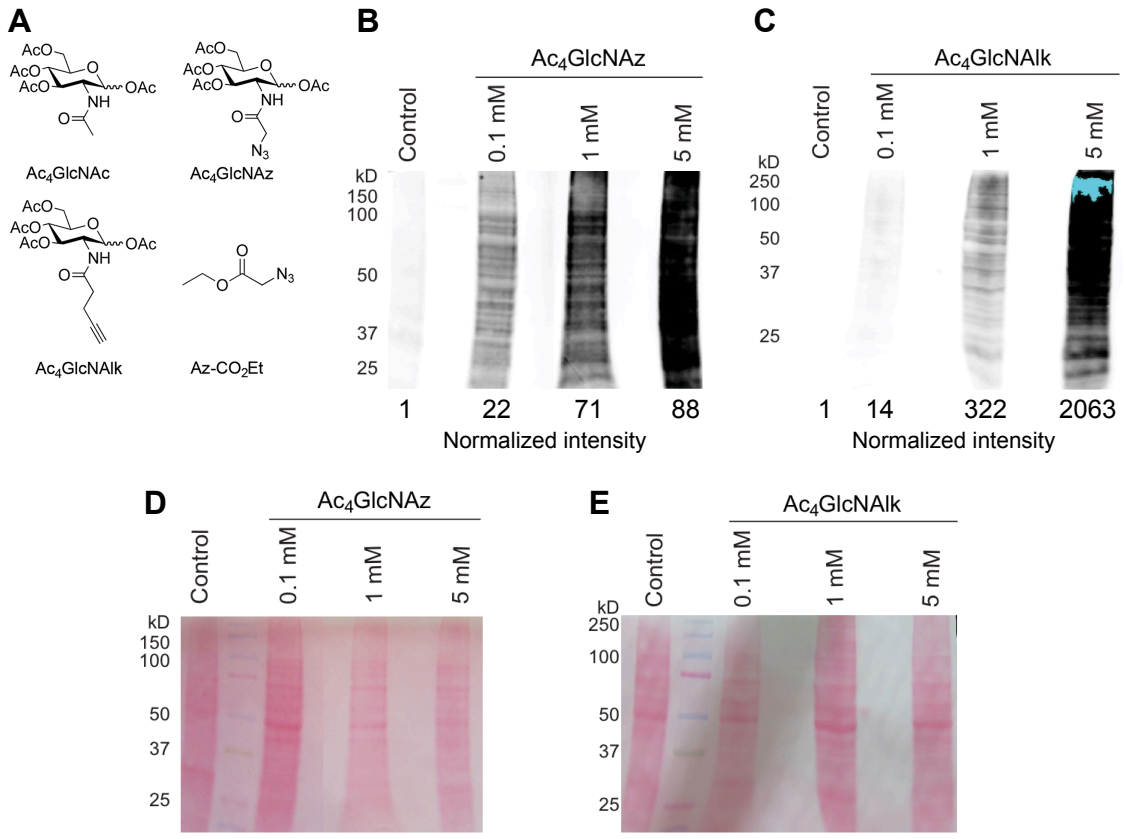

Figure 2-1 *Toxoplasma* tachyzoites metabolize unnatural sugars in a dose-dependent manner. (A) Structures of peracetylated N-acetylglucosamine ($Ac_4GlcNAc$) and the corresponding alkynyl ($Ac_4GlcNAlk$) and azido ($Ac_4GlcNAz$) analogs used in metabolic labeling studies. The acetyl groups facilitate sugar uptake into cells and are removed by the action of non-specific esterases in the cytoplasm. An azide-functionalized acyl chain ($Az\text{-}CO_2Et$) used in various control experiments is also pictured. The azide and alkyne functional groups can be detected using bioorthogonal "click" chemistries. (B) *Toxoplasma* tachyzoites incorporate $Ac_4GlcNAz$ in a dose-dependent manner. Parasites were incubated with unnatural sugar (0.1-5 mM) or the control sugar $Ac_4GlcNAc$ for 8 hours, lysed, and reacted with a biotin-alk tag via "click" chemistry. The labeled proteins were separated via gel electrophoresis and detected via immunoblot with streptavidin. (C) *Toxoplasma* tachyzoites incorporate $Ac_4GlcNAlk$ in a dose-dependent manner. Parasites were incubated with unnatural sugar (0.1-5 mM) or the control sugar $Ac_4GlcNAc$ for 8 hours, lysed, and reacted with a biotin-az tag via "click" chemistry. (D) Equivalent protein loading for the blot pictured in Figure 2-1B was confirmed via staining with Ponceau S. (E) Equivalent protein loading for the blot pictured in Figure 2-1C was confirmed via staining with Ponceau S.

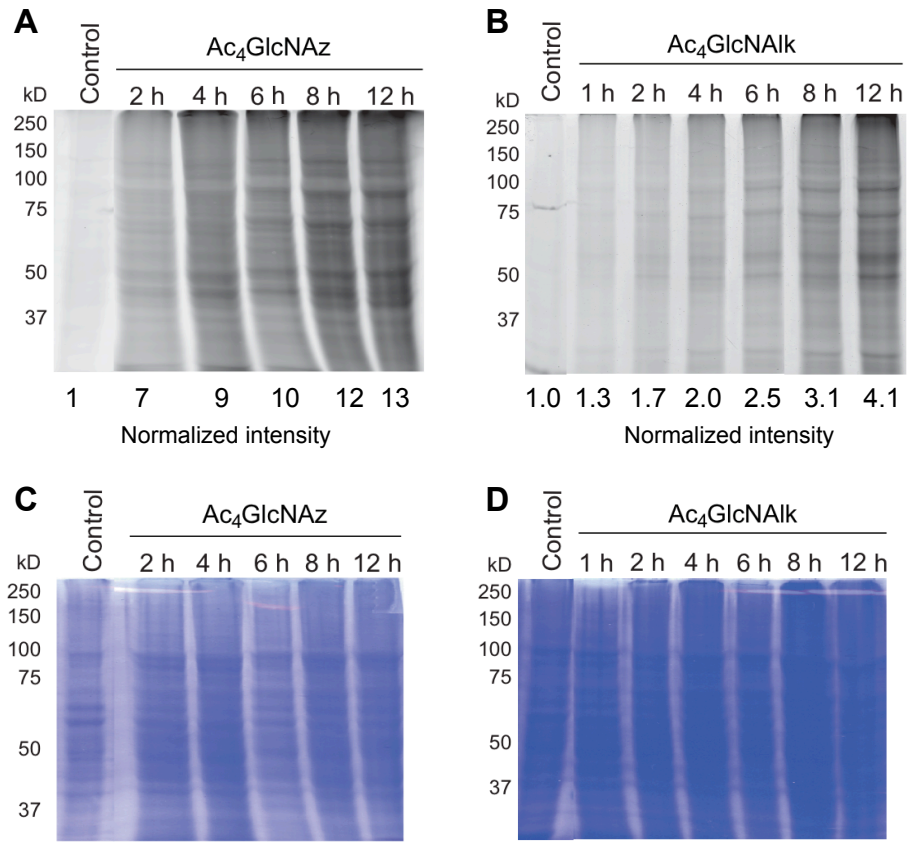

Figure 2-2 *Toxoplasma* tachyzoites metabolize unnatural sugars in a time-dependent manner. (A) *Toxoplasma* tachyzoites incorporate Ac_4GlcNAz in a time-dependent manner. Parasites were incubated with Ac_4GlcNAz (1 mM) or the control sugar Ac_4GlcNAc (1 mM) for 2-12 h hours, lysed, and reacted with a rhodamine-alkyne probe. Labeled proteins were separated via gel electrophoresis and analyzed via in-gel fluorescence. (B) *Toxoplasma* tachyzoites incorporate Ac_4GlcNAlk in a time-dependent manner. Parasites were incubated with Ac_4GlcNAlk (1 mM) or the control sugar Ac_4GlcNAc (1 mM) for 1-12 h hours, lysed, and reacted with a rhodamine-azide probe. Labeled proteins were separated via gel electrophoresis and analyzed via in-gel fluorescence. (C) Equivalent protein loading for the gel pictured in Figure 2-2A was confirmed via staining with Coomassie Brilliant Blue. (D) Equivalent protein loading for the gel pictured in Figure 2-2B was confirmed via staining with Coomassie Brilliant Blue.

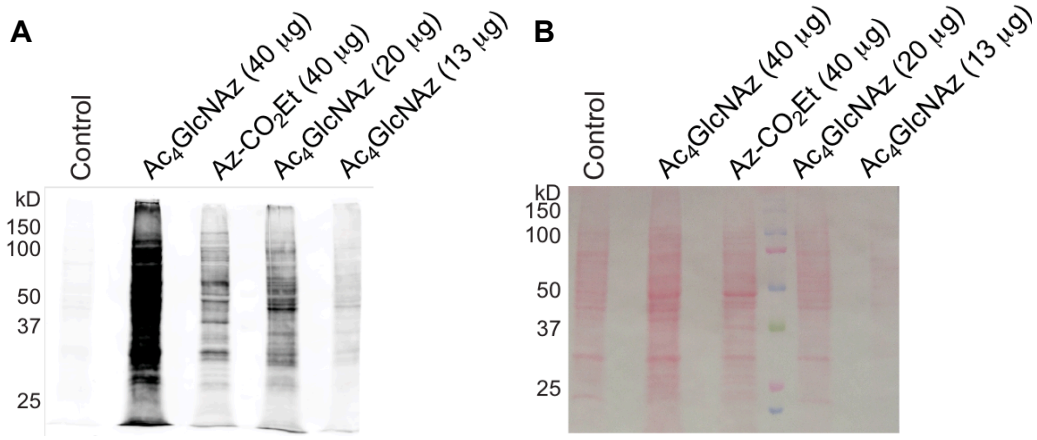

Figure 2-3 $Ac_4GlcNAz$ treatment reveals a unique glycoprotein fingerprint. (A) Parasites were incubated with $Ac_4GlcNAz$ (1 mM), $Ac_4GlcNAc$ (1 h) or a non-sugar probe ($Az\text{-}CO_2Et$) for 8 hours, lysed, and reacted with a biotin-alk tag. Labeled proteins were analyzed via immunoblot as in Figure 2-1. (B) Equivalent protein loading for the blot pictured in Figure 2-3A was confirmed via staining with Ponceau S.

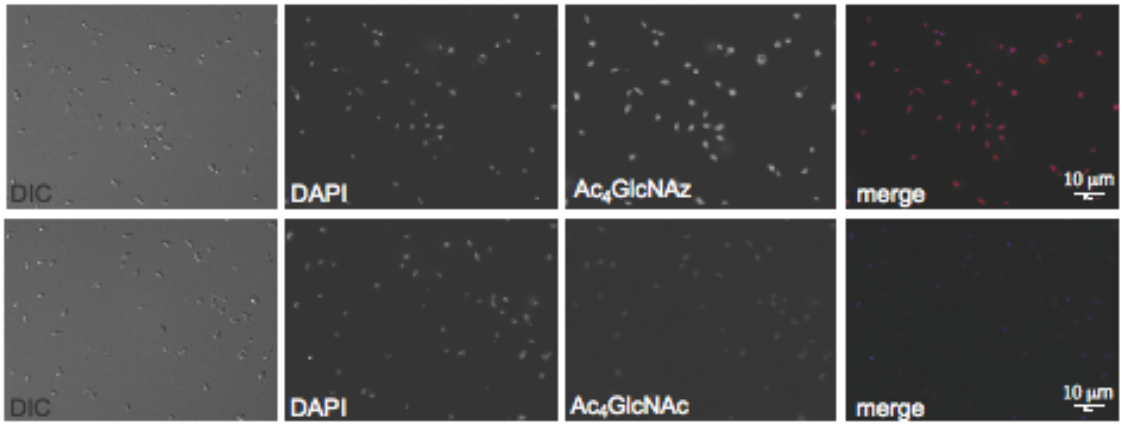

Figure 2-4 Labeling of *Toxoplasma* tachyzoites with unnatural sugars in DMEM media. Parasites were incubated with $Ac_4GlcNAz$ (1 mM) or $Ac_4GlcNAc$ (1 mM) for 8 h, prior to fixation with 4% paraformaldehyde in PBS for 15 min at rt Subsequent reaction with biotin-alk and incubation with streptavidin-AlexaFluor594 enabled fluorescence detection of modified glycoconjugates.

Azido and alkynyl variants of N-acetylglucosamine (Ac_4GlcNAz and Ac_4GlcNAlk, Figure 2-1A) have been used to target O-linked and O-GlcNAcylated proteins in mammalian cells as well as in bacteria [43], and have the potential to target N-linked structures as well [44]. When these reagents were administered to extracellular *Toxoplasma* tachyzoites, they labeled similar subsets of proteins, suggesting that the distinct chemical reporters do not influence incorporation of the monosaccharide (Figures 2-1B, 2-1C). Importantly, tachyzoites incorporate Ac_4GlcNAz and Ac_4GlcNAlk in a concentration and time dependent manner (Figures 2-1B, 2-1C, 2-2A, 2-2B). To investigate whether the N-acyl sugar modifications were simply removed from the sugar scaffolds and appended to proteins, we synthesized N-azidoacetyl and N-alkynylacetyl units and examined their incorporation into *Toxoplasma* proteins (Figure 2-3A). Since the incorporation pattern is distinct, we believe that the bulk of the proteins that are detected are modified by intact unnatural sugars rather than a catabolic product. Metabolic incorporation was also visualized using fluorescence microscopy. Ac_4GlcNAz-labeled parasites were reacted with biotinylated probes and subsequently stained with streptavidin-conjugated Alexa Fluor 488 (Figure 2-5A). Signal was specific to Ac_4GlcNAz-treated parasites and was most concentrated in the region around the nucleus, perhaps reflecting ER localization. Importantly, Ac_4GlcNAz-treated samples were still able to infect host cells, suggesting that metabolic labeling was tolerated by the parasites (Figures 2-5B).

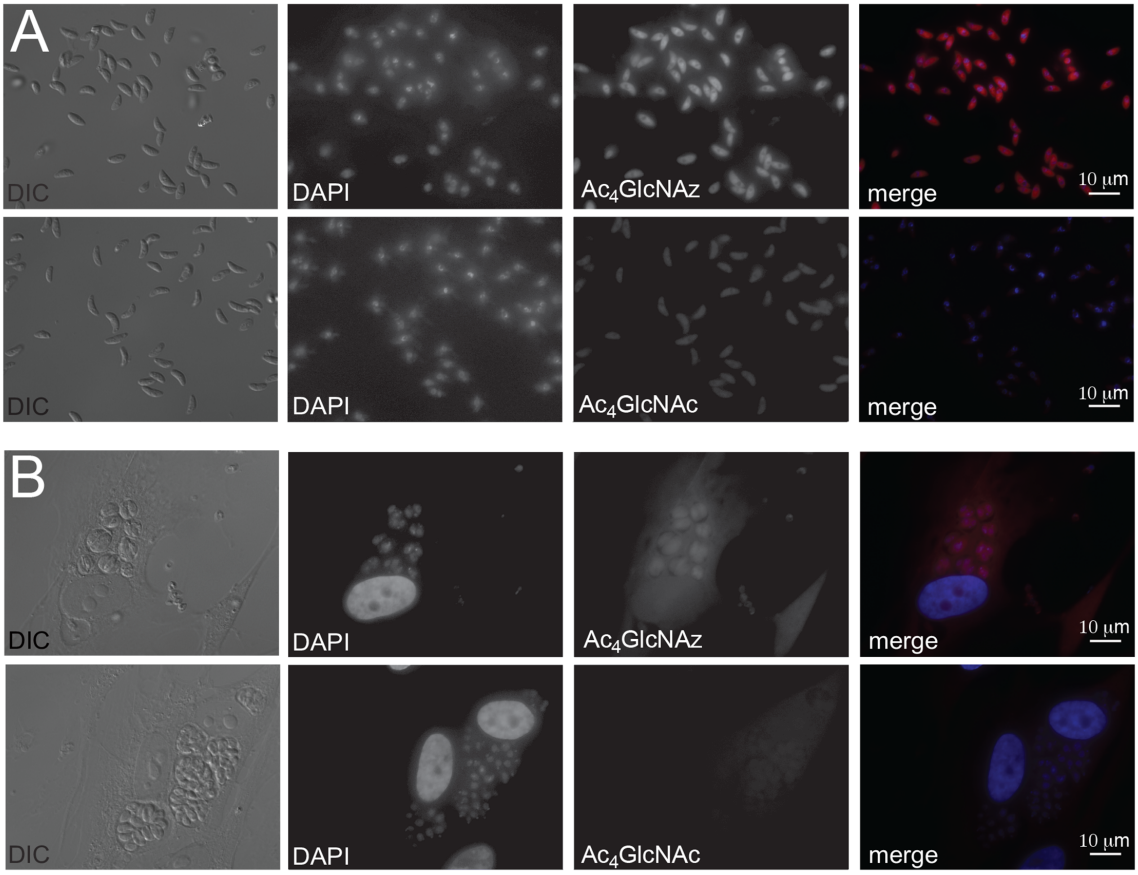

Figure 2-5 Unnatural sugars can be visualized in *Toxoplasma* tachyzoites via fluorescence microscopy. (A) Parasites were incubated with $Ac_4GlcNAz$ (0.5 mM) or $Ac_4GlcNAc$ (0.5 mM) for 8 h, prior to fixation with 4% paraformaldehyde in PBS for 15 min at rt Subsequent reaction with biotin-alk and incubation with streptavidin-AlexaFluor594 enabled fluorescence detection of modified glycoconjugates. (B) $Ac_4GlcNAz$-treated parasites remain viable. Parasites were incubated with $Ac_4GlcNAz$ (250 μM) or $Ac_4GlcNAz$ (250 μM) for 8 h and then added to HFF monolayers. After 36 h, the samples were fixed, labeled, and imaged as in (A).

2.3 Most proteins appear to be modified by O-linked sugars

To elucidate the type of labeled glycans, we first investigated the common carbohydrate cleaving enzyme *N*-glycosidase F (PNGaseF). PNGaseF treatment did not eliminate $Ac_4GlcNAz$-dependent signal in our immunoblot analyses, suggesting that the

majority of the label is not present in N-linked glycans or that the enzyme may not recognize features of carbohydrate modification in *Toxoplasma* (Figures 2-6A). We also examined the effect of tunicamycin treatment on Ac_4GlcNAz-labeled parasites. Tunicamycin blocks the synthesis of all N-linked glycoproteins in vertebrate cells. However, cells must be treated for 24-72 h with this drug to observe an effect and extracellular parasites are not viable for that length of time. We chose to treat host cells with tunicamycin prior to infection with tachyzoites. Parasites were allowed to replicate in treated cells for 24 h, and then were released and subjected to further tunicamycin treatment (extracellularly) in the presence of the unnatural sugars. Minimal reduction in Ac_4GlcNAz-dependent signal was observed in this experiment, indicating that most of the labeled proteins are not N-linked and therefore not susceptible to the drug (Figures 2-6B).

Ac_4GlcNAz does appear to target a second major class of glycans in eukaryotes: O-linked glycans. Boothroyd and coworkers recently reported a *Toxoplasma* line that is deficient in certain mucin-type O-linked glycans. This strain is null for a nucleotide sugar transporter (NST1) relevant to complex glycan biosynthesis (Figures 2-6C). When these parasites were treated with Ac_4GlcNAz, though, no reduction in labeling was observed compared to the complemented strain. While it is not possible to rule out the incorporation of azido sugar into complex mucins, our data suggest that the majority of Ac_4GlcNAz likely targets proteins with simpler O-linked structures or β-O-GlcNAc residues. Attempts to verify the fate of Ac_4GlcNAz by treating lystates with O-GlcNAcase (OGA), an enzyme capable of removing single β-O-GlcNAc residues found on numerous intracellular proteins, were not successful (data not shown). Additionally,

no diminishment in signal was observed with a related recombinant lysosomal hexosaminidase-*f* (Figures 2-7A). However, beta-elimination conditions drastically reduced Ac_4GlcNAz-dependent signal in the parasites, consistent with the label being primarily localized to O-linked structures (Figures 2-7B).

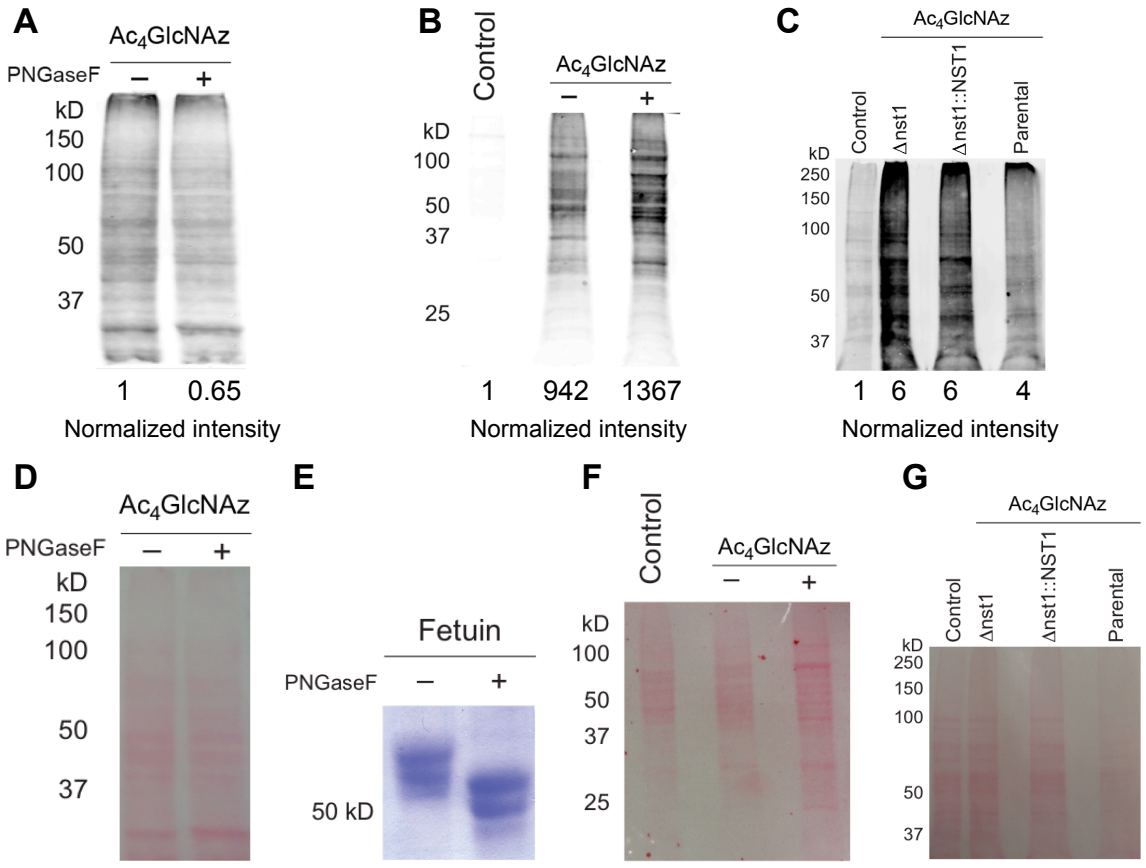

Figure 2-6 N-linked glycans are not a primary target of $Ac_4GlcNAz$ in *Toxoplasma* tachyzoites. (A) Parasites were incubated with $Ac_4GlcNAz$ (1 mM) or $Ac_4GlcNAc$ (1 mM), then lysed and treated with PNGase F. All samples were labeled with biotin-alk and analyzed via immunoblot as in Figure 2-1. (B) Parasites were grown in tunicamycin-treated HFFs for 24 h, then harvested and incubated in Endo Buffer with $Ac_4GlcNAz$ (1 mM) or $Ac_4GlcNAc$ (1 mM) and additional tunicamycin. After 8 h, the parasites were lysed and protein samples were reacted and analyzed via immunoblot as in Figure 2-1. (C) Parasites deficient in a UDP-GlcNAc nucleotide sugar transporter (Δnst1) were treated with $Ac_4GlcNAz$ (1 mM) or $Ac_4GlcNAc$ (1 mM) for 8 h, then lysed and analyzed as in Figure 2-1. The complemented strain (Δnst1::NST1) and parental strain (Me49) were similarly processed and analyzed. (D) Equivalent protein loading for the blot pictured in Figure 2-5A was confirmed via staining with Ponceau S. (E) Fetuin protein was treated with PNGase F. The samples were analyzed via gel electrophoresis and stained with Coomassie Brilliant Blue. (F) Equivalent protein loading for the blot pictured in Figure 2-6B was confirmed via staining with Ponceau S. (G) Equivalent protein loading for the blot pictured in Figure 2-6C was confirmed via staining with Ponceau S.

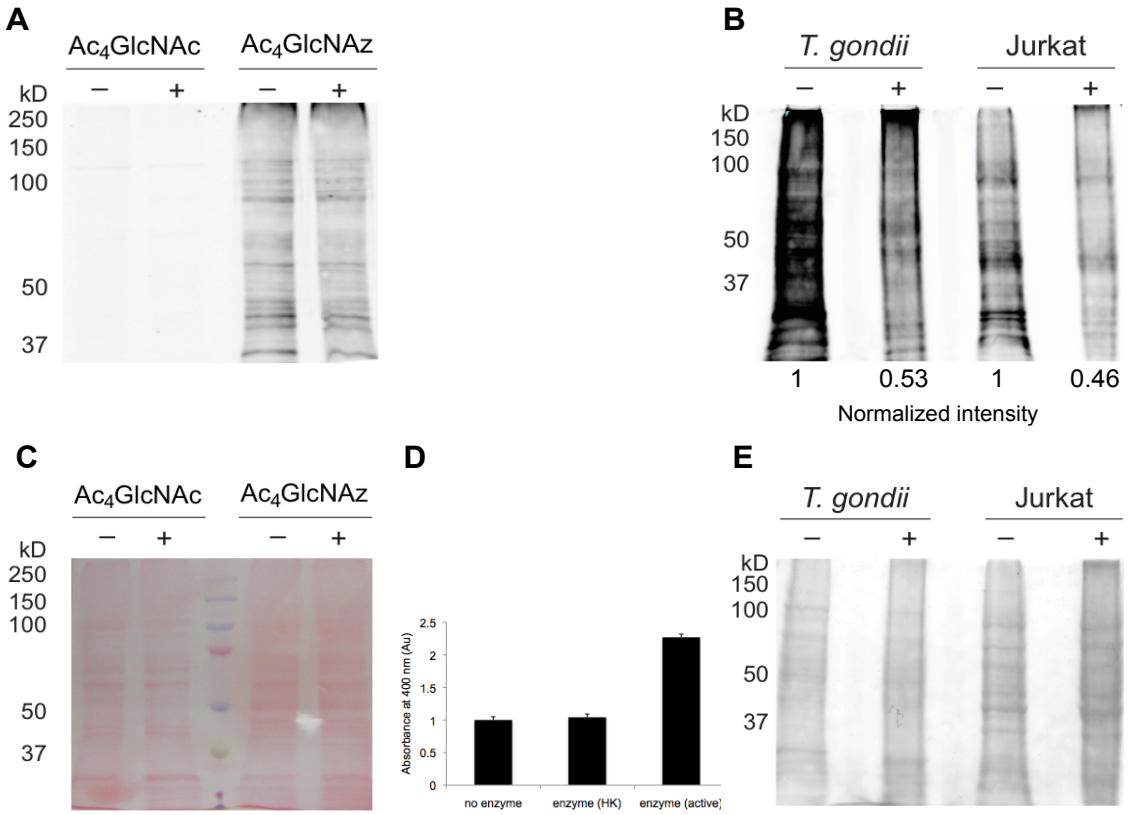

Figure 2-7 $Ac_4GlcNAz$ appears to target O-linked glycans in *Toxoplasma* tachyzoites. (A) Parasites were incubated with $Ac_4GlcNAz$ (1 mM) or $Ac_4GlcNAc$ (1 mM), then lysed and treated with hexosaminidase-*f*. All samples were labeled with biotin-alk and analyzed via immunoblot as in Figure 2-1. (B) Parasites were treated with $Ac_4GlcNAz$ (1 mM) or $Ac_4GlcNAc$ (1 mM) for 8 h. The samples were then lysed, and proteins were then subjected to mild base-catalyzed elimination, labeled with biotin-alk and analyzed as in Figure 2-1. As a control, Jurkat cells were labeled with $Ac_4GlcNAz$ (0.1 mM) for 48 h, then lysed and subjected to the same conditions as parasite cell lysate. (C) Equivalent protein loading for the blot pictured in Figure 2-7A was confirmed via staining with Ponceau S. (D) As a control for enzyme activity in Figure 2-7A, 45 µL of 0.1 mg/mL 4-Nitrophenyl-N-acetyl-β-D-glucosaminide (Sigma) was incubated with 5 µL of G2 reaction buffer and 1 µL of hexosaminidase-*f* (active or heat-killed) or 1 µL of water for 2 h at RT. The amount of released 4-Nitrophenol was measured by reading absorbance at 400 nm. (E) Equivalent protein loading for the blot pictured in Figure 2-7B was confirmed via staining with Ponceau S.

2.4 Global profiling reveals both predicted and novel glycosylated proteins

We purified a set of proteins that incorporated the Ac_4GlcNAz label using biotinylated reactants and streptavidin beads. The captured and eluted proteins were analyzed via mass spectrometry (MS) and the resulting 89 candidate proteins are listed in Table 2-1. MS hits included orthologs of proteins that are known to be O-GlcNAcylated in other species (HSP60, enolase, GAPDH) [45,46] as well as proteins that were identified in two lectin MS surveys [16,17] of tachyzoite proteins (myosin A, GAP50). Some proteins are previously characterized components that are specific to Toxoplasma (SAG1, SAG2) [47,48] while others are novel hypothetical proteins identified in the *Toxoplasma* genome. This dataset included orthologs of proteins that are markers of the ER (protein disulfide isomerase, a reticulon domain containing protein and the SERCA calcium ATPase) as well as components that mediate membrane trafficking (BET1, Sec63 and the dynamin family member Gbp1p). Lastly, we identified a set of parasite-specific effectors that have been shown to be secreted from the rhoptries, micronemes or dense granules (AMA1, NTPase1, NTPase2, ROP5, ROP7, ROP13 and ROP44). We anticipate that the membrane compartment markers and secreted effectors are likely to be modified by more complex glycan structures.

Table 2-1 Glycosylated proteins identified by mass spectroscopy

Protein Name	Uniprot Number	Predicted Function	MS Expt	Other Evidence	Lectin MS Surveys
Chaperones/stress (11)					
CDC48 (ATPase, proteasome)	B9PFU8	chaperone	2		
Heat shock protein 90	Q2Y2Q8	stress response	1,2	yes	yes
Heat shock protein 90	F0VBM9	stress response	2	yes	
Heat shock protein 90	F0VEH8	stress response	2	yes	
Heat shock protein 70	Q9U540	stress response	1,2	yes	yes
Heat shock protein 70	Q9UAE9	stress response	1	yes	
Heat shock protein 70	O76274	stress response	2	yes	
Heat shock protein 70	B6KHU4	stress response	2	yes	
Heat shock protein 60	F0VQU9	stress response	1	yes	yes
Heat shock protein 20	B9PGE9	stress response	2		
TCP-1 cpn60 family chaperonin	B6KFE8	chaperone	2		
Cytoskeleton (8)					
Actin	P53476	cytoskeleton	1,2		yes
α-tubulin1	B9PJD4	cytoskeleton	2	yes	
β-tubulin1	F0V8J8	cytoskeleton	1,2		
GAP50 (Acid phosphatase)	Q6PQ42	myosin complex	1,2	yes	yes
IMC3	Q6GYB1	cytoskeleton	2		
Myosin A	B9PW84	myosin complex	1,2	yes	yes
Myosin light chain 1	Q95UJ7	myosin complex	2		
Myosin D	MYOD	myosin complex	2		
Enzymes (32)					
Acid phosphatase	B9PQM6	phosphatase	1	yes	
Aconitate hydratase (aconitase)	B9PMS3	TCA	2		
ADP-ATP carrier (translocase)	Q9BJ36	mitochondria	1,2		
Asparaginyl tRNA synthetase	B6KCZ4	tRNA synthetase	2		
ATP dependent DNA helicase II	B9PQX8	helicase	2		yes
ATP synthase α-subunit	B9PUY4	ATP synthesis	1,2	yes	
ATP synthase β-subunit	Q309Z7	ATP synthesis	1,2	yes	
Ca^{2+}-dependent protein kinase 1	Q3HNM6	Ca^{2+} signaling	2	yes	
Citrate synthase	B6KCK9	mitochondria	2		
Cytochrome P450	B6K9N1	mitochondria	2		
Cytosol aminopeptidase	B9PTG8	protein turnover	2	yes	
Enolase	B9PH46	glycolysis	2	yes	
Fructose 1,6-bisphosphatase	Q8MY84	gluconeogenesis	1		
Fumarase	B9Q1R2	aa metabolism	2		
Isocitrate dehydrogenase 2	B9PW21	ox decarboxylation	2		
Long chain fatty acid CoA ligase	B9PJN2	FA breakdown	2	yes	
Long chain fatty acid CoA ligase	B9PJM7	FA breakdown	2	yes	yes
Malate quinone oxidoreductase	B6KKB7	pyruvate metabol	2		
Branch ch α-keto acid dehydrogenase	Q1KSF2	mitochondria	2		
Mitochondrial processing peptidase			1,2		
α-subunit	B9PUJ6	mitochondria			
β-subunit	B9PW21	mitochondria	2		

Peroxiredoxin 3	Q86GL5	antioxidant	2		
Phosphate carrier protein (TMD)	B9PRN1	mitochondria	2		
Prolyl endopeptidase	B9QH13	endopeptidase	2	yes	
Phosphofructokinase	B9Q857	glycolysis	2	yes	
Pyridine nucleotide diS oxidoreductase	B9PXF3	oxidoreductase	2		
Pyruvate carboxylase	B9PSZ5	mitochondrial	2	yes	
Pyruvate kinase	B6KVA2	glycolysis	2	yes	
Succinate CoA synthetase α-subunit	B9PTH6	mitochondrial	1,2		
Succinate CoA synthetase β-subunit	Q1KSE5	mitochondrial	1,2		
Succinate dehydrogenase	B9PZU5	mitochondrial	2		
Tryptophanyl tRNA synthetase	B6KKA3	tRNA synthetase	2		
Other Cellular Processes (13)					
Histone H2A	F0VGI1	histone	1	yes	
AP2 transcription factor (AP2X-9)	B9PZQ1	transcription factor	1	yes	
Calmodulin	B9PZ33	Ca^{2+} signaling	2		
Elongation Factor-1α	B6KN45	transcription	2	yes	yes
Elongation Factor-2	F0VEU2	transcription	2	yes	
Elongation factor Tu	B6KC06	transcription	2	yes	
Nucleosome assembly protein	B6KAS9	nucleosomes	1		
Prohibitin	B9PP22	transcription	2	yes	
Prohibitin	B9PGD2	transcription	2	yes	
Ribosomal S3Ae family	F0VIB8	translation	2		
Ribosomal: 60s ribosomal protein	F0VBQ9	translation	1		yes
Thioredoxin	B9PM19	redox signaling	2		
Ubiquitin	F0VPK9	ubiquitination	1,2		yes
Membrane Compartments & Trafficking (10)					
α-importin (nuclear transport)	B9QIQ9	transport	2		
Gbp1p protein	B9PLQ7	dynamin superfam	2		
Protein disulfide isomerase	Q9BLM8	ER, diS bonds	1,2	yes	yes
Rab23 (nuclear transport)	B9PSV9	transport	2		
Ranbp1 domain containing protein	F0V739	transport	2		
Reticulon domain containing protein	B9PMP2	ER curvature	2		
SERCA Calcium ATPase	Q5IH90	Ca^{2+} pump	2	yes	
Signal recognition particle	B9Q211	rough ER	2		
Vacuolar ATP synthase β-subunit	B9PQR4	H^{+} pump	2	yes	
Vacuolar ATP synthase subunit E	F0VAR6	H^{+} pump	2	yes	
Secretory Pathway (11)					
Apical membrane antigen (AMA1)	B9Q2L9	secreted, MN	2		yes
Mitochondrial association factor	B9Q3S3	secreted, DG	2		yes
Nucleoside triphosphatase 1 (DG)	Q27893	secreted, DG	2		
Nucleoside triphosphatase 2 (DG)	Q27895	secreted, DG	1		
Rhoptry protein ROP5B (rhoptries)	F2YGS5	secreted, rhoptries	2		yes
Rhoptry protein ROP5C	F2YGS4	secreted, rhoptries	1,2		yes

Rhoptry protein ROP5C (rhoptries)	F2YGS4	secreted, rhoptries	1,2		yes
Rhoptry protein ROP7 (rhoptries)	B6KR07	secreted, rhoptries	2		yes
Rhoptry protein ROP13 (rhoptries)	B9PK73	secreted, rhoptries	2		yes
Rhoptry protein ROP44 (rhoptries)	B6KPH7	secreted, rhoptries	1		
Surface antigen-1 (SAG1, P30)	C7E5U4	secreted, surface	1,2	yes	yes
Surface antigen-2 (SAG2)	Q27004	secreted, surface	2		yes
Uncharacterized (4)					
M protein repeat containing protein	B9PQT9	No predicted TMD	2	N/A	
Uncharacterized protein	B6K8Z6	*Borrelia* motif, TMD	1,2	N/A	
Uncharacterized protein	B9Q2P2	No predicted TMD	2	N/A	
Uncharacterized protein	F0VB85	No predicted TMD	2	N/A	

2.5 SAG1 is modified with the metabolic probe

One of the most well-characterized-proteins identified by our survey is surface antigen 1 (SAG1). Immunoprecipitation of SAG1 from Ac_4GlcNAz-labeled cells confirmed that it was labeled with the unnatural sugar (Figure 2-8). We also attempted to determine the site of modification with MS. We were unable to detect the altered peptide fragment, most likely because the bulk of SAG1 was synthesized prior to incorporation of the unnatural sugar and the signal from the minor fraction that is Ac_4GlcNAz-modified was too low. SAG1 is a GPI-linked protein [49]. Therefore, the unnatural sugar could be associated with the GPI modification or may reflect an N-linked (at N178 and/or N241) or O-linked modification of the protein.

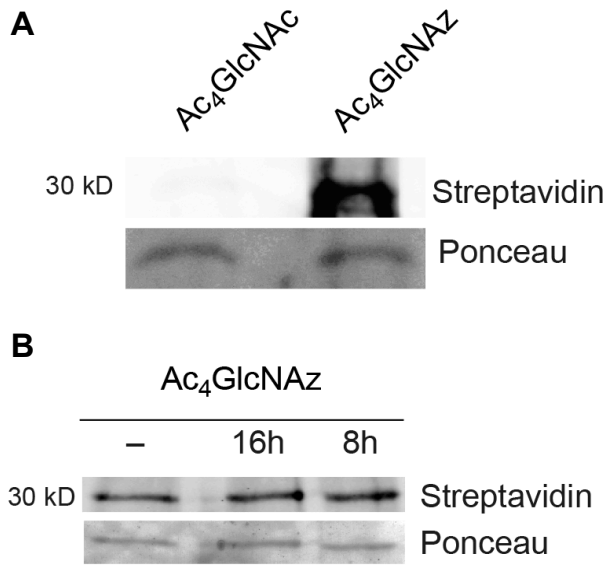

Figure 2-8 Ac_4GlcNAz label is detected in TgSAG1. (A) Parasites were labeled with Ac_4GlcNAz (1 mM) or Ac_4GlcNAc (1 mM, control) for 8 h. The samples were lysed and treated with biotin-alk as above, then incubated with anti-gp30/SAG1 (DG52) antibody overnight at 4°C. The protein-antibody complex was isolated using Pierce Protein A/G Magnetic Beads and analyzed via immunoblot. (B) Parasites were labeled with Ac_4GlcNAz (1 mM) or Ac_4GlcNAc (1 mM, control) for 8 h. The samples were then lysed, and proteins were then subjected to mild base-catalyzed elimination, labeled with biotin-alk as above, then incubated with anti-gp30/SAG1 (DG52) antibody overnight at 4°C. The protein-antibody complex was isolated using Pierce Protein A/G Magnetic Beads and analyzed via immunoblot.

2.6 Conclusions and future directions

The details of protein glycosylation in *Toxoplasma* are less well understood than the process of carbohydrate modification in vertebrate cells, but important features are beginning to emerge from studies that have used a variety of reagents to demonstrate carbohydrate incorporation into modified proteins. Our understanding of glycan biology in *Toxoplasma* or other apicomplexan parasites is complicated by the need to dissect contributions of the host cell away from parasite-specific processes. This is critically

important, as previous results suggest that the specific nature of carbohydrate modification of parasite proteins is influenced by host cell type [50]. However, the *Toxoplasma* genome has between 14 and 18 annotated glycosyltransferases [51] and the results described here demonstrate that parasites incorporate unnatural sugars into glycoproteins in the absence of host cells. Previous studies indicate that the predominant glycans in *Toxoplasma* are oligomannosidic ($Man_{5-8}(GlcNAc)_2$) and paucimannosidic ($Man_{3-4}(GlcNAc)_2$) sugars, which are rarely present on mature vertebrate glycoproteins [17]. This is consistent with the observation that the *Toxoplasma* genome lacks annotated glycosidases, suggesting that transferred sugars are not further trimmed.

We present results that are complementary to two reports that identified other types of glycosylated proteins in *Toxoplasma* tachyzoites using lectin affinity chromatography and MS. The first study profiled ConA-purified components while the second survey used ConA, WGA and Jacalin for affinity chromatography. There is a significant overlap of our results with both lectin datasets. In several instances, all three surveys identify the same specific proteins (GAP50, Myosin A, TgAMA1, ROP7, β-tubulin and actin). Our identification of an overlapping protein dataset reinforces the evidence that these components are indeed modified by glycosylation. Moreover, we also identified proteins that were not identified in the previous surveys. This is not surprising, as lectins bind to subsets of glycan structures and may not identify all glycosylated proteins in *Toxoplasma*. A limitation of our strategy is that the unnatural sugars were only reproducibly incorporated into proteins when we labeled extracellular parasites. This is likely due to the action of esterases in the host cell cytoplasm, which may prevent the sugar probes from accessing the parasite cytoplasm. While we were able to identify a

number of secreted and surface proteins, these may be less abundantly synthesized in non-replicating parasites.

2.7 Methods and materials

2.7a Culture of host cells and parasites

Toxoplasma (RH and Me49 strains, and Me49-derived lines) were grown in human foreskin fibroblast (HFF) host cells [33]. HFF cells were cultured in DMEM media (GIBCO, Invitrogen) supplemented with 10% fetal bovine serum in a humidified incubator (37 °C, 5.0% CO_2).

2.7b Metabolic labeling of parasites

Confluent monolayers of HFF cells were infected with Toxoplasma 24-48 h prior to metabolic labeling. Once the host cells were infected to maximum capacity, they were washed with Endo buffer (44.7 mM K_2SO_4, 106 mM sucrose, 10 mM $MgSO_4$, 20 mM Tris, 5 mM glucose, 3.5% BSA pH 8.2), a buffer that mimics intracellular conditions [34], and then collected by scraping. Parasites were released from host cells by syringe passage (27-gauge needle) and filtered through a 3-μm mesh. The parasites were pelleted at 1500 xg for 20 min, aspirated, and resuspended in 5 mL of Endo buffer. The parasites were added to 60-mm plates that had been pre-coated with Ac_4GlcNAc [35], Ac_4GlcNAz, Ac_4GalNAz, Ac_4ManNAz [36], Ac_4GlcNAlk [37], Ac_4GalNAlk [35].

2.7c Cell lysate preparation

Labeled parasites were collected by centrifugation (1500xg for 20 min), washed twice with PBS and resuspended in 75 µL of lysis buffer (1% NP-40, 150 mM NaCl, 50 mM triethanolamine, pH 7.4) containing protease inhibitors (Roche Biosciences). Samples were subjected to five freeze-thaw cycles, pelleted, and the resulting supernatants were collected for analyses. Total protein concentrations were measured using a bicinchoninic acid (BCA) assay (Pierce, ThermoScientific).

2.7d Covalent protein labeling and SDS-PAGE

Cu(I)-catalyzed "click" reactions

Toxoplasma lysates (50 µg) were diluted with lysis buffer to a final concentration of 1 µg/µL. To each sample was added rho-alk, rho-az, biotin-alk [38], or biotin-az [39] (100 µM, from a 10 mM stock solution in DMSO), along with a freshly prepared cocktail of "click" chemistry reagents (sodium ascorbate: 1 mM, from a 50 mM stock solution in water; tris[(1-benzyl-1-H-1,2,3-triazol-4-yl)methyl]amine (TBTA): 100 µM, from a 10 mM stock solution in DMSO); $CuSO_4 \cdot 5H_2O$: 1 mM, from a 50 mM stock solution in water). The final reaction volume was 50 µL in all cases. The reaction mixtures were vortexed and incubated at RT for 1 h. To precipitate the labeled proteins, the samples were treated with ice-cold methanol (1 mL) and placed at -80 °C for 2 h. The precipitates were pelleted at 13,000 xg for 10 min (at 4 °C), and the supernatants were discarded. The samples were air-dried for 1 h at RT prior to the addition of 15 µL of resuspension buffer (4% SDS, 150 mM NaCl, 50 mM thiethanolamine pH 7.4) and 15 µL of 2x SDS-PAGE loading buffer (20% glycerol, 0.2% bromophenol blue, 1.4% β-mercaptoethanol). The

proteins were denatured at 95°C and then resolved on Tris-glycine SDS-PAGE gels. Labeled proteins were detected with antibodies on immunoblots or in-gel fluorescence was used (below).

The Staudinger ligation

Toxoplasma lysates (50 μg) were reacted with phosphine-FLAG-His6 or phosphine-biotin (250 μM, 500 μM stock solution in PBS) at RT for 12 h [40]. The samples were then treated with 4x SDS-PAGE loading buffer (4% SDS, 40% glycerol, 0.4% bromophenol blue, 2.8% β-mercaptoethanol). The samples were then incubated at 95 °C and the proteins were resolved on Tris-glycine SDS-PAGE gels. In some cases, the labeled proteins were detected with antibodies on immunoblots, whereas in other cases, in-gel fluorescence was used (below).

2.7e Visualization of labeled proteins

Immunoblots

Proteins separated by SDS-PAGE were electroblotted to nitrocellulose membranes. Blots with biotinylated proteins were blocked using a solution of 7% BSA in PBS containing 0.1% Tween-20 (PBS-T) for 1 h at RT. FLAG-His6-labeled blots were blocked using a solution of 5% non-fat milk (in PBS-T) for 1 h at RT. The blots were incubated with HRP-α-biotin (Jackson ImmunoResearch, 1:10,000 dilution), IRDye 800 CW streptavidin (Li-Cor, 1:10,000 dilution) or HRP-α-FLAG (Sigma, 1:5,000 dilution) in the appropriate blocking buffer for 1 h at RT, then rinsed with PBS-T (6 x 10 min). Detection of membrane-bound antibodies was accomplished by chemiluminescence (SuperSignal chemiluminescence substrate, Pierce) or near infrared spectroscopy on an

Odyssey Infrared Imaging System. Densitometry analyses were performed using imageJ software. The intensity of signal of each lane from visualized immunoblot was divided by the intensity of the corresponding lane from the Ponceau S stain image. The resulting numbers were adjusted to the negative control (background) lane.

In-gel fluorescence scanning

Following SDS-PAGE, some gels were incubated with destaining solution (50% methanol/10% acetic acid in water, 10 min), followed by water (10 min). In-gel fluorescent signals were measured on a Typhoon Trio+ scanner. Densitometry analyses were performed using imageJ software. The intensity of signal of each lane from visualized gel was divided by the intensity of the corresponding lane from the Coomassie stained gel. The resulting numbers were adjusted to the negative control (background) lane.

2.7f Immunoprecipitation

Toxoplasma samples were prepared and reacted as previously described. In order to purify TgSAG1, samples were incubated with anti-P30/SAG1 (DG52) [41] overnight at 4°C, with mixing. The protein-antibody complex was isolated using Pierce Protein A/G Magnetic Beads (Thermo Scientific). Samples were analyzed on immunoblots as above.

2.7g Fluorescence microscopy

Syringe-lysed parasite cultures were purified using a PD-10 desalting column (GE Healthcare) or filter (Millipore, Millex-SV, 5.00 um PVDF membrane) and washed with

DMEM media (Corning) supplemented with 3% (vol/vol) heat inactivated FBS (Omega Scientific), penicillin (100 U/mL), and streptomycin (10 μg/mL). The parasites were resuspended in Endo buffer containing Ac_4GlcNAz (250-1000 μM) or Ac_4GlcNAc (250-1000 μM). After 8 h, the parasites were washed with PBS (3 x 0.5 mL) and DMEM (3 x 0.5 mL). The parasites were then centrifuged onto poly-L lysine coated (0.01%, Sigma) glass coverslips (1500 rpm for 7 min) and fixed with 4% paraformaldehyde in PBS for 15 min at RT. After washing with PBS (3 x 0.25 mL), the parasites were permeabilized with 0.1% Triton-X in PBS for 5 min at RT. The parasites were rinsed with PBS (3 x 0.25 mL) and treated with freshly prepared "click" chemistry cocktail containing biotin-alk as described above. The samples were washed with PBS (3 x 0.25 mL), then blocked for 1 h at RT with PBS + 5% BSA (0.5 mL). The parasite samples were then treated with streptavidin-AlexaFluor594 (Jackson Labs; 1:1000 in PBS) for 30 min at RT, then washed with PBS (3 x 0.25 mL). In some cases streptavidin-AlexaFluor488 (Jackson Labs; 1:1000 in PBS) was used, the resulting images were false colored red for consistency. The cover slips were mounted on glass slides with Vectashield mounting media (Vector Laboratories). All samples were prepared in triplicate. Images were acquired on a Nikon Eclipse Ti inverted microscope with NIS-Elements Microscope imaging Software and analyzed with ImageJ.

In some cases, parasites incubated with unnatural sugars in Endo buffer were used to infect HFF cells. HFF cells were grown on glass coverslips submerged in 0.5 mL DMEM media supplemented with 10% FBS (vol/vol), penicillin (100 U/mL), and streptomycin (100 μg/mL). The cells were infected at a multiplicity of infection (MOI) of 5-15 in duplicate, then processed and imaged as above.

2.7h Deglycosylation experiments

PNGaseF treatment

Toxoplasma lysates (40 μg) were diluted with lysis buffer (to total 10 μL), 10% NP-40 (1.3 μL), and reaction buffer (New England Biolabs deglycosylation kit, 1.3 μL). PNGaseF (New England Biolabs 200 U, 0.4 μL) was added to each sample, and the reactions were incubated at 37 °C for 8 h. Proteins were then labeled with biotin-alk and analyzed via immunoblot as above.

Hexosaminidase-*f* treatment

Toxoplasma lysates (50 μg) were diluted with lysis buffer (to total 54 μL), G2 reaction buffer (New England Biolabs, 6 μL). Hexosaminidase-*f* (New England Biolabs 5 U, 1.0 μL) was added to each sample, and the reactions were incubated at 37°C for 16 h. Proteins were then labeled with biotin-alk and analyzed via immunoblot as above. As a control, 45 μL of 0.1 mg/mL 4-Nitrophenyl-N-acetyl-β-D-glucosaminide (Sigma) was incubated with 5 μL of G2 reaction buffer and 1 μL of hexosaminidase-*f* (active or heat-killed) or 1 μL of water for 2 h at RT. The amount of released 4-Nitrophenol was measured by reading absorbance at 400 nm.

Tunicamycin treatment

HFF cells were cultured in T-175 flasks for 12 d, then treated with 5μg/mL tunicamycin for 48 h. The cells were then infected with Toxoplasma tachyzoites. After 24 h growth in tunicamycin-treated host cells, the parasites were isolated as above. Extracellular parasites were then incubated with unnatural sugars in the presence of tunicamycin for an additional 8 h prior to covalent labeling and immunoblot analysis.

OGA treatment

Toxoplasma lysates (40 μg) were diluted with lysis buffer (to total 20 μL) and treated with OGA enzyme as in [42] at 37 °C for 24 h. Proteins were then labeled with biotin-alk and analyzed via immunoblot as above.

β-Elimination

Toxoplasma lysates (40 μg) were diluted with lysis buffer (to total 20 μL) and then labeled with biotin-alk. After addition of 5 μL of β-elimination reagent mixture (Sigma) the reaction was incubated at 4 °C for 8-24 h. Proteins were then analyzed via immunoblot as above.

2.7i Enrichment of proteins for MudPIT analysis

Toxoplasma lysate (6 mg total protein in 1 mL of lysis buffer) was treated with 110 μL of 10 mM phosphine-biotin in DMSO (working concentration = 1 mM). The reaction mixture was incubated under an Ar atmosphere for 4 h at 37 °C. Next, 1 mL of ice-cold methanol for each 250 μL of reaction mixture was added, and the samples were incubated at -80 °C for 2 h to precipitate proteins. The precipitates were pelleted at 13,000xg (4 °C, 10 min). The supernatants were discarded, and the samples were re-suspended in ice-cold methanol and precipitated at -80 °C two more times. Precipitates were dissolved in 1% SDS in PBS, and incubated with avidin agarose beads at RT overnight. The beads were washed with 2 column volumes of 1% SDS in PBS (pH 7.4), followed by 2 column volumes of 6 M urea in PBS (pH 7.4), then 2 column volumes of 4

M NaCl in PBS (pH 7.4), and 2 column volumes of 100 mM NH_4HCO_3 (pH 7.4). The bound species were eluted by boiling the beads in SDS-PAGE loading buffer at 95 °C for 10 min, and then loaded onto Tris-glycine SDS-PAGE gels. The gels were stained with Coomasssie blue and submitted to the UCI Mass Spectrometry Facility for MudPIT analysis. Similar data were obtained from two replicate experiments (labeled 1 and 2 in Table 2-1).

2.7j MudPIT analysis

Following in-gel digestion with porcine trypsin, extracted peptides were separated on a C18 column and analyzed by MSE on a SYNAPT G2 instrument with a TRIZIAC source (Waters). The data was analyzed using ProteinLynx Global Server software (PLGS 3.0) with the Toxoplasma UniProt database.

2.7k Toxoplasma proteins identified by MudPIT analysis

A spread-sheet of Toxoplasma proteins identified by mass spectrometry using the ToxoDB/uniprot database was further organized using BLASTP and NCBI data to categorize hits into subgroups (Chaperones/stress, Cytoskeleton, Enzymes, Membrane Compartments and Trafficking, Secretory Pathway and Other Cellular Processes). A set of uncharacterized protein hits was also noted and annotated with any available information on protein motifs.

References

(1) Varki, A; Cummings, R. D.; Esko, J. D.; Freeze, H. H.; Stanley, P; Bertozzi, C. R.; Hart, G. W.; Etzler, M. E. *Essentials of Glycobiology*; Cold Spring Harbor: New York, 2009.

(2) Moremen, K. W.; Tiemeyer, M.; Nairn, A. V. Vertebrate protein glycosylation: diversity, synthesis and function. *Nat. Rev. Mol. Cell Biol.* **2012**, *13*, 448-462.

(3) Tomavo, S.; Dubremetz, J. F.; Schwarz, R. T. Biosynthesis of glycolipid precursors for glycosylphosphatidylinositol membrane anchors in a *Toxoplasma gondii* cell-free system. *J. Biol. Chem.* **1992**, *267*, 21446-21458.

(4) Tomavo, S.; Dubremetz, J. F.; Schwarz, R. T. A family of glycolipids from *Toxoplasma gondii*. Identification of candidate glycolipid precursor(s) for *Toxoplasma gondii* glycosylphosphatidylinositol membrane anchors. *J. Biol. Chem.* **1992**, *267*, 11721-11728.

(5) Ma, J.; Hart, G. W. O-GlcNAc profiling: from proteins to proteomes. *Clin. Proteomics* **2014**, *11*, 8.

(6) Hanover, J. A.; Krause, M. W.; Love, D. C. Bittersweet memories: linking metabolism to epigenetics through O-GlcNAcylation. *Nat. Rev. Mol. Cell Biol.* **2012**, *13*, 312-321.

(7) Levine, N. D. *The protozoan phylum Apicomplexa*; CRC Press: Boca Raton, FL, 1988.

(8) Lekutis, C.; Ferguson, D. J.; Grigg, M. E.; Camps, M.; Boothroyd, J. C. Surface antigens of *Toxoplasma gondii*: variations on a theme. *Int. J. Parasitol.* **2001**, *31*, 1285-1292.

(9) Boulanger, M. J.; Tonkin, M. L.; Crawford, J. Apicomplexan parasite adhesins: novel strategies for targeting host cell carbohydrates. *Curr. Opin. Struct. Biol.* **2010**, *20*, 551-559.

(10) Carruthers, V.; Boothroyd, J. C. Pulling together: an integrated model of *Toxoplasma* cell invasion. *Curr. Opin. Microbiol.* **2007**, *10*, 83-89.

(11) Boothroyd, J. C.; Dubremetz, J. F. Kiss and spit: the dual roles of *Toxoplasma* rhoptries. *Nature Rev. Microbiol.* **2008**, *6*, 79-88.

(12) Hager, K. M.; Striepen, B.; Tilney, L. G.; Roos, D. S. The nuclear envelope serves as an intermediary between the ER and Golgi complex in the intracellular parasite *Toxoplasma gondii*. *J. Cell Sci.* **1999**, *112*, 2631-2638.

(13) Stedman, T. T.; Sussmann, A. R.; Joiner, K. A. *Toxoplasma gondii* Rab6 mediates a retrograde pathway for sorting of constitutively secreted proteins to the Golgi complex. *J. Biol. Chem*. **2003**, *278*, 5433-5443.

(14) Sheiner, L.; Dowse, T. J.; Soldati-Favre, D. Identification of trafficking determinants for polytopic rhomboid proteases in *Toxoplasma gondii. Traffic* **2008**, *9*, 665-677.

(15) Prescher, J. A.; Bertozzi, C. R. Chemical technologies for probing glycans. *Cell* **2006**, *126*, 851-854.

(16) Luo, Q.; Upadhya, R.; Zhang, H.; Madrid-Aliste, C.; Nieves, E.; Kim, K.; Angeletti, R. H.; Weiss, L. M. Analysis of the glycoproteome of *Toxoplasma gondii* using lectin affinity chromatography and tandem mass spectrometry. *Microbes Infect.* **2011**, *13*, 1199-1210.

(17) Fauquenoy, S.; Morelle, W.; Hovasse, A.; Bednarczyk, A.; Slomianny, C.; Schaeffer, C.; Dorsselaer, A. V.; Tomavo, S. Proteomics and glycomics analyses of N-glycosylated structures involved in *Toxoplasma gondii*--host cell interactions. *Mol. Cell. Proteomics* **2008**, *7*, 891-910.

(18) Perez-Cervera, Y.; Harichaux, G.; Schmidt, J.; Debierre-Grockiego, F.; Dehennaut, V.; Bieker, U.; Meurice, E.; Lefebvre, T.; Schwarz, R. T. Direct evidence of O-GlcNAcylation in the apicomplexan *Toxoplasma gondii*: a biochemical and bioinformatic study. *Amino Acids* **2011**, *40*, 847-856.

(19) Gowda, D. C.; Gupta, P.; Davidson, E. A. Glycosylphosphatidylinositol anchors represent the major carbohydrate modification in proteins of intraerythrocytic stage *Plasmodium falciparum*. *J. Biol. Chem.* **1997**, *272*, 6428-6439.

(20) Striepen, B.; Zinecker, C. F.; Damm, J. B.; Melgers, P. A.; Gerwig, G. J.; Koolen, M.; Vliegenthart, J. F.; Dubremetz, J. F.; Schwarz, R. T. Molecular structure of the "low molecular weight antigen" of *Toxoplasma gondii*: a glucose alpha 1-4 N-acetylgalactosamine makes free glycosyl-phosphatidylinositols highly immunogenic. *J. Mol. Biol.* **1997**, *266*, 797-813.

(21) Zinecker, C. F.; Striepen, B.; Geyer, H.; Geyer, R.; Dubremetz, J. F.; Schwarz, R. T. Two glycoforms are present in the GPI-membrane anchor of the surface antigen 1 (P30) of *Toxoplasma gondii*. *Mol. Biochem. Parasitol.* **2001**, *116*, 127-135.

(22) Stwora-Wojczyk, M. M.; Dzierszinski, F.; Roos, D. S.; Spitalnik, S. L.; Wojczyk, B. S. Functional characterization of a novel *Toxoplasma gondii* glycosyltransferase: UDP-N-acetyl-D-galactosamine:polypeptide N-acetylgalactosaminyltransferase-T3. *Arch Biochem. Biophys.* **2004**, *426*, 231-240.

(23) Stwora-Wojczyk, M. M.; Kissinger, J. C.; Spitalnik, S. L.; Wojczyk, B. S. O-glycosylation in *Toxoplasma gondii*: identification and analysis of a family of UDP-

GalNAc: polypeptide N-acetylgalactosaminyltransferases. *Int. J. Parasitol.* **2004**, *34*, 309-322.

(24) West, C. M.; van der Wel, H.; Blader, I. J. Detection of cytoplasmic glycosylation associated with hydroxyproline. *Methods Enzymol.* **2006**, *417*, 389-404.

(25) Xu, Y.; Brown, K. M.; Wang, Z. A.; van der Wel, H.; Teygong, C.; Zhang, D.; Blader, I. J.; West, C. M. The Skp1 protein from *Toxoplasma* is modified by a cytoplasmic prolyl 4-hydroxylase associated with oxygen sensing in the social amoeba Dictyostelium. *J. Biol. Chem.* **2012**, *287*, 25098-25110.

(26) Shams-Eldin, H.; Blaschke, T.; Anhlan, D.; Niehus, S.; Muller, J.; Azzouz, N.; Schwarz, R. T. High-level expression of the *Toxoplasma gondii* STT3 gene is required for suppression of the yeast STT3 gene mutation. *Mol. Biochem. Parasitol.* **2005**, *143*, 6-11.

(27) Luk, F. C.; Johnson, T. M.; Beckers, C. J. N-linked glycosylation of proteins in the protozoan parasite *Toxoplasma gondii*. *Mol. Biochem. Parasitol.* **2008**, *157*, 169-178.

(28) Schwarz, R. T.; Tomavo, S. The current status of the glycobiology of *Toxoplasma gondii*: glycosylphosphatidylinositols, N- and O-linked glycans. *Res. Immunol*. **1993**, *144*, 24-31.

(29) Fauquenoy, S.; Hovasse, A.; Sloves, P. J.; Morelle, W.; Dilezitoko Alayi, T.; Slomianny, C.; Werkmeister, E.; Schaeffer, C.; Van Dorsselaer, A.; Tomavo, S. Unusual N-glycan structures required for trafficking *Toxoplasma gondii* GAP50 to the inner membrane complex regulate host cell entry through parasite motility. *Mol. Cell. Proteomics* **2011**, *10*, M111.008953.

(30) Prescher, J. A.; Bertozzi, C. R. Chemistry in living systems. *Nat. Chem. Biol.* **2005**, *1*, 13-21.

(31) Grammel, M.; Hang, H. C. Chemical reporters for biological discovery. *Nat. Chem. Biol.* **2013**, *9*, 475-484.

(32) Patterson, D. M.; Nazarova, L. A.; Prescher, J. A. Finding the right (bioorthogonal) chemistry. *ACS Chem. Biol.* **2014**, *9*, 592-605.

(33) Roos, D. S.; Donald, R. G.; Morrissette, N. S.; Moulton, A. L. Molecular tools for genetic dissection of the protozoan parasite *Toxoplasma gondii*. *Methods Cell. Biol.* **1994**, *45*, 27-63.

(34) Endo, T.; Tokuda, H.; Yagita, K.; Koyama, T. Effects of extracellular potassium on acid release and motility initiation in *Toxoplasma gondii*. *J. Protozool.* **1987**, *34*, 291-295.

(35) Kretzschmar, G.; Stahl, W. Large scale synthesis of linker-modified sialyl LewisX, LewisX and N-acetyllactosamine. *Tetrahedron* **1998**, *54*, 6341-6358.

(36) Luchansky, S. J.; Hang, H. C.; Saxon, E.; Grunwell, J. R.; Yu, C.; Dube, D. H.; Bertozzi, C. R. Constructing azide-labeled cell surfaces using polysaccharide biosynthetic pathways. *Methods Enzymol.* **2003**, *362*, 249-272.

(37) Gurcel, C.; Vercoutter-Edouart, A. S.; Fonbonne, C.; Mortuaire, M.; Salvador, A.; Michalski, J. C.; Lemoine J. Identification of new O-GlcNAc modified proteins using a click-chemistry-based tagging. *Anal. Bioanal. Chem.* **2008**, *390*, 2089-2097.

(38) Charron, G.; Zhang, M. M.; Yount, J. S.; Wilson, J.; Raghavan, A. S.; Shamir, E.; Hang, H. C. Robust fluorescent detection of protein fatty-acylation with chemical reporters. *J. Am. Chem. Soc.* **2009**, *131*, 4967-4975.

(39) Hang, H. C.; Yu, C.; Pratt, M. R.; Bertozzi, C. R. Probing glycosyltransferase activities with the Staudinger ligation. *J. Am. Chem. Soc.* **2004**, *126*, 6-7.

(40) Laughlin, S. T.; Agard, N. J.; Baskin, J. M.; Carrico, I. S.; Chang, P. V.; Ganguli, A. S.; Hangauer, M. J.; Lo, A.; Prescher, J. A.; Bertozzi, C. R. Metabolic labeling of glycans with azido sugars for visualization and glycoproteomics. *Methods Enzymol.* **2006**, *415*, 230-250.

(41) Burg, J. L.; Perelman, D.; Kasper, L. H.; Ware, P. L.; Boothroyd, J. C. Molecular analysis of the gene encoding the major surface antigen of *Toxoplasma gondii*. *J. Immunol.* **1988**, *141*, 3584-3591.

(42) Boyce, M.; Carrico, I. S.; Ganguli, A. S.; Yu, S. H.; Hangauer, M. J.; Hubbard, S. C.; Kohler, J. J.; Bertozzi, C. R. Metabolic cross-talk allows labeling of O-linked beta-N-acetylglucosamine-modified proteins via the N-acetylgalactosamine salvage pathway. *Proc. Natl. Acad. Sci. U.S.A.* **2011**, *108*, 3141-3146.

(43) Dube, D. H.; Champasa, K.; Wang, B. Chemical tools to discover and target bacterial glycoproteins. *Chem. Commun.* **2011**, *47*, 87-101.

(44) Breidenbach, M. A.; Gallagher, J. E.; King, D. S.; Smart, B. P.; Wu, P.; Bertozzi, C. R. Targeted metabolic labeling of yeast N-glycans with unnatural sugars. *Proc Natl Acad Sci U.S.A.* **2010**, *107*, 3988-3993.

(45) Hayoun, D.; Kapp, T.; Edri-Brami, M.; Ventura, T.; Cohen, M.; Avidan, A.; Lichtenstein, R. G. HSP60 is transported through the secretory pathway of 3-MCA-induced fibrosarcoma tumour cells and undergoes N-glycosylation. *FEBS J.* **2012**, *279*, 2083-2095.

(46) Love, D. C.; Hanover, J. A. The hexosamine signaling pathway: deciphering the "O-GlcNAc Code". *Sci. STKE* **2005**, *312*, re13.

(47) Manger, I. D.; Hehl, A. B.; Boothroyd, J. C. The surface of *Toxoplasma* tachyzoites is dominated by a family of glycosylphosphatidylinositol-anchored antigens related to SAG1. *Infect. Immun.* **1998**, *66*, 2237-2244.

(48) Pollard, A. M.; Onatolu, K. N.; Hiller, L.; Haldar, K.; Knoll, L. J. Highly polymorphic family of glycosylphosphatidylinositol-anchored surface antigens with evidence of developmental regulation in *Toxoplasma gondii*. *Infect. Immun.* **2008**, *76*, 103-110.

(49) Nagel, S. D.; Boothroyd, J. C. The major surface antigen, P30, of *Toxoplasma gondii* is anchored by a glycolipid. *J. Biol. Chem.* **1989**, *264*, 5569-5574.

(50) Garenaux, E.; Shams-Eldin, H.; Chirat, F.; Bieker, U.; Schmidt, J.; Michalski, J. C.; Cacan, R.; Guérardel, Y.; Schwarz, R. T. The dual origin of *Toxoplasma gondii* N-glycans. *Biochemistry* **2008**, *47*, 12270-12276.

(51) Kissinger, J. C.; Gajria, B.; Li, L.; Paulsen, I. T.; Roos, D. S. ToxoDB: accessing the *Toxoplasma gondii* genome. *Nucleic Acids Res.* **2003**, *31*, 234–236.

CHAPTER 3: Expanding the chemical reporter toolkit for visualizing host-pathogen interactions

3.1 Introduction

The bioorthogonal chemical reporter strategy has been widely used to interrogate glycans and other biopolymers in living systems [1-5]. This approach relies on the introduction of a uniquely reactive functional group (i.e., a "chemical reporter") into a biomolecule of interest. The chemical reporter can be ligated to probes for visualization or retrieval using highly selective (i.e., "bioorthogonal") chemistries [2,6]. Intriguingly, in addition to glycosylated structures, parasites and host cells exchange numerous other metabolites. Monitoring these communication pathways simultaneously requires multiple cell-compatible reactions that can be used concurrently, or "mutually orthogonal" bioorthogonal chemistries. Unfortunately, the existing toolbox of bioorthogonal chemistries is rather sparse and has been largely limited to examining one biological feature at a time in live cells and tissues. This is because many bioorthogonal reactions are incompatible with one another and cannot be used in tandem to monitor multiple species [7-12].

To fill this void, we aimed to identify transformations that can be used concurrently to tag biomolecules in complex environments. Organic azides have dominated the lanscape of bioorthogonal reactions for the last few years [6,8,13]. Organic azides can be easily installed into various biomolecules, including glycans, proteins, lipids, and numerous metabolites [4,14,15]. Once attached to the biomolecule of interest,

they can be selectively reacted with phosphines via Staudinger ligation, with terminal alkynes via copper-catalyzed "click" chemistry, or with strained cyclooctynes [16-20].

In recent years, strained alkenes and alkynes have been identified that meet several of the criteria for broadly applicable chemical reporters [7]. These scaffolds, including *trans*-cyclooctene (TCO), norbornene (NB), and bicyclononyne (BCN), are abiotic and relatively stable in cellular environs [21-24]. Furthermore, they react rapidly with electron-poor tetrazines via inverse-electron-demand Diels-Alder (IED-DA) reactions. The remarkable speed of these reactions is well suited for sensitive imaging applications, and a variety of TCO- and NB- conjugated nanoparticles and antibodies have been utilized for this purpose [8,25,26]. While useful for some applications, strained alkenes and alkynes have been slow to transition as chemical reporter groups for metabolic pathways that are sensitive to steric hindrance due to their large size. Many of these reporters have also been found to cross-react with organic azides, which made their simultaneous use for looking at different biomolecules impossible.

Recently, the Prescher lab and others have developed a smaller strained olefin—1,3-disubstituted cyclopropene—for use as a chemical reporter. This microcycle is small in size and possesses a high amount of strain energy, which enables it to react efficiently with electron-poor diens (e.g., tetrazine) via EAD-DA reaction (Figure 3-1, top). Cyclopropene itself is prone to polymerization at room temperature and susceptible to attack by thiols and other biological nucleophiles. However, it was demonstrated that a combination of steric and electronic modifications to the cyclopropene core at C-3 position provides a stable chemical reporter suitable for metabolic labeling without compromising cycloaddition reactivity. Additionally, 1,3-disubstituted cyclopropene does

not cross-react with organic azides, which makes it a promising chemical reporter for use in combination with strain-promoted "click" chemistries (Figure 3-1, bottom) [27,28].

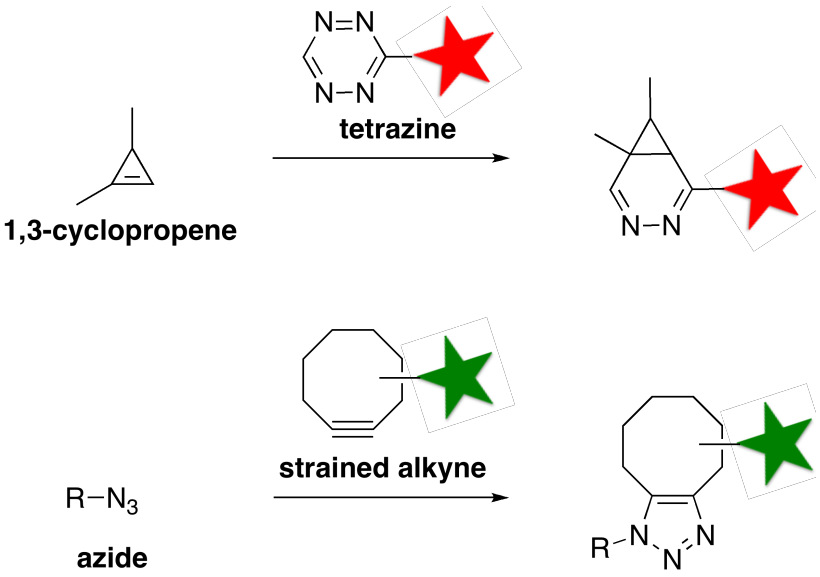

Figure 3-1 1,3-Disubsituted cyclopropene scaffolds can be used in conjunction with strain-promoted "click" chemistries. 1,3-Disubstituted cyclopropenes (top) react with tetrazines. Organic azides (bottom) react with strained alkynes.

3.2 Metabolic incorporation of 1,3-disubstituted cyclopropenes onto live cell surfaces

To investigate whether cyclopropenes would be useful for cellular labeling studies, we constructed a methyl cyclopropene-sialic acid conjugate (**9-Cp-NeuAc**, Scheme 3-1). Modified sialic acids of this sort are known to be metabolized by cells and incorporated into cell surface glycans [29-32]. I collaborated with others in the Prescher lab to explore whether disubstituted cyclopropenes can be metabolically incorporated into cellular glycans and modified via EAD-DA with tetrazines. Jurkat cells were incubated with various concentrations of **9-Cp-NeuAc** for 24-48 h. The presence of cell surface

cyclopropenes was subsequently probed by reaction with a tetrazine-biotin conjugate **Tz-biotin** and avidin staining (Figure 3-2A). The fluorescence of each cell population was measured using flow cytometry. As shown in Figure 3-2B, a dose-dependent increase in signal was observed when cells were incubated with increasing concentrations of **9-Cp-NeuAc**, indicating successful metabolic incorporation of the chemical reporter. The incorporation efficiency of **9-Cp-NeuAc** was lower than that of a similarly functionalized azido sugar (**9-Az-NeuAc**), but on par with other unnatural sialic acids used in metabolic engineering studies (Figure 3-3) [29-32]. Importantly, the fluorescence signal also diminished when 9-Cp-NeuAc-treated cells were cultured in the presence of unlabeled sugars (sialic acid, NeuAc or peracetylated *N*-acetylmannosamine, $Ac_4ManNAc$) targeting the same metabolic pathway [29].

Scheme 3-1 Synthesis of Cp-derivatives for biomolecule labeling. (A) Synthesis of NHS-cyclopropenyl ester (**Cp-NHS**). (B) Synthesis of cyclopropene-modified sialic acid (**9-Cp-NeuAc**).

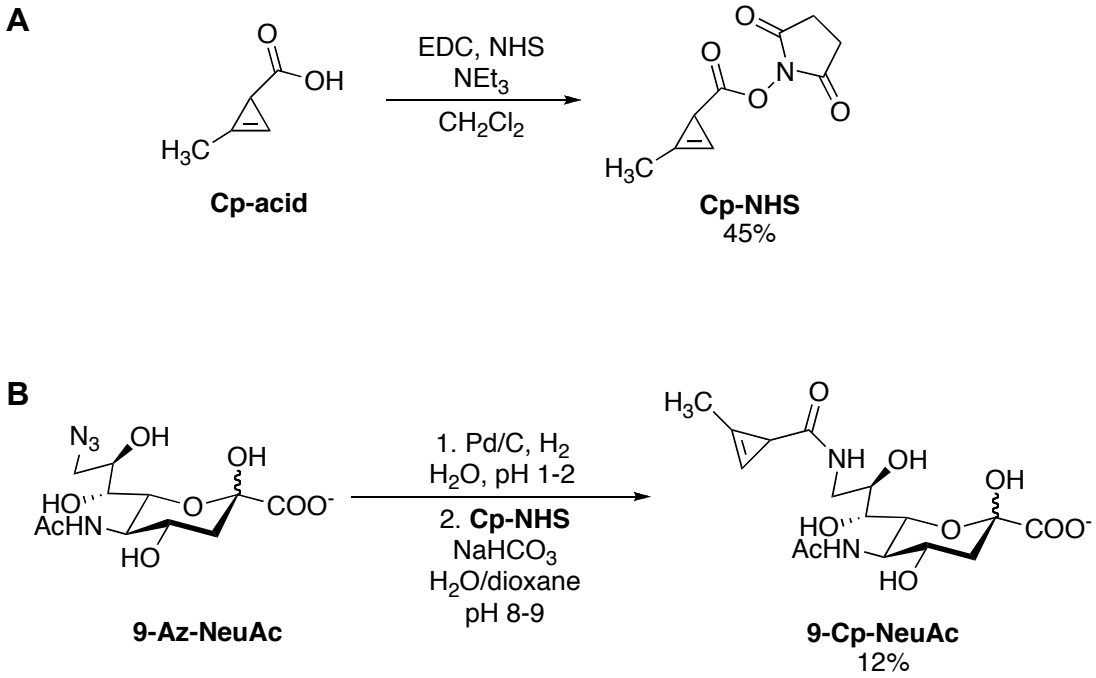

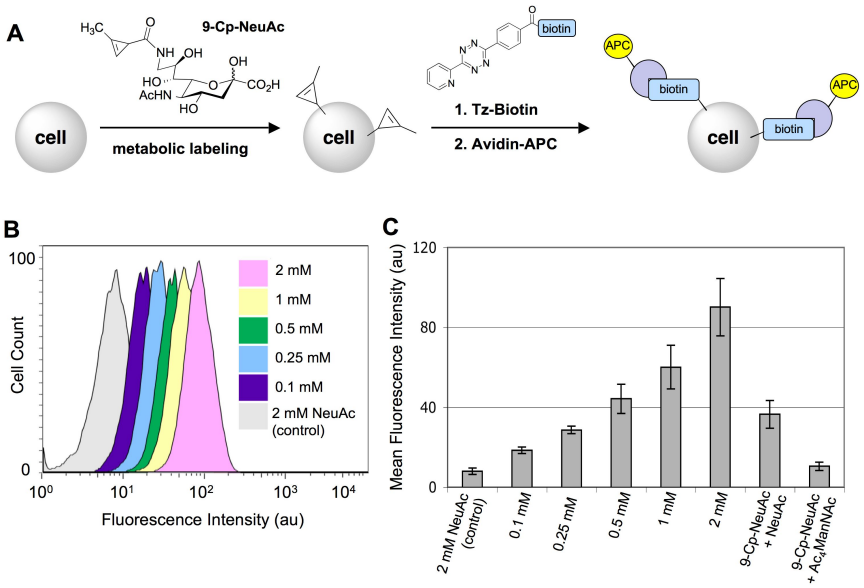

Figure 3-2 Cyclopropenes can be metabolically incorporated onto live cell surfaces. (A) Jurkat cells were incubated with **9-Cp-NeuAc** (0-2 mM), a control sugar (**NeuAc**, 2 mM) or both **9-Cp-NeuAc** and **NeuAc** (or **Ac_4ManNAc**) for 24 h. After washing, the cells were reacted with **Tz-Biotin** (100 μM) for 1 h at 37 °C. Subsequent staining with APC-avidin and flow cytometry analysis provided the plots in (B). (C) Mean fluorescence intensities (in arbitrary units, au) for the histograms in (B). Error bars represent the standard deviation of the mean for three experiments.

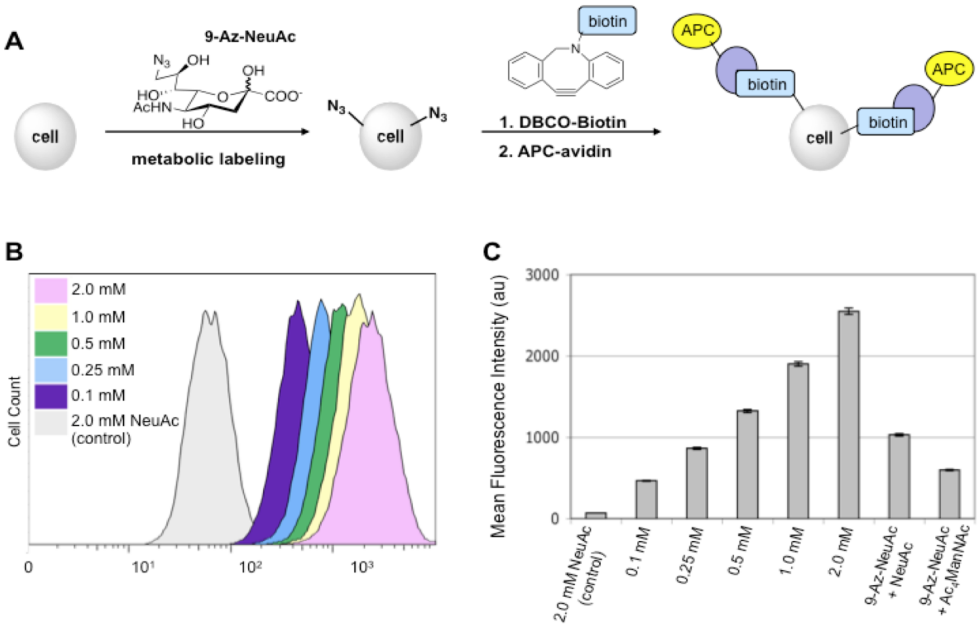

D

9-Cp-NeuAc (μM)	9-Az-NeuAc (μM)	Ac_4ManNAc (μM)	NeuAc (μM)	Label	MFI Difference over Background
—	—	—	2000	Tz-Biotin	1.0
100	—	—	—		2.3
250	—	—	—		3.6
500	—	—	—		5.6
1000	—	—	—		7.5
2000	—	—	—		11.3
1000	—	—	1000		4.6
1000	—	25	—		1.3
—	—	—	2000	DBCO-Biotin	1.0
—	100	—	—		6.7
—	250	—	—		12.5
—	500	—	—		19.2
—	1000	—	—		27.6
—	2000	—	—		37.0
—	1000	—	1000		15.0
—	1000	25	—		8.7

Figure 3-3 Flow cytometry analysis of 9-Az-NeuAc metabolism in Jurkat cells. (A) Cells incubated with **9-Az-NeuAc** (0-2 mM) were treated with 100 μM DBCO-Biotin followed by APC-avidin. (B) Flow cytometry histograms revealing a dose-dependent increase in fluorescence correlating with **9-Az-NeuAc** concentration. (C) Mean fluorescence intensities (in arbitrary units, au) for the histograms in (B). Error bars represent the standard deviation of the mean for three experiments A reduction in signal was observed when cells were incubated simultaneously with **9-Az-NeuAc** and unlabeled sugars (sialic acid and **Ac_4ManNAc**). (D) Comparison of the metabolic incorporation efficiencies of **9-Cp-NeuAc** and **9-Az-NeuAc**.

3.3 Simultaneous use of organic azides and cyclopropenes on live cell surfaces

We further investigated whether cyclopropene- and azide-modified sugars could be utilized concurrently for live cell labeling. In one setup, Jurkat cells were incubated with **9-Cp- NeuAc**, **9-Az-NeuAc**, or no sugar. After 24 h, portions of the sugar-treated cells were combined. In a second setup, Jurkat cells were cultured with both sugars simultaneously. All samples were subsequently reacted with either **Tz-Biotin**, a water-soluble cyclooctyne-fluorophore conjugate (**DBCO-Rho**), or both reagents. Cells treated with **Tz-Biotin** were also stained with APC-avidin. The fluorescence of the resulting cell populations was analyzed via two-color flow cytometry, and the corresponding plots are depicted in Figure 3-4. For cells cultured separately with the unnatural sugars prior to mixing and covalent reaction, flow analysis revealed two distinct cell populations—one with robust APC fluorescence (corresponding to the **9-Cp-NeuAc**-treated cells) and one with robust rhodamine fluorescence (corresponding to the **9-Az-NeuAc**-treated cells) (Figure 3-4A). For cells cultured with the cyclopropenyl and azido sugars simultaneously, treatment with both covalent probes and flow analysis revealed a single population of cells labeled with both fluorophores (Figure 3-4B). The overall fluorescence signal attributed to the cyclopropene modification was reduced in this case, though, likely due to the lower incorporation efficiency of **9-Cp-NeuAc** compared to **9-Az-NeuAc**. Non-specific reactivity with DBCO-Rho was also observed in the cell labeling studies, but importantly, no cross-reactivity was observed when **9-Az-NeuAc**-treated cells were labeled with **Tz-Biotin** or when **9-Cp-NeuAc**-treated cells were

labeled with DBCO-Rho (Figure 3-5). Collectively, these results suggest that cyclopropene- and azide-based chemical reporters can be utilized together in live cells and will be useful for multiplexed metabolic engineering strategies. Work along these lines is being further pursued to study protein function and imaging other biomolecules [33].

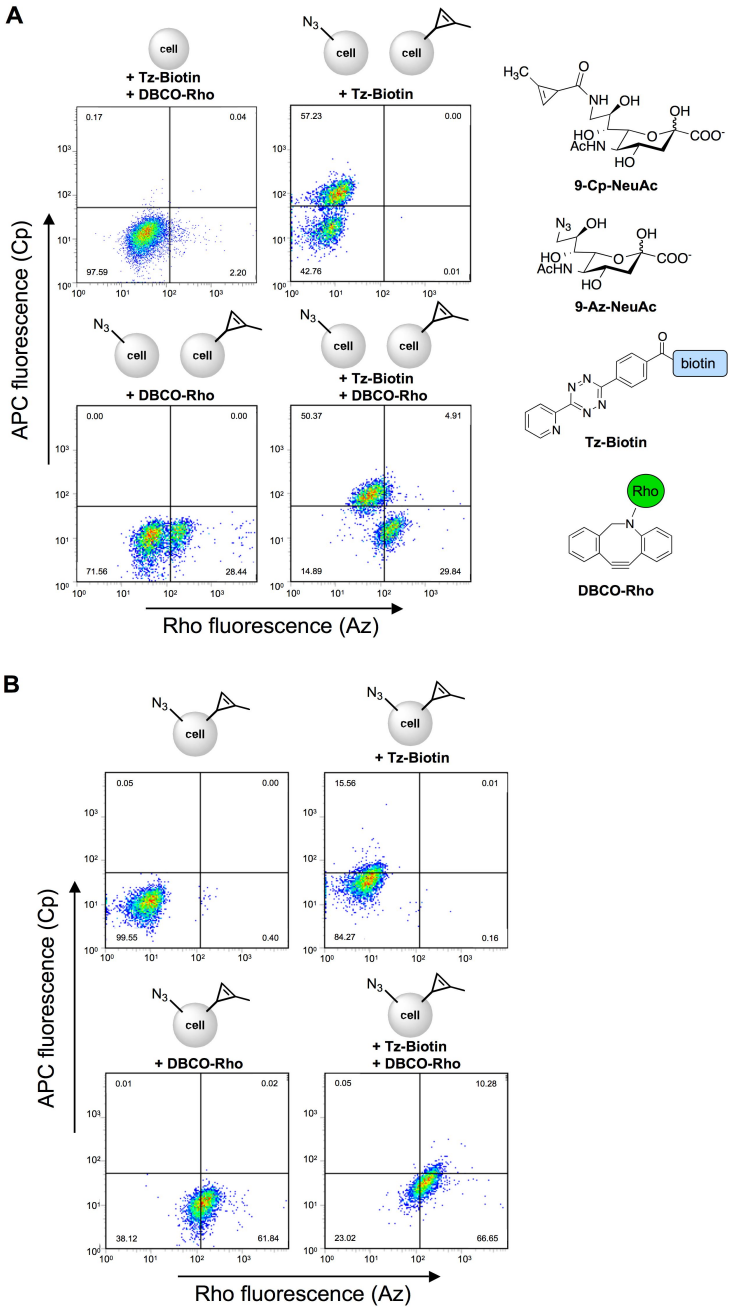

Figure 3-4 Methylcyclopropenes and organic azides can be utilized in tandem for cellular metabolic labeling. (A) Flow cytometry analysis of Jurkat cells treated with **9-Cp-NeuAc** (1 mM), **9-Az-NeuAc** (1 mM), or no sugar for 24 h. After washing, a portion of the **9-Cp-** and **9-Az-NeuAc** cells were mixed. Cell samples were then washed and subsequently reacted with **Tz-biotin** (100 μM), **DBCO-Rho** (100 μM) or both reagents for 1 h at 37 °C. Following staining with APC-avidin, cellular fluorescence was measured. Plots are shown with Rho (azide) and APC (cyclopropene) levels on the x- and y-axes, respectively. (B) Flow cytometry analysis of Jurkat cells incubated with **9-Cp-NeuAc** (1 mM) and **9-Az-NeuAc** (1 mM) simultaneously. After 24 h, the cells were washed, reacted, and analyzed as in (A). For (A) and (B), the same patterns of labeling were apparent in replicate experiments.

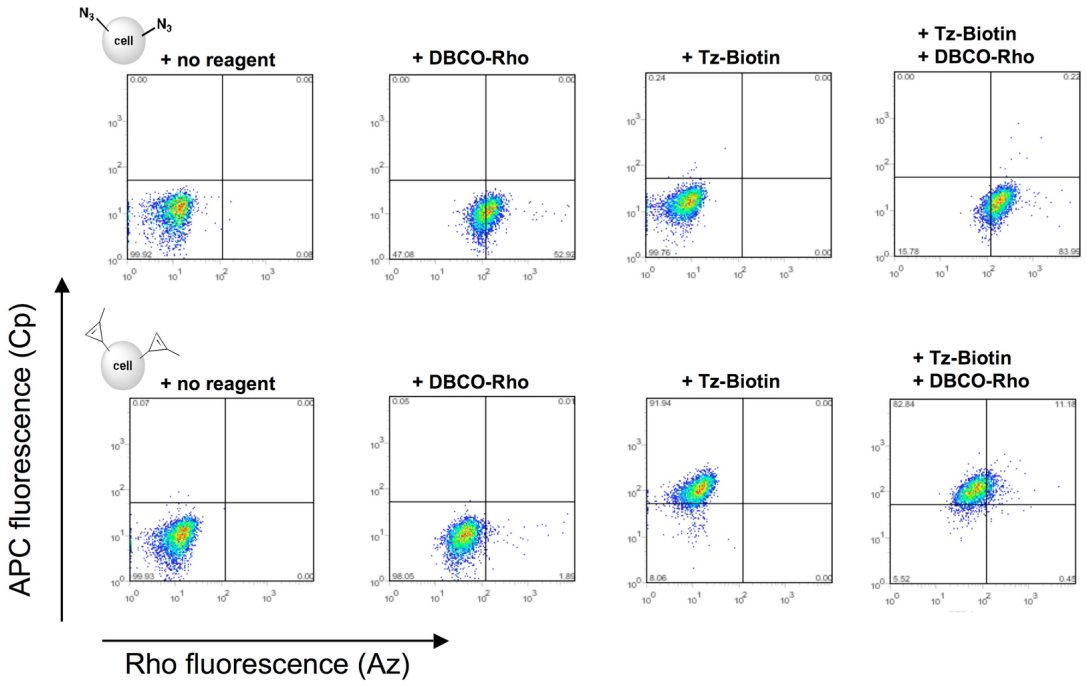

Figure 3-5 Orthogonality of cyclopropene-tetrazine and azide-alkyne reactions. Cells incubated with **9-Cp-NeuAc** (lower panels) or **9-Az-NeuAc** (upper panels) (1 mM) were treated with DBCO-Rho (100 μM), Tz-biotin (100 μM), both reagents, or no reagent and analyzed as in Figure 3-3.

3.4 Isomeric 1,3- and 3,3-disubstituted cyclopropenes can be used to label two distinct sets of biomolecules

In addition to being stable in physiological environments and small in size, cyclopropenes can be readily tuned to access unique reactions. For example, Lin and colleagues demonstrated that 3,3-disubstituted cyclopropenes—regioisomers of the previously discussed 1,3-disubstituted cyclopropenes—can be introduced into proteins and ultimately detected via 1,3-dipolar cycloaddition with nitrile imines (Scheme 3-2) [34]. This reaction, similar to the cyclopropene-tetrazine ligation, proceeds readily in cellular environments. Our lab has later demonstrated that cyclopropene IED-DA and dipolar cycloadditions are orthogonal to one another and, thus, could potentially be used for visualization of biomolecules in tandem [35].

To test this hypothesis, we functionalized model proteins (BSA and lysozyme) with the isomeric cyclopropenes **Cp-NHS** and **3,3-Cp-NHS** using standard coupling conditions (Figure 3-6A). When the proteins were treated with a tetrazine-rhodamine conjugate (**Tz-Rho**), only samples functionalized with 1,3-disubstituted cyclopropenes (**Cp (1,3)**) showed robust dose- and time-dependent labeling, in agreement with our kinetic data (Figures 3-6B, 3-7, and 3-8). No labeling above background was observed with proteins outfitted with 3,3-disubstituted cyclopropenes (**Cp (3,3)**). Both **Cp (1,3)** and **Cp (3,3)** samples were covalently modified with nitrile imines using "photo-click" conditions (Figures 3-6C and 3-8). The fluorescent intensities of the **Cp (1,3)** adducts were somewhat reduced, though, likely due to the decreased absorption efficiency of the

products. When conjugates **Cp (1,3)** and **Cp (3,3)** were subjected to both cycloaddition reactions (treatment with **Tz-Rho**, followed by tetrazole), tetrazine labeling was again only observed for **Cp (1,3)** samples. The **Cp (3,3)** samples, along with unmodified scaffolds on **Cp (1,3)**, were detected following nitrile imine generation (Figures 3-6D and 3-8).

Scheme 3-2 Isomeric 1,3- and 3,3-disubstituted cyclopropenes can be used to label two distinct sets of biomolecules (A) Nitrile imines can be generated from tetrazoles *in situ* via UV irradiation. (B) Cyclopropene derivatives react with tetrazines and 1,3-dipoles.

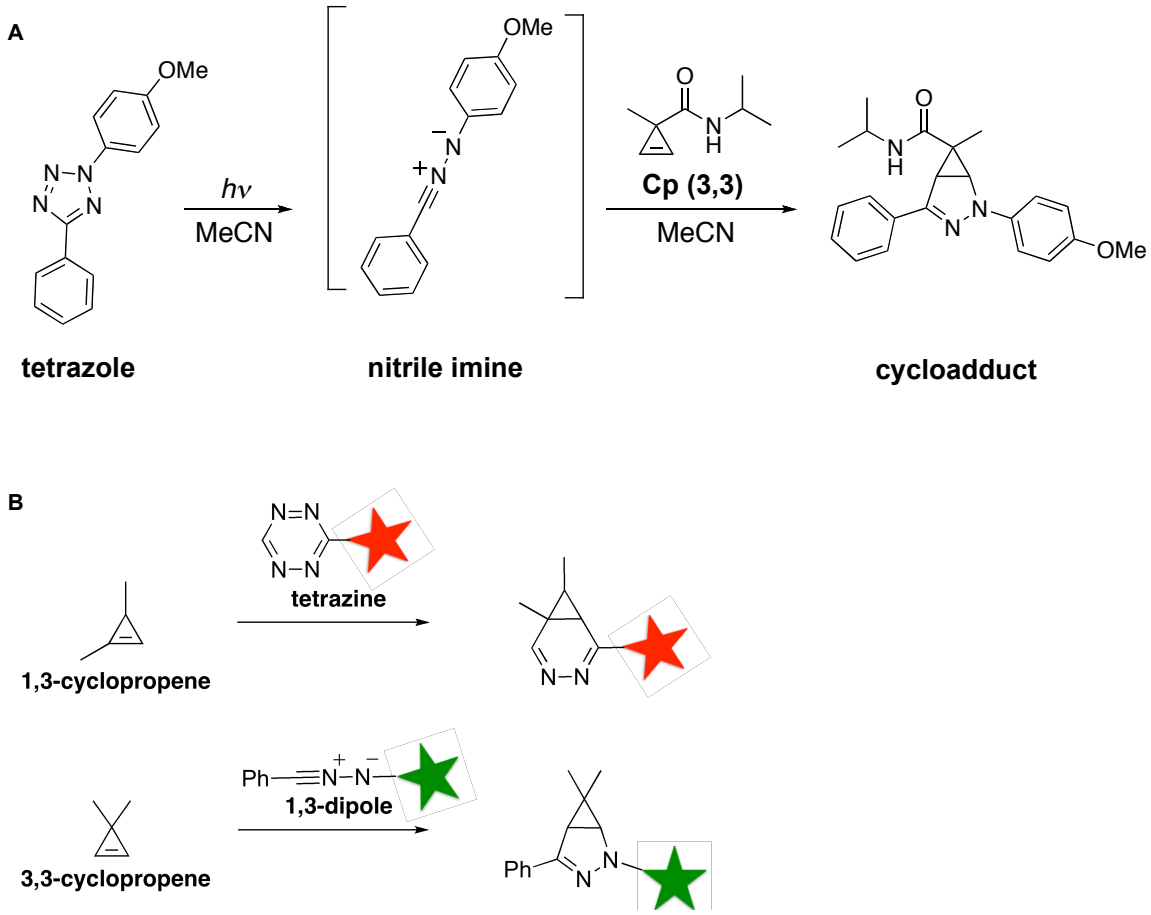

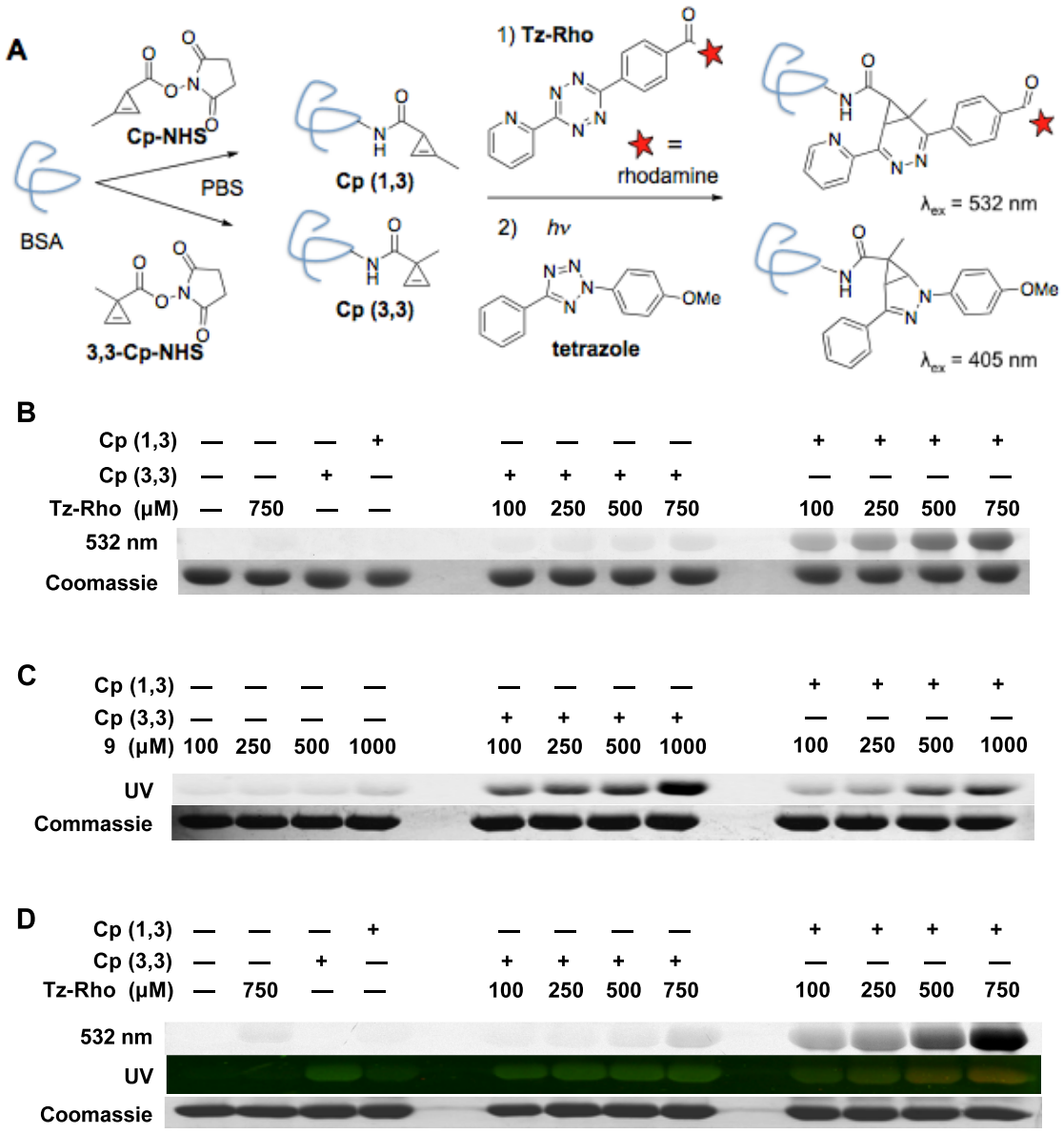

Figure 3-6 Cyclopropenes can be selectively detected on model proteins. (A) Cyclopropenes were appended to BSA. The modified proteins **Cp (1,3)** and **Cp (3,3)** were subsequently reacted with either a tetrazine-rhodamine conjugate (**Tz-Rho**) or **nitrile imine** (generated via photolysis of **tetrazole**). (B) Gel analysis of **Cp (1,3)** or **Cp (3,3)** incubated with **Tz-Rho** (100-750 μM) or no reagent (—) for 1 h. (C) Gel analysis of **Cp (1,3)** or **Cp (3,3)** treated with **tetrazole** (100-1000 μM) and UV irradiation. (D) Analysis of samples treated with **Tz-Rho** (100-750 μM) or no reagent (—), followed by tetrazole (5 mM) and UV irradiation (in gel). The gel was scanned at 532 nm (top) to visualize rhodamine, and also illuminated with UV light (middle) to visualize **nitrile imine** cycloadducts (green). The red color in the UV-illuminated gel (middle) is due to rhodamine fluorescence. For B-D, protein loading was assessed with Coomassie stain.

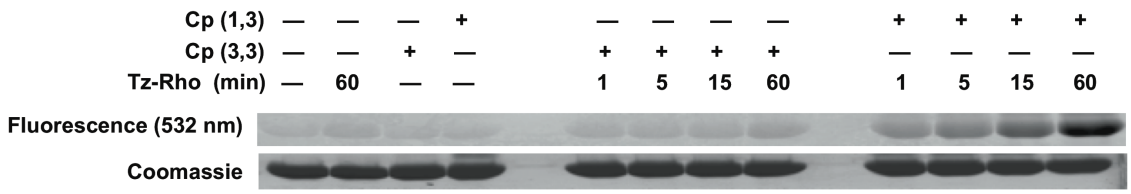

Figure 3-7 Proteins can be labeled with **Tz-Rho** in a time-dependent manner. Gel analysis of **Cp (1,3)** or **Cp (3,3)** incubated with **Tz-Rho** (500 μM) for 0-60 min.

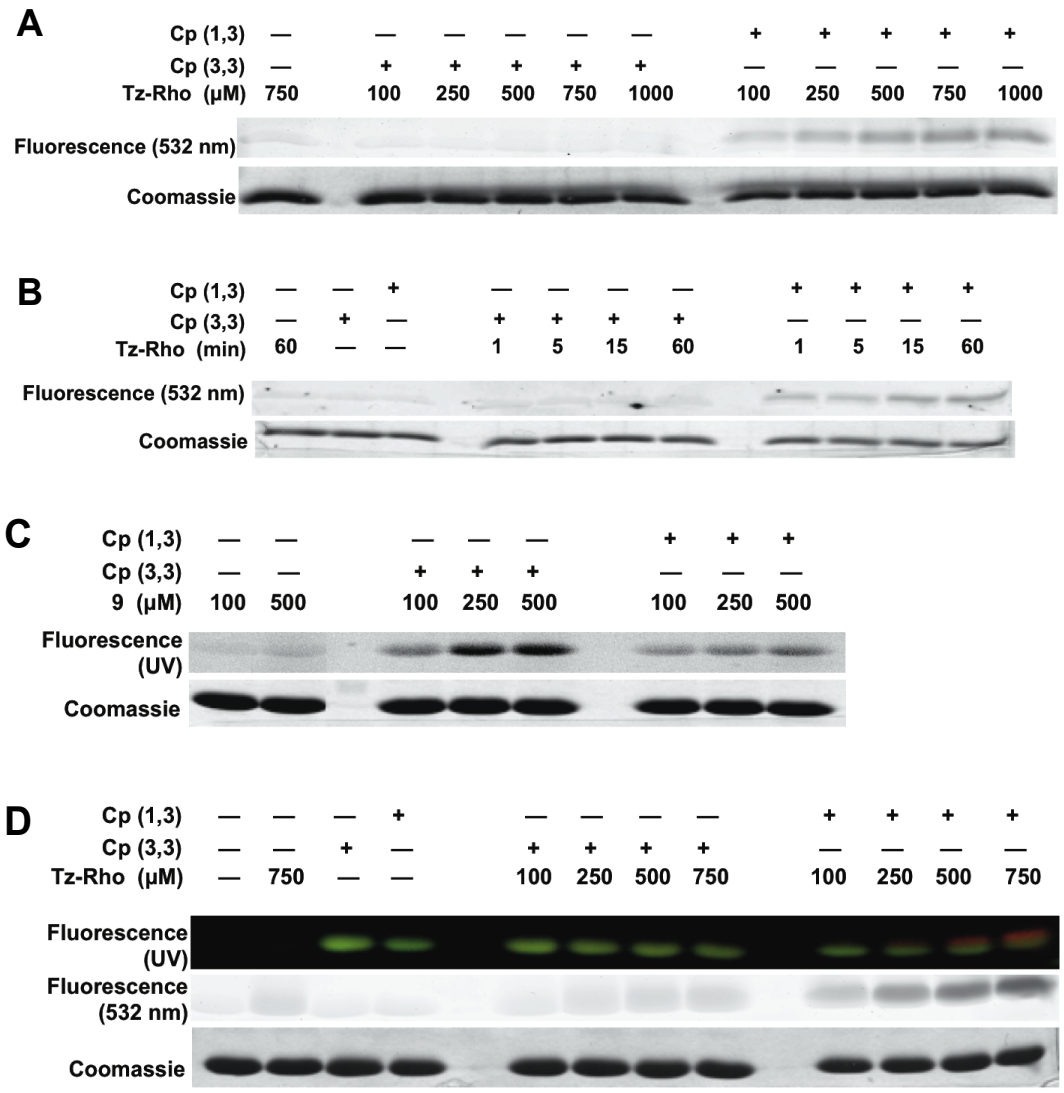

Figure 3-8 Selective cyclopropene reactivity observed with lysozyme conjugates. (A) Gel analysis of the cyclopropene-modified proteins **Cp (1,3)** or **Cp (3,3)** incubated with **Tz-Rho** (100-750 μM) or no reagent (—) for 60 min. (B) Gel analysis of **Cp(1,3)** or **Cp(3,3)** treated with **Tz-Rho** (500 μM) for 0-60 min. (C) Gel analysis of **Cp (1,3)** or **Cp (3,3)** treated with **tetrazole** (100-500 μM) and irradiated with UV light. (D) Gel analysis of **Cp (1,3)** or **Cp (3,3)** treated with **Tz-Rho** (100-750 μM) or no reagent (—), followed by **tetrazole** (500 mM) and UV irradiation. The gel was illuminated with UV light (top panel) to visualize nitrile imine cycloadducts (green) and scanned at 532 nm (middle panel) to visualize rhodamine fluorescence. For B-D, protein loading was assessed with Coomassie stain (lower panels).

3.5 Conclusions and future directions

Functionalized cyclopropenes have been developed for use as chemical reporters in living systems. These scaffolds react with tetrazines to form covalent adducts in high yield and with reaction rates comparable to existing bioorthogonal chemistries. The cyclopropene units are stable in biological environs and can be used to derivatize proteins and other biomolecules. Moreover, these functional groups can be metabolically introduced into cellular glycans, suggesting they are small enough to traverse biosynthetic pathways in live cells. Methylcyclopropenes can also be used concurrently with organic azides, and we anticipate that combinations of these chemical reporters will be widely used for targeting multiple classes of biomolecules in living systems.

We have also identified cyclopropenes that exhibit unique modes of bioorthogonal reactivity. Upon *in vitro* characterization of model proteins tagged with cyclopropenes, we discovered that scaffolds that differ in the placement of a single methyl group (C-1 vs. C-3) exhibit vastly different IED-DA reaction profiles: 1-methyl cyclopropenes can be selectively ligated with tetrazine probes in the presence of 3-methyl cyclopropenes; the unmodified 3-methyl substituted scaffolds can be efficiently ligated via dipolar cycloaddition. The ability to selectively modify isomeric cyclopropenes—and ultimately target them to discrete biomolecules—will facilitate multi-component imaging studies *in vitro* and in live cells. The cyclopropene scaffold also offers unique opportunities for further biocompatible reaction development, including selective nucleophilic additions and normal-demand Diels–Alder reactions. An arsenal of such orthogonal reactions will continue to provide insight into complex biological systems [22,36].

The disubstituted cyclopropenes are also well suited to unraveling the molecular cross-talk between host cells and parasites, a topic introduced in Chapter 2. *T. gondii* has a number of special organelles that it uses for secretion of various signaling molecules into the host cells (Figure 3-9) [37-41]. At the same time the parasite is capable of pilfering the host's complex biomolecules and even parts of organelles (Chapter 2). The biomolecules that are exchanged between the host and the pathogen in this manner are not limited to proteins and glycans, but can also be lipid-based and resemble other metabolites. Being able to attach small chemical reporters to such signaling molecules and trace their locations could reveal important patterns of these types of interactions and, thus, lead to better diagnostics and therapeutics.

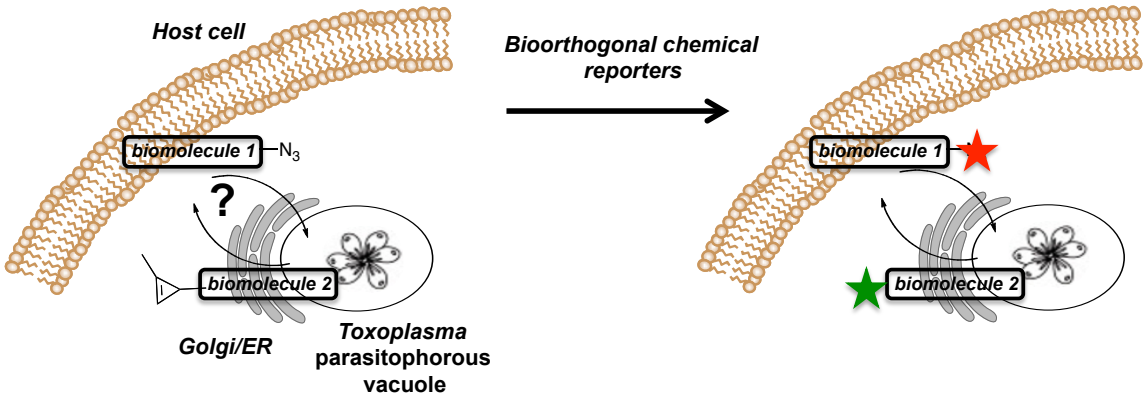

Figure 3-9 Bidirectional visualization of host-pathogen interactions with bioorthogonal chemical reporters.

3.6 Methods and materials

General Synthetic Procedures

Compounds **Cp-acid** [27], **9-Az-NeuAc** [30], **Tz-biotin** [27], **tetrazole** [35], and **3,3-Cp-NHS** [35] were synthesized as previously reported. All other reagents were purchased from commercial sources and used as received without further purification. Reactions were carried out under an inert atmosphere of nitrogen or argon in oven- or flame-dried glassware. Dichloromethane (CH_2Cl_2), tetrahydrofuran (THF), diethyl ether (Et_2O), N,N-dimethylformamide (DMF), methanol (CH_3OH) and triethylamine (NEt_3) were degassed with argon and passed through two 4 x 36 inch columns of anhydrous neutral A-2 (8 x 14 mesh; LaRoche Chemicals; activated under a flow of argon at 350 °C for 12 h). The remaining solvents were of analytical grade and purchased from commercial suppliers. Thin-layer chromatography was performed using Silica Gel 60 F254 plates. Plates were visualized using UV radiation and/or staining with $KMnO_4$. Flash column chromatography was performed with 60 Å (240-400 mesh) silica gel from Sorbent Technologies. ^1H and ^{13}C NMR spectra were recorded on Bruker GN-500 (500 MHz ^1H, 125.7 MHz ^{13}C), CRYO-500 (500 MHz ^1H, 125.7 MHz ^{13}C) or DRX-400 (400 MHz ^1H, 100 MHz ^{13}C) spectrometers. All spectra were collected at 298 K unless otherwise noted. Chemical shifts are reported in ppm values relative to tetramethylsilane or residual non-deuterated NMR solvent, and coupling constants (*J*) are reported in Hertz (Hz). High-resolution mass spectrometry was performed by the University of California, Irvine Mass Spectrometry Center. HPLC runs were conducted on a Varian ProStar equipped with 325 Dual Wavelength UV-Vis Detector. Analytical runs were performed using an Agilent

Polaris 5 C18-A column (4.6 x 150 mm, 5 μm) with a 1 mL/min flow rate. Semi-preparative runs were performed using an Agilent Prep-C18 Scalar column (9.4 x 150 mm, 5 μm) with a 5 mL/min flow rate. The elution gradients for the relevant separations are specified below.

*3.5a Synthesis of NHS-cyclopropenyl ester (**Cp-NHS**)*

Cyclopropene **Cp-acid** (100 mg, 1.02 mmol) was dissolved in 1 mL of CH_2Cl_2. *N*-Hydroxysuccinimide (121 mg, 1.05 mmol) was added, followed by 1-ethyl-3-(3-dimethylaminopropyl)carbodiimide hydrochloride salt (128 mg, 1.07 mmol) and triethylamine (0.3 mL, 2 mmol). The reaction mixture was allowed to stir at rt overnight, then diluted with 50 mL of ethyl acetate and washed with saturated NH_4Cl (2 x 20 mL) followed by brine (1 x 20 mL). The organic layers were combined, dried with MgSO4, filtered, and concentrated in vacuo to afford **Cp-NHS** (90.0 mg, 0.461 mmol, 45%) as a pale yellow oil. The product was used without further purification; TLC R*f* = 0.6 (50% ethyl acetate in hexanes); ^{1}H NMR (400 MHz, $CDCl_3$) δ 6.38 (t, *J* = 1.2 Hz, 1H), 2.78 (br s, 4H), 2.32 (d, *J* = 1.6 Hz, 1H), 2.20 (d, *J* = 1.2 Hz, 3H); ^{13}C NMR (125 MHz, $CDCl_3$) δ 171.1, 169.5, 110.5, 93.3, 25.6, 17.5, 10.3; HRMS (ESI) m/z calcd for $C_9H_9O_4N$ $[M+Na]^+$ 218.0429, found 218.0427.

*3.5b Synthesis of sialic acid-cyclopropene conjugate (**9-Cp-NeuAc**).*

9-Az-NeuAc (0.34 g, 1.0 mmol) was dissolved in 11.0 mL of water and the pH of the reaction mixture was adjusted to 1-2 with acetic acid. After the addition of Pd/C (33 mg), the reaction mixture was stirred under H_2 at rt overnight. The reaction mixture was

then filtered through Celite and concentrated *in vacuo*. The residue was dissolved in 28 mL of dioxane:water (3:2), and the pH of the reaction mixture was adjusted to 8-9 with saturated $NaHCO_3$. NHS-cyclopropenyl ester **Cp-NHS** (0.250 g, 1.26 mmol) was added, and the reaction mixture was stirred at rt overnight. The resulting reaction mixture was then concentrated *in vacuo* and purified via HPLC (0-30% CH_3CN in water over 20 min). Fractions containing the desired product were combined and lyophilized to yield a white solid (45 mg, 12% yield, α:β = 1:5); TLC R*f* = 0.5 (50% CH_3OH in CH_2Cl_2); ^{1}H NMR (500 MHz, CD_3OD, β-anomer) δ 6.56 – 6.57 (m, 1H), 4.01 – 4.03 (m, 2H), 3.94 – 3.98 (m, 1H), 3.71 – 3.74 (m, 1H), 3.66 (dt, *J* = 5.0, 14.0 Hz, 1H), 3.32 (app d, *J* = 9.0 Hz, 1H), 3.26 (ddd, *J* = 5.5, 14.0 Hz, 1H), 2.17 – 2.18 (m, 3H), 2.14 (d, *J* = 4.5 Hz, 1H), 2.10 (d, *J* = 1.5 Hz, 1H), 2.04 (s, 3H), 1.90 (app t, *J* = 12.5 Hz, 1H); ^{13}C NMR (125 MHz, CD_3OD): δ 178.6, 176.1, 172.9, 112.7, 96.3, 95.0, 70.4, 70.2, 69.6, 67.4, 52.6, 43.2, 40.5, 21.5, 21.3, 9.1; HRMS (ESI) m/z calcd $C_9H_9O_4N$ $[M-H]^-$ 387.1404, found 387.1412.

3.5c Metabolic labeling studies

Jurkat cells were plated at a density of ~1 x 10^6 cells/mL in RPMI media (Gibco) supplemented with 10% fetal bovine serum (FBS), 10% penicillin/streptomycin, and either **9-Cp-NeuAc** (0-2 mM), **9-Az-NeuAc** (0-2 mM), both sugars in tandem (1 mM each) no sugar, or a control sugar (**NeuAc**, 1-2 mM or peracetylated **ManNAc**, 25 mM). All cell cultures were incubated for 24-48 h in a 5% CO_2, water-saturated incubator at 37 °C. The presence of cyclopropenes or azides in cell-surface glycoconjugates was determined by reaction with **Tz-Biotin**, sulfo-dibenzocyclooctyne-biotin (**DBCO-Biotin**; Click Chemistry Tools, Scotsdale, AZ), or dibenzocyclooctyne-PEG-carboxyrhodamine

(**DBCO-Rho**, Click Chemistry Tools, Scotsdale, AZ). Briefly, the cells were rinsed with PBS containing 1% bovine serum albumin (FACS buffer), and then reacted with **Tz-Biotin** (100 mM, 1 h, 37 °C), **DBCO-Biotin** (100 uM, 1 h, 37 °C) or **DBCO-Rho** (100 uM, 1 h, 37 °C). The cells were subsequently washed with FACS buffer and, when necessary, stained with APC-avidin (Invitrogen, 1:100 dilution in FACS buffer) for 30 min on ice. The fluorescence of the labeled cells was analyzed by flow cytometry on an LSR-II flow cytometer (BD Biosciences). For each cell population, 10,000 live cells were analyzed for each replicate experiment. Data were analyzed using FloJo software (Tree Star, Inc.).

3.5d Cyclopropene conjugation to protein scaffolds

Bovine serum albumin (BSA) or lysozyme conjugates were prepared by treating the proteins with cyclopropene esters as previously described. In brief, BSA or lysozyme (400 μL of a 20 mg/mL solution in PBS, pH 7.4) was treated with **Cp-NHS** or **3,3-Cp-NHS** (100 μL of a 25 mM solution in DMSO). The lysozyme solutions were incubated at 37 °C (with shaking) for 4 h, while the BSA solutions were allowed to stand at RT for 12 h. The modified proteins were isolated using P-10 BioGel® (BioRad), eluting with nanopure water.

3.5e In-gel fluorescence analysis of cyclopropene-tetrazine reactivity

Purified protein conjugates were diluted to 2 mg/mL with PBS (pH 7.4), treated with **Tz-Rho** (1-7.5 μL of a 5 mM DMSO/PBS solution), and combined with additional PBS to total 50 μL. The labeling reactions were run for 1-60 min, and protein isolates (4-

9 μg) were analyzed on SDS-PAGE as previously described.6 Gels were analyzed by in-gel fluorescence scanning (GE Typhoon TRIO+ Variable Mode Imager, 532 nm excitation/580 nm emission). Gels were also stained with Coomassie Brilliant Blue. Purified protein conjugates (40 μL of 2 mg/mL solutions in PBS) were treated with **Tz-Rho** (1-7.5 μL of a 5 mM stock solution in 1:1 DMSO:PBS), and combined with additional PBS to a total volume of 50 μL. After 1-60 min of fluorophore labeling, the modified protein samples were purified by passage over P-10 BioGel® and eluting with PBS.The concentrations of the isolated protein samples were measured using a DC Protein Assay kit (BioRad). Protein isolates (4-9 μg) were analyzed by gel electrophoresis using 10% or 12% polyacrylamide gels. Gels were rinsed in destain buffer (50% D.I. H_2O, 40% CH_3OH, 10% acetic acid) and analyzed by in-gel fluorescence measurements on a GE Typhoon TRIO+ Variable Mode Imager. **Tz-Rho** fluorescence was measured with a 532 nm excitation wavelength and 580 nm emission. **Tetrazole** fluorescence was measured on UV-transilluminator (MultiDoc-It Digital Imaging System). Total protein loading was confirmed by subsequent staining with Coomassie Brilliant Blue.

3.5f In-gel fluorescence analysis of nitrile imine reactivity

Protein conjugates were labeled with nitrile imines using a procedure reported by Lin and coworkers [34]. Purified proteins (40 μL of 2 mg/mL solutions in PBS) were added to a 96-well plate and treated with tetrazole 9 (1-10 μL of a 5 mM solution in DMSO). The samples were irradiated with a UV lamp (302 nm, Zilla UVB 20 watts) for 5 min. For these experiments, the lamp was placed directly on top of the 96-well plate.

The labeled samples were subsequently analyzed via SDS-PAGE as described above. Gels were visualized with a UV-transilluminator (MultiDoc-It Digital Imaging System) and stained with Coomassie Brilliant Blue.

3.5g Dual protein modification

Solution reactions

Protein conjugates (40 μL of 2 mg/mL solutions in PBS) were added to a 96-well plate and treated with **Tz-Rho** (1-7.5 μL of a 5 mM stock in 1:1 DMSO:PBS) for 1 h at rt. **Tetrazole** (5.6 μL of a 5 mM solution in DMSO) or no reagent was added to each well, and the mixtures were irradiated with a UV lamp for 5 min (302 nm, Zilla UVB 20 watts). For these experiments, the lamp was placed directly on top of the 96-well plate. The samples were then analyzed via SDS-PAGE as described above. Gels were visualized using a fluorescence scanner (GE Typhoon TRIO+ Variable Mode Imager, 532 nm excitation/580 nm emission) and a UV-transilluminator (MultiDoc-It Digital Imaging System) prior to staining with Coomassie Brilliant Blue.

In-gel reactions

Following reaction with **Tz-Rho**, some protein samples were analyzed via SDS-PAGE and visualized by in-gel fluorescence scanning (GE Typhoon TRIO+ Variable Mode Imager, 532 nm excitation/580 nm emission). The gels were then soaked in a solution of 9 (5 mM in DMSO) for 1 h at RT, rinsed in destain buffer (10% AcOH, 40% MeOH), and photoirradiated (302 nm, Zilla UVB 20 watts). Gels were visualized using a UV-transilluminator (MultiDoc-It Digital Imaging System) and stained with Coomassie Brilliant Blue.

References

(1) Chang, P. V.; Prescher, J. A.; Hangauer, M. J.; Bertozzi, C. R. Imaging cell surface glycans with bioorthogonal chemical reporters. *J. Am. Chem. Soc.* **2007**, *129*, 8400.

(2) Prescher, J. A.; Bertozzi, C. R. Chemistry in living systems. *Nat. Chem. Biol.* **2005**, *1*, 13.

(3) Prescher, J. A.; Dube, D. H.; Bertozzi, C. R. Chemical remodelling of cell surfaces in living animals. *Nature* **2004**, *430*, 873.

(4) Hang, H. C.; Wilson, J. P.; Charron, G. Bioorthogonal chemical reporters for analyzing protein lipidation and lipid trafficking. *Acc. Chem. Res.* **2011**, *44*, 699.

(5) Haun, J. B.; Devaraj, N. K.; Hilderbrand, S. A.; Lee, H.; Weissleder, R. Bioorthogonal chemistry amplifies nanoparticle binding and enhances the sensitivity of cell detection. *Nat. Nanotechnol.* **2010**, *5*, 660.

(6) Sletten, E. M.; Bertozzi, C. R. Bioorthogonal chemistry: fishing for selectivity in a sea of functionality. *Angew. Chem., Int. Ed.* **2009**, *48*, 6974.

(7) Debets, M. F.; van Berkel, S. S.; Dommerholt, J.; Dirks, A. J.; Rutjes, F. P. J. T.; van Delft, F. L. Bioconjugation with strained alkenes and alkynes. *Acc. Chem. Res.* **2011**, *44*, 805.

(8) Lang, K.; Davis, L.; Wallace, S.; Mahesh, M.; Cox, D. J.; Blackman, M. L.; Fox, J. M.; Chin, J. W. Genetic encoding of bicyclononynes and trans-cyclooctenes for site-specific protein labeling in vitro and in live mammalian cells via rapid fluorogenic Diels-Alder reactions. *J. Am. Chem. Soc.* **2012**, *134*, 10317.

(9) Chen, W.; Wang, D.; Dai, C.; Hamelberg, D.; Wang, B. Clicking 1,2,4,5-tetrazine and cyclooctynes with tunable reaction rates. *Chem. Commun.* **2012**, *48*, 1736.

(10) Plass, T.; Milles, S.; Koehler, C.; Schultz, C.; Lemke, E. A. Genetically encoded copper-free click chemistry. *Angew. Chem., Int. Ed.* **2011**, *50*, 3878.

(11) Liang, Y.; Mackey, J. L.; Lopez, S. A.; Liu, F.; Houk, K. N. Control and design of mutual orthogonality in bioorthogonal cycloadditions. *J. Am. Chem. Soc.* **2012**, *134*, 17904.

(12) Sanders, B. C.; Friscourt, F.; Ledin, P. A.; Mbua, N. E.; Arumugam, S.; Guo, J.; Boltje, T. J.; Popik, V. V.; Boons, G. J. Metal-free sequential [3 + 2]-dipolar cycloadditions using cyclooctynes and 1,3-dipoles of different reactivity. *J. Am. Chem. Soc.* **2011**, *133*, 949.

(13) Braše, S.; Gil, C.; Knepper, K.; Zimmermann, V. Organic azides: an exploding diversity of a unique class of compounds. *Angew.Chem. Int. Ed.* **2005**, *44*, 5188.

(14) El-Sagheer, A. H.; Sanzone, A. P.; Gao, R.; Tavassoli, A.; Brown, T. Biocompatible artificial DNA linker that is read through by DNA polymerases and is functional in Escherichia coli. *Proc. Natl. Acad. Sci. U.S.A.* **2011**, *108*, 11338.

(15) Ngo, J. T.; Tirrell, D. A. Noncanonical amino acids in the interrogation of cellular protein synthesis. *Acc. Chem. Res.* **2011**, *44*, 677.

(16) Saxon, E.; Bertozzi, C. R. Cell surface engineering by a modified Staudinger reaction. *Science* **2000**, *287*, 2007.

(17) Agard, N. J.; Prescher, J. A.; Bertozzi, C. R. A strain-promoted [3 + 2] azide-alkyne cycloaddition for covalent modification of biomolecules in living systems. *J. Am. Chem. Soc.* **2004**, *126*, 15046.

(18) Baskin, J. M.; Prescher, J. A.; Laughlin, S. T.; Agard, N. J.; Chang, P. V.; Miller, I. A.; Lo, A.; Codelli, J. A.; Bertozzi, C. R. Copper-free click chemistry for dynamic in vivo imaging. *Proc. Natl. Acad. Sci. U.S.A.* **2007**, *104*, 16793.

(19) Jewett, J. C.; Sletten, E. M.; Bertozzi, C. R. Rapid Cu-free click chemistry with readily synthesized biarylazacyclooctynones. *J. Am. Chem. Soc.* **2010**, *132*, 3688.

(20) Ning, X.; Guo, J.; Wolfert, M. A.; Boons, G. J. Visualizing metabolically labeled glycoconjugates of living cells by copper-free and fast huisgen cycloadditions. *Angew. Chem. Int. Ed.* **2008**, *47*, 2253.

(21) Blackman, M. L.; Royzen, M.; Fox, J. M. The Tetrazine Ligation: Fast Bioconjugation based on Inverse-electron-demand Diels-Alder Reactivity. *J. Am. Chem. Soc.* **2008**, *130*, 13518.

(22) Willems, L. I.; Verdoes, M.; Florea, B. I.; van der Marel, G. A.; Overkleeft, H. S. Two-step labeling of endogenous enzymatic activities by Diels-Alder ligation. *ChemBioChem* **2010**, *11*, 1769.

(23) Dommerholt, J.; Schmidt, S.; Temming, R.; Hendriks, L. J.; Rutjes, F. P.; van Hest, J. C.; Lefeber, D. J.; Friedl, P.; van Delft, F. L. Readily accessible bicyclononynes for bioorthogonal labeling and three-dimentional imaging of living cells. *Angew. Chem. Int. Ed.* **2010**, *49*, 9422.

(24) Devaraj, N. K.; Weissleder, R. Biomedical applications of tetrazine cycloadditions. *Acc. Chem. Res.* **2011**, *44*, 816.

(25) Karver, M. R.; Weissleder, R.; Hilderbrand, S. A. Bioorthogonal reaction pairs enable simultaneous, selective, multi-target imaging. *Angew. Chem. Int. Ed.* **2012**, *51*, 920.

(26) Devaraj, N. K.; Weissleder, R.; Hilderbrand, S. A. Tetrazine-based cycloadditions: application to pretargeted live cell imaging. *Bioconjugate Chem.* **2008**, *19*, 2297.

(27) Patterson, D. M.; Nazarova, L. A.; Xie, B.; Kamber, D. N.; Prescher, J. A. Functionalized cyclopropenes as bioorthogonal chemical reporters. *J. Am. Chem. Soc.* **2012**, *134*, 18638.

(28) Yang, J.; Šeckute, J.; Cole, C. M.; Devaraj, N. K. Live-cell imaging of cyclopropene tags with fluorogenic tetrazine cycloadditions. *Angew. Chem. Int. Ed.* **2012**, *51*, 7476.

(29) Campbell, C. T.; Sampathkumar, S.-G.; Yarema, K. J. Metabolic oligosaccharide engineering: perspectives, applications, and future directions. *Mol. BioSyst.* **2007**, *3*, 187.

(30) Han, S.; Collins, B. E.; Bengtson, P.; Paulson, J. C. Homomultimeric complexes of CD22 in B cells revealed by protein-glycan cross-linking. *Nat. Chem. Biol.* **2005**, *1*, 93.

(31) Luchansky, S. J.; Hang, H. C.; Saxon, E.; Grunwell, J. R.; Yu, C.; Dube, D. H.; Bertozzi, C. R. Constructing azide-labeled cell surfaces using polysaccharide biosynthetic pathways. *Methods Enzymol.* **2003**, *362*, 249.

(32) Oetke, C.; Brossmer, R.; Mantey, L. R.; Hinderlich, S.; Isecke, R.; Reutter, W.; Keppler, O. T.; Pawlita, M. Versatile biosynthetic engineering of sialic acid in living cells using synthetic sialic acid analogues. *J. Biol. Chem.* **2002**, *277*, 6688.

(33) Sachdeva, A.; Wang, K.; Elliott, T.; Chin, J. W. Concerted, rapid, quantitative, and site-specific dual labeling of proteins. *J. Am. Chem. Soc.* **2014**, *136*, 7785-7788.

(34) Yu, Z.; Pan, Y.; Wang, Z.; Wang, J.; Lin, Q. Genetically encoded cyclopropene directs rapid, photoclick-chemistry-mediated protein labeling in mammalian cells. *Angew. Chem. Int. Ed.* **2012**, *51*, 10600.

(35) Kamber, D. N.; Nazarova, L. A.; Liang, Y.; Lopez, S. A.; Patterson, D. M.; Shih, H.-W.; Houk, K. N.; Prescher, J. A. Isomeric cyclopropenes exhibit unique bioorthogonal reactivities. *J. Am. Chem. Soc.* **2013**, *135*, 13680−13683.

(36) Sletten, E. M.; Bertozzi, C. R. A bioorthogonal quadricyclane ligation. *J. Am. Chem. Soc.* **2011**, *133*, 17570.

(37) Carruthers, V.; Boothroyd, J. C. Pulling together: an integrated model of *Toxoplasma* cell invasion. *Curr. Opin. Microbiol.* **2007**, *10*, 83-89.

(38) Boothroyd, J. C.; Dubremetz, J. F. Kiss and spit: the dual roles of *Toxoplasma* rhoptries. *Nat. Rev. Micro* **2008**, *6*, 79-88.

(39) Hager, K. M.; Striepen, B.; Tilney, L. G.; Roos, D. S. The nuclear envelope serves as an intermediary between the ER and Golgi complex in the intracellular parasite *Toxoplasma gondii*. *J. Cell Sci.* **1999**, *112*, 2631-2638.

(40) Stedman, T. T.; Sussmann, A. R.; Joiner, K. A. *Toxoplasma gondii* Rab6 mediates a retrograde pathway for sorting of constitutively secreted proteins to the Golgi complex. *J. Biol. Chem*. **2003**, *278*, 5433-5443.

(41) Sheiner, L.; Dowse, T. J.; Soldati-Favre, D. Identification of trafficking determinants for polytopic rhomboid proteases in *Toxoplasma gondii. Traffic* **2008**, *9*, 665-677.

CHAPTER 4: Methylene cyclopropanes are robust chemical reporters

4.1 Introduction

Bioorthogonal chemical reporters have been widely used to probe biological systems. Only a handful of organic functional groups and potential chemical reporters can be used to study biological systems, as the majority of biomolecules reside in aqueous media, and in the presence of molecular oxygen and various nucleophiles [1-5]. The chemical reporter also needs to be small in size to not perturb the biomolecule's function, and possess specific reactivity towards its corresponding probe (Figure 4-1A). With many functional groups known to date, only a few of them show promise for use in complex biological environments.

One functional moiety that has recently attracted attention is a small three-membered ring microcycle—cyclopropene [6-9]. This chemical reporter is small in size and, thus, compatible with a variety of biomolecules, such as lipids, glycans and proteins. The earliest reported 1,3-disubstituted cyclopropene reacts efficiently with tetrazines, and can be used for biomolecule labeling [6,7]. The isomer of this motif—3,3-disubstituted cyclopropene—is similarly bioorthogonal. It differs by the placement of one methyl group, and, intriguingly, has no reactivity with tetrazines. It reacts readily with nitrile imines to form stable cycloadducts [8,9]. This remarkable tunability of the cyclopropene core (Figure 4-1B) shows a great promise for developing new bioorthogonal reactions

that are orthogonal to one another and, thus, can be used for simultaneous studying of multiple biomolecules.

Despite their versatility, cyclopropenes have some liabilities with reporter stability in biological media, precluding long-term visualization studies. Cyclopropenes are prone to nucleophilic attack in biological media and polymerization at room temperature [10-12]. Thus, finding new chemical reporters that are both stable in biological environments and orthogonal to other reporters would be a tremendous help for studying complex biological systems.

To address these issues, we became interested in a related microcycle—methylene cyclopropane. This motif is found in the natural product hypoglycin A, occuring in Jamaican fruit (Figure 4-1C), suggesting that it is stable in biological environments and likely compatible with a number of metabolic and biosynthetic pathways [13]. Importantly, this functionality possesses a significant amount of strain energy, suggesting that it might also make a good candidate for IED-DA reactivity.

To test these hypotheses, I first synthesized a set of model methylene cyclopropane derivatives. I then evaluated methylene cyclopropane's stability in biological media. Furthermore, I found that methylene cyclopropane reacts with tetrazines via IED-DA. I also tested its stability and usability for labeling model biomolecules.

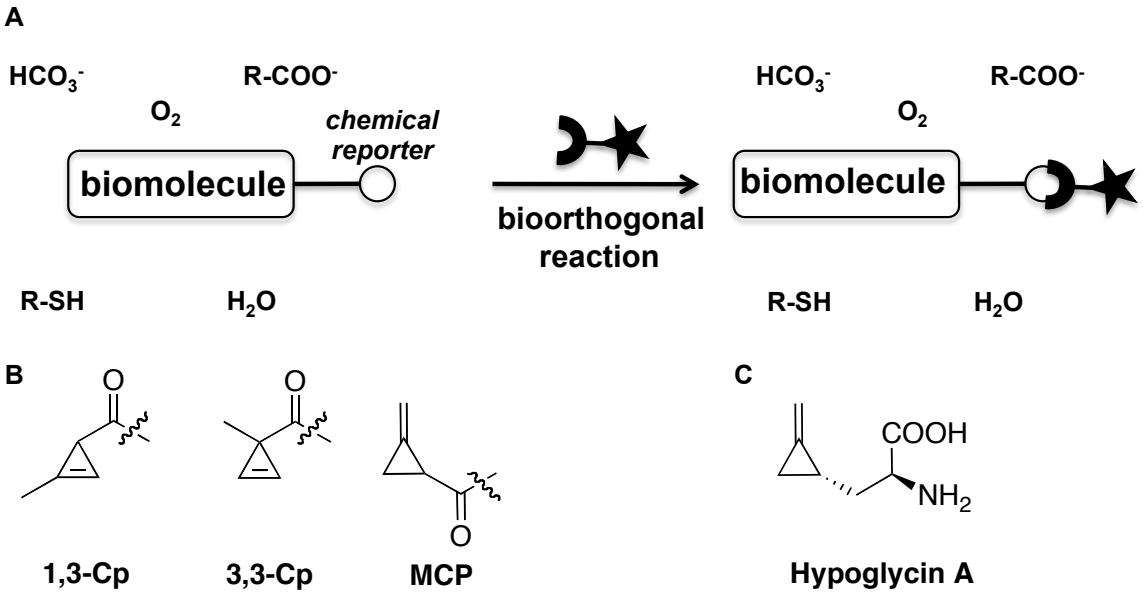

Figure 4-1 Series of isomeric cyclopropenes as chemical reporters. (A) A bioorthogonal reaction. (B) Structures of isomeric three-member ring microcycles. (C) Structure of hypoglycin A.

4.2 Design and synthesis of methylene cyclopropane units

We first synthesized a model methylene cyclopropane derivative **4.4** (Scheme 4-1). We initially converted the commercially available 2-bromopropene to ester **4.1** via rhodium-catalyzed cyclopropanation [14-16]. The resulting product **4.1** was then subjected to β-hydride elimination with sodium hydride. The resulting ester **4.2** was then hydrolyzed with KOH in aqueous methanol. Upon isolation, the free acid **4.3** was activated with pentafluorophenyl trifluoroacetate and then treated with isopropylamine to furnish the desired methylene cyclopropane amide **4.4**.

Scheme 4-1 Synthesis of methylene cyclopropane amide **4.4**.

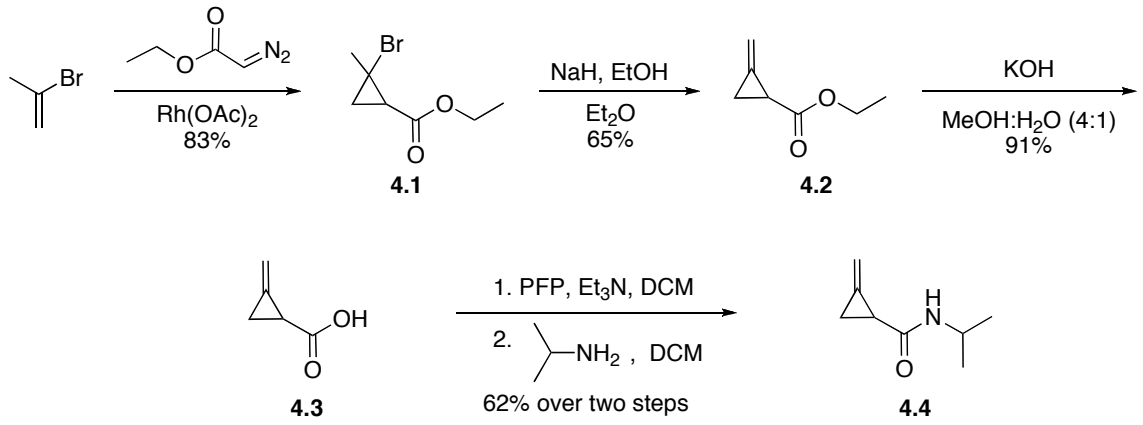

4.3 Methylene cyclopropanes are stable in aqueous solution and in the presence of cysteine

To test the stability of the model methylene cyclopropane amide **4.4**, I incubated **4.4** in the presence of 5 mM L-cysteine in 8% DMSO-d_6 in deuterated PBS. The reaction mixture was monitored via NMR. No cysteine addition products were observed after 8 h of incubation at 37°C. This result implies that methylene cyclopropane unit should be stable under physiological conditions and, thus, has the potential to be a novel chemical reporter.

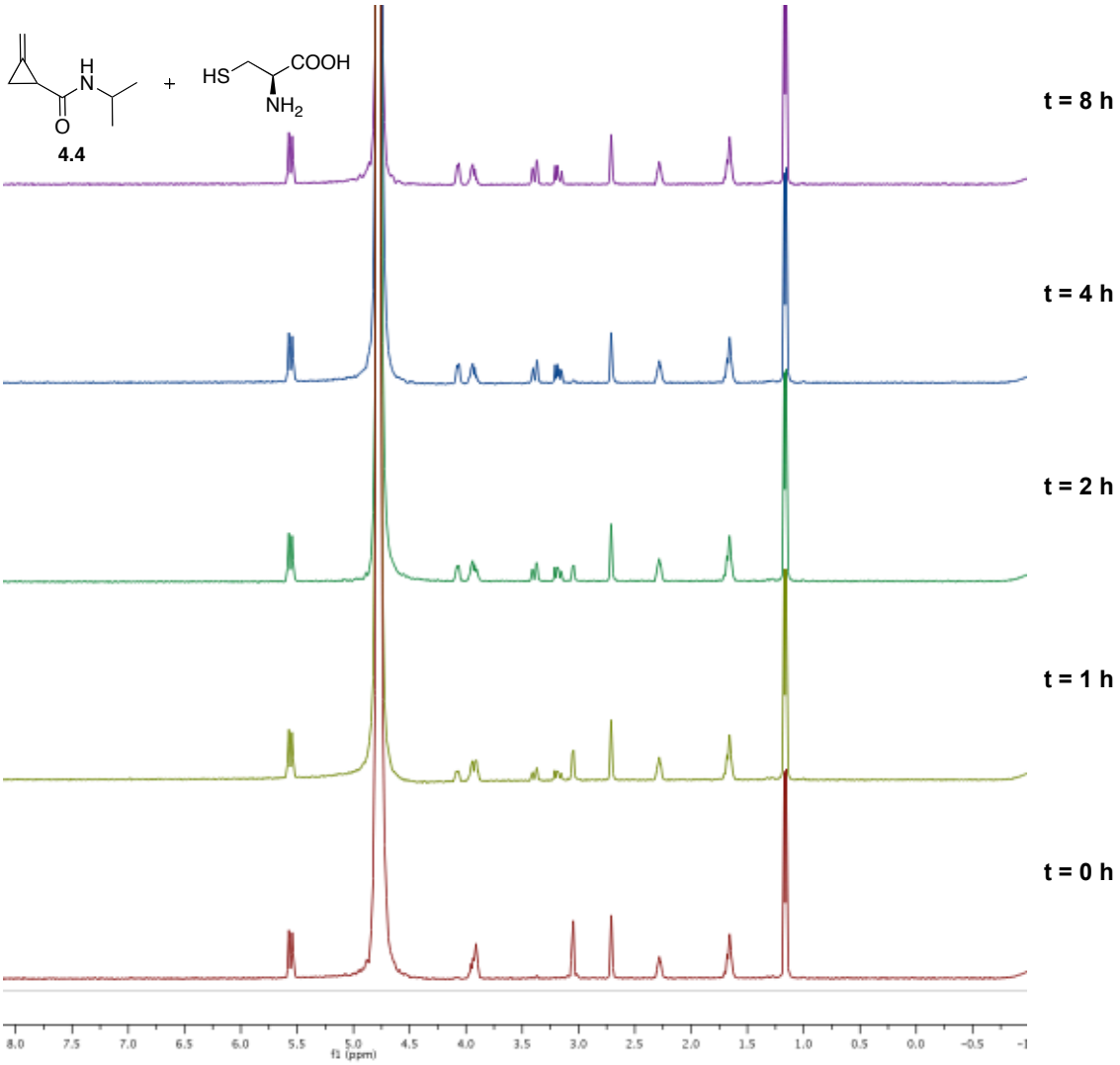

Figure 4-2 Methylene cyclopropane amide **4.4** was incubated with 5 mM of L-cysteine at 37°C and monitored by NMR.

4.4 Methylene cyclopropanes can be covalently ligated via IED-DA reactions

Encouraged by the stability data, we investigated the reactivity of **4.4.** The amide was treated with mono- and di-substituted tetrazine probes. Upon reacting commercially available dipyridyl tetrazine with **4.4** in deuterated chloroform, we observed clean conversion of the starting microcycle to the cycloadduct **4.6**. The second-order reaction rate was calculated to be (1.14 ± 0.22) x 10^{-4} $M^{-1}s^{-1}$. We did not observe any reactivity between amide **4.4** and dipyridyl tetrazine **4.5** in a mixture of 10% DMSO in deuterated PBS due to the limited solubility of the tetrazine and its decreased stability in aqueous media. The reaction between **4.4** and mono-substituted tetrazines **4.6** and **4.7** exhibited second-order rate constants of (6.93 ± 1.07 – 7.33 ± 1.14) x 10^{-4} $M^{-1}s^{-1}$ (Table 4-1). While not as fast as the disubstituted cyclopropene-tetrazine cycloadditions, these reactions rates are on par with some bioorthogonal transformations, such as the Staudinger ligation. Interestingly, the product of the reaction of dipyridyl tetrazine with methylene cyclopropane undergoes an intriguing rearrangement, which ultimately provides an aromatic product (Scheme 4-2).

Table 4-1 Second-order rate constants for the reaction between tetrazine and amide **4.4**. The reactions were run at rt and monitored via ^{1}H NMR.

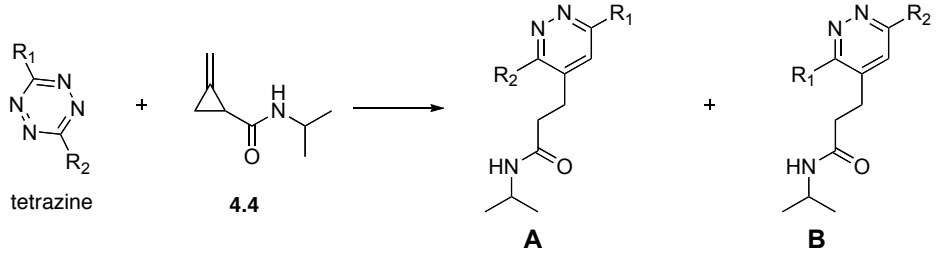

tetrazine	R_1	R_2	solvent	k_2 (x 10^{-4} M^{-1} s^{-1})	A:B
4.5	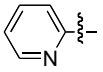	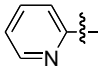	10% DMSO/PBS	N/R*	–
4.5	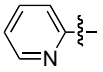	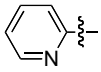	$CDCl_3$	1.14 ± 0.22	N/A
4.6	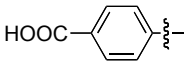	H	10% DMSO/PBS	7.33 ± 1.14	1.3
4.7	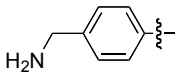	H	10% DMSO/PBS	6.93 ± 1.07	2.1-2.6

Scheme 4-2 Putative mechanism for the formation of the cycloadduct of methylene cyclopropane amide **4.4** and dipyridyl tetrazine.

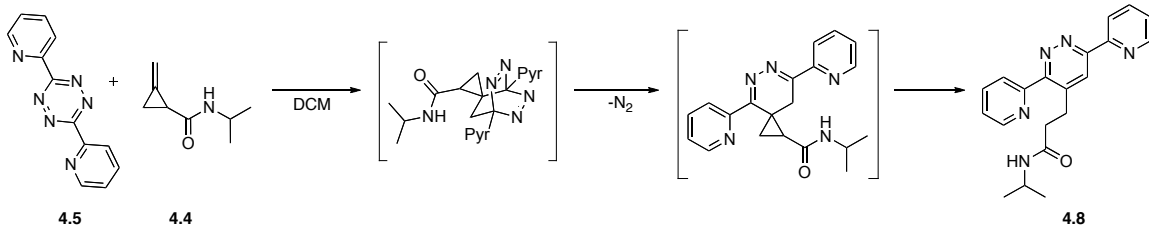

4.5 Labeling a model protein with the methylene cyclopropane-tetrazine ligation

The stability of methylene cyclopropane and the structure of the resulting cycloadduct render this transformation particularly useful for some applications, such as protein labeling. Toward this end, I attached it to a model protein—lysozyme (Figure 4-3A). The modified protein was detected by ESI mass spectrometry. As can be seen from Figure 4-3B, one to two modifications were observed on lysozyme.

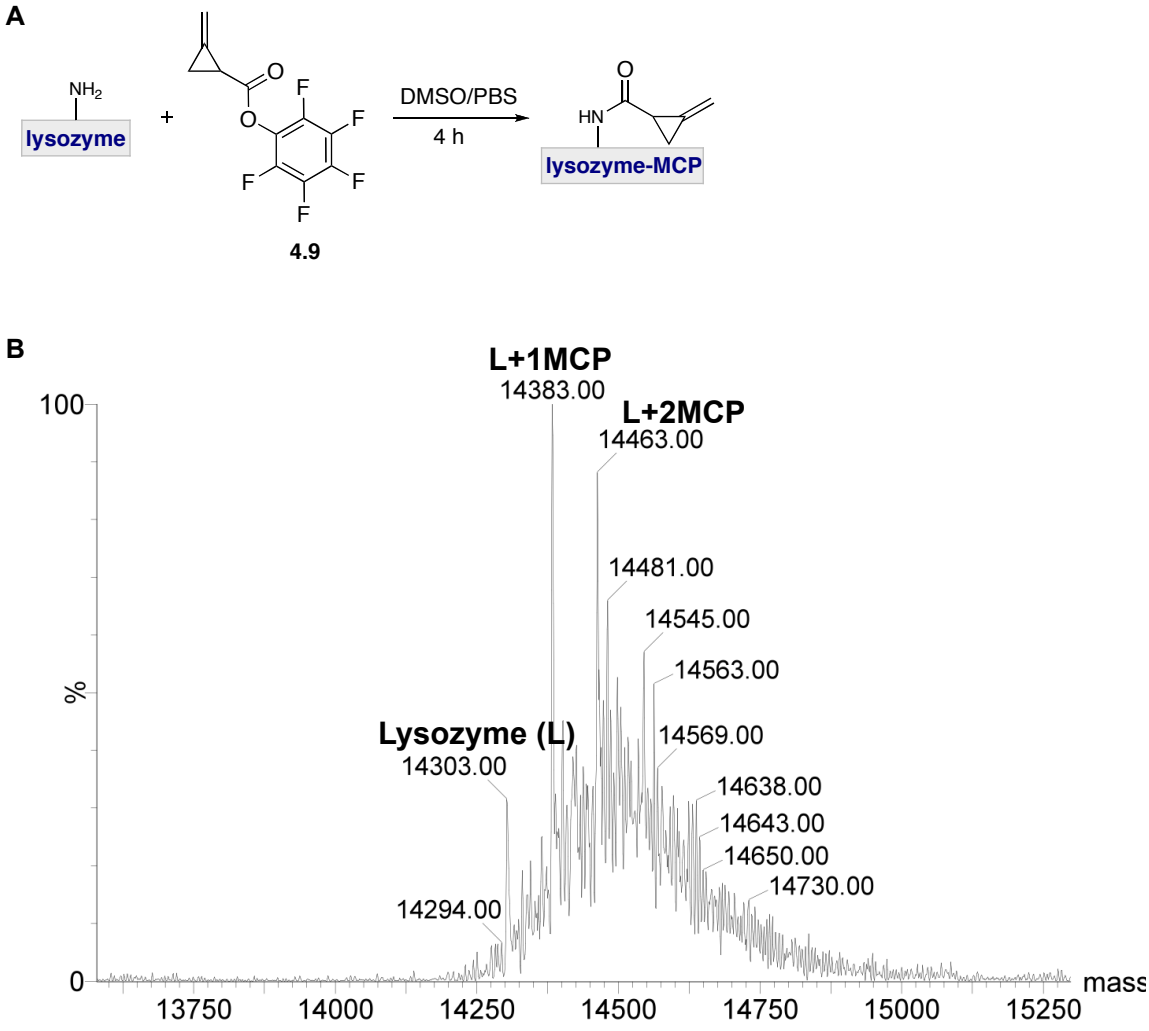

Figure 4-3 Labeling lysozyme with methylene cyclopropane. (A) Methylene cyclopropane can be attached to a model protein (lysozyme) via reaction with MCP-PFP ester. (B) MS-ESI analysis of lysozyme sample labeled with methylene cyclopropane.

I then tested the lysozyme-MCP conjugate's reactivity with model tetrazine **4.7**. The modified protein was reacted with aqueous solution of **Tz-biotin** and then visualized via Western blot, probing with Streptavidin (Figure 4-4A). The intensity of the observed signal was found to be both time- and dose-dependent (Figures 4-4B and 4-4C).

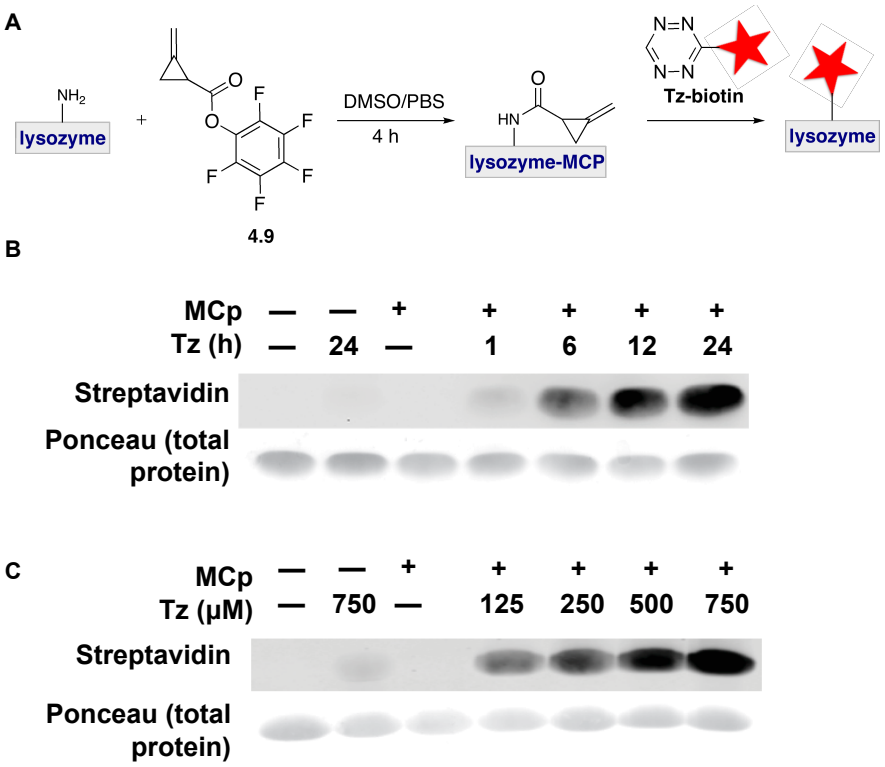

Figure 4-4 Labeling lysozyme with the methylene cyclopropane-tetrazine ligation. (A) Methylene cyclopropane-modified lysozyme was reacted with **Tz-biotin**. (B) Western blot analysis of MCP-lysozyme treated with 2.5 mM of **Tz-biotin** at 37° C for 1-24 h. Equivalent protein loading was confirmed by Ponceau S stain. (C) Western blot analysis of MCP-lysozyme treated with 0-750 μM of **Tz-biotin** at 37° C for 12 h. Equivalent protein loading was verified by Ponceau S stain.

4.6 Conclusions and future directions

A model methylene cyclopropane—an isomer of bioorthogonal cyclopropenes—was synthesized and confirmed to be stable under physiological conditions for over 8 h. This small microcycle was also found to react with tetrazines with rate constants in the 10^{-4} $M^{-1}s^{-1}$ range. The methylene cyclopropane-tetrazine reaction proceeds through an intriguing rearrangement, which leads to an aromatic cycloadduct (Scheme 4-2). Initial attempts to visualize the resulting cycloadduct on the model were not successful, which indicates the need for design of tetrazine derivatives with improved UV profile. This unique feature could be explored to derive "turn-on" probes, molecules that produce signal only upon ligation. Since the resulting transformation leads to the ring-opening of the methylene cyclopropane cycle, it should also be possible to exploit this reaction for catch and release applications (e.g., drug delivery). Even though the methylene cyclopropane-tetrazine reaction rate is modest, the remarkable stability of MCP core should prove valuable for long-term imaging purposes.

4.7 Methods and materials

4.7a Cyclopropene stability

To analyze of methylene cyclopropane amide **4.4** stability in the presence of biological nucleophiles, **4.4** was incubated with cysteine (5 mM of each reagent in 8% DMSO-d_6/deuterated PBS, pH 7.4) and the resulting solutions were monitored via ^{1}H-NMR at rt or 37°C.

4.7b Rate studies by ^{1}H NMR

The cycloaddition reaction between methylene cyclopropane amide **4.4** and dipyridyl tetrazine (Table 4-1, entry 1) was monitored by ^{1}H-NMR. Methylene cyclopropane amide **4.4** (150 mM final concentration) and dipyridyl tetrazine **4.5** (100 mM final concentration) were combined in $CDCl_3$, and the ensuing reaction was monitored over 72 h. An internal standard (TMS) was used to determine peak integration values and, ultimately, the concentrations of the relevant species.

In some cases, the reaction rate was measured in a mixture of 10% DMSO-d_6/deuterated PBS, pH 7.4. Methylene cyclopropane amide **4.4** (20 mM final concentration) and the corresponding tetrazine **4.5**-**4.7** (40 mM final concentration) were combined in a mixture of 10% DMSO-d_6/deuterated PBS, pH 7.4, and the reaction was monitored over 72 h. An internal standard (TMS) was used to determine peak integration values and, ultimately, the concentrations of the relevant species.

4.7c Protein labeling

Lysozyme conjugates were prepared by treating the proteins with methylene cyclopropane PFP-ester **4.7** using standard coupling conditions. Lysozyme (0.5 mL, 20 mg/mL in PBS) was treated with 100 µL of PFP ester (67 mM in DMSO) and an additional 200 µL DMSO. The final protein solution (12.5 mg/mL protein) was incubated at 37 °C (with shaking) for 4 h.

4.7d Mass spectrometry analysis of lysozyme conjugates

Lysozyme samples modified with **4.7** (see above) were purified via P-10 BioGel® (BioRad), eluted with LCMS grade water, and subsequently analyzed by ESI-MS via direct infusion onto a QTOF2 instrument.

4.7e Western blot analysis of lysozyme conjugates

The labeled lysozyme samples were subsequently isolated using P-10 BioGel® (BioRad), eluting with 2 mL PBS (pH 7.4). The derivatized lysozyme eluents (10 μL, 6 mg/mL) were treated with **Tz-biotin** (1.25 – 7.5 μL of a 2 mM solution in DMSO) or DMSO as a control. After 1-24 hr of labeling, the modified lysozyme samples were separated by gel electrophoresis using 10% polyacrylamide gels. The gels were then electroblotted to nitrocellulose membranes. Blots were blocked using a solution of 7% BSA in PBS containing 0.1% Tween-20 (PBS-T) for 1 h at rt. The blots were incubated with IRDye 800 CW streptavidin (Li-Cor, 1:10,000 dilution) in the blocking buffer for 1 h at RT, then rinsed with PBS-T (6 x 10 min). Detection of membrane-bound antibodies was accomplished by near infrared spectroscopy on an Odyssey Infrared Imaging System. The equivalent protein loading was demonstrated by Ponceau S stain.

4.7f General synthetic procedures

Compound **4.3** [16], and tetrazines **4.6** and **4.7** [17] were synthesized as previously reported. All other reagents were purchased from commercial sources and

used as received without further purification. Reactions were carried out under an inert atmosphere of nitrogen or argon in oven- or flame-dried glassware. Dichloromethane (CH_2Cl_2), tetrahydrofuran (THF), diethyl ether (Et_2O), *N,N*-dimethylformamide (DMF), methanol (CH_3OH) and triethylamine (NEt_3) were degassed with argon and passed through two 4 x 36 inch columns of anhydrous neutral A-2 (8 x 14 mesh; LaRoche Chemicals; activated under a flow of argon at 350 °C for 12 h). The remaining solvents were of analytical grade and purchased from commercial suppliers. Thin-layer chromatography was performed using Silica Gel 60 F254 plates. Plates were visualized using UV radiation and/or staining with $KMnO_4$. Flash column chromatography was performed with 60 Å (240-400 mesh) silica gel from Sorbent Technologies. ^1H and ^{13}C NMR spectra were recorded on Bruker GN-500 (500 MHz ^1H, 125.7 MHz ^{13}C), CRYO-500 (500 MHz ^1H, 125.7 MHz ^{13}C) or DRX-400 (400 MHz ^1H, 100 MHz ^{13}C) spectrometers. All spectra were collected at 298 K unless otherwise noted. Chemical shifts are reported in ppm values relative to tetramethylsilane or residual non-deuterated NMR solvent, and coupling constants (*J*) are reported in Hertz (Hz). High-resolution mass spectrometry was performed by the University of California, Irvine Mass Spectrometry Center. HPLC runs were conducted on a Varian ProStar equipped with 325 Dual Wavelength UV-Vis Detector. Analytical runs were performed using an Agilent Polaris 5 C18-A column (4.6 x 150 mm, 5 μm) with a 1 mL/min flow rate. Semi-preparative runs were performed using an Agilent Prep-C18 Scalar column (9.4 x 150 mm, 5 μm) with a 5 mL/min flow rate. The elution gradients for the relevant separations are specified below.

4.7g Synthetic procedures

Synthesis of pentafluorophenyl methylene cyclopropane ester (**4.9**)

Methylene cyclopropane acid **4.3** (50 mg, 0.51 mmol) was dissolved in 2 mL of CH_2Cl_2. Triethylamine (0.13 mL, 1.02 mmol) was added and the solution was cooled to 4 °C. Pentafluorophenyltrifluoracetate (0.13 mL, 0.77 mmol) was then added dropwise over 1 min via syringe. The reaction mixture was allowed to stir at rt for 1 hr, then diluted with 50 mL of CH_2Cl_2 and washed with saturated NH_4Cl (3 x 20 mL) followed by brine (1 x 20 mL). The organic layers were combined, dried with $MgSO_4$, filtered, and concentrated *in vacuo* to afford methylene cyclopropane PFP ester **4.7** as a pale yellow oil. The product was used without further purification due to instability on silica gel. TLC R_f = 0.5 (10% ethyl acetate in hexanes, $KMnO_4$ stain); ^1H NMR (400 MHz, $CDCl_3$) δ 5.68 (dd, J = 1.6 Hz, J = 14 Hz, 2H), 2.57-2.60 (m, 1H), 2.07-2.10 (m, 1H), 1.92-1.97 (m, 1H).

Synthesis of methylene cyclopropane amide (**4.4**)

Pentafluorophenyl methylene cyclopropane ester **4.9** (70 mg, 0.51 mmol) was dissolved in 2 mL of CH_2Cl_2. Isopropyl amine (0.12 mL, 1.53 mmol) was added and the solution was allowed to stir at rt for overnight, then diluted with 50 mL of CH_2Cl_2 and washed with saturated NH_4Cl (3 x 20 mL) followed by brine (1 x 20 mL). The organic layers were combined, dried with $MgSO_4$, filtered, and concentrated *in vacuo* to afford a yellow oil. The crude product was purified by flash column chromatography (eluting with 50% ethyl acetate in hexanes) to yield **4.4** as a white crystalline solid (0.044 g, 0.98 mmol, 0.32 mmol, 62% over two steps): TLC R_f = 0.5 (50% ethyl acetate in hexanes,

$KMnO_4$ stain); ^1H NMR (500 MHz, $CDCl_3$) δ 5.55 (d, J = 2.0 Hz, 2H), 5.34 (br s, 1H), 4.06-4.10 (m, 1H), 2.08-2.12 (m, 1H), 1.66-1.68 (m, 1H), 1.56-1.59 (m, 1H), 1.13-1.16 (m, 6H). ^{13}C NMR (125.7 MHz, $CDCl_3$) δ 170.0, 130.9, 105.1, 41.5, 22.9, 22.8, 20.3, 11.0; HRMS (ESI) m/z calcd for $C_8H_{13}ON$ $[M+Na]^+$ 162.0895, found 162.0891.

Synthesis of cycloadduct of dipyridyl tetrazine and methylene cyclopropane (**4.8**)

Amide **4.4** (35 mg, 0.25 mmol) and dipyridyl tetrazine **4.5** (40 mg, 0.17 mmol) were dissolved in 5 mL of CH_2Cl_2 and allowed to react for 2 d. Then the reaction mixture was concentrated *in vacuo* and purified via flash chromatography (eluting with 100% CH_2Cl_2 to 5% MeOH in CH_2Cl_2 to 7% MeOH in CH_2Cl_2) to yield **4.8** (54 mg, 0.16 mmol, 92%) as pale yellow solid: TLC R_f = 0.5 (10% MeOH in CH_2Cl_2, $KMnO_4$ stain); ^1H NMR (400 MHz, $CDCl_3$) δ 8.67-8.69 (m, 3H), 8.52 (s, 1H), 8.18 (d, J = 8.0 Hz, 1H), 7.87 (qd, J = 1.6 Hz, 2H), 7.35-7.40 (m, 2H), 6.25 (br d, J = 7.6 Hz, 1H), 3.99-4.04 (m, 1H), 3.34 (t, J = 7.6 Hz, 2H), 1.03 (d, J = 6.4 Hz, 6H); ^{13}C NMR (125.7 MHz, $CDCl_3$) δ 170.5, 158.6, 157.5, 156.1, 153.3, 149.5, 148.3, 141.0, 137.3, 137.2, 125.7, 125.1, 124.8, 123.9, 121.7, 41.3, 36.6, 27.9, 22.7; HRMS (ESI) m/z calcd for $C_{20}H_{21}ON_5$ $[M+Na]^+$ 370.1644, found 370.1650.

References

(1) Chang, P. V.; Prescher, J. A.; Hangauer, M. J.; Bertozzi, C. R. Imaging cell surface glycans with bioorthogonal chemical reporters. *J. Am. Chem. Soc.* **2007**, *129*, 8400.

(2) Prescher, J. A.; Bertozzi, C. R. Chemistry in living systems. *Nat. Chem. Biol.* **2005**, *1*, 13.

(3) Prescher, J. A.; Dube, D. H.; Bertozzi, C. R. Chemical remodelling of cell surfaces in living animals. *Nature* **2004**, *430*, 873.

(4) Hang, H. C.; Wilson, J. P.; Charron, G. Bioorthogonal chemical reporters for analyzing protein lipidation and lipid trafficking. *Acc. Chem. Res.* **2011**, *44*, 699.

(5) Haun, J. B.; Devaraj, N. K.; Hilderbrand, S. A.; Lee, H.; Weissleder, R. Bioorthogonal chemistry amplifies nanoparticle binding and enhances the sensitivity of cell detection. *Nat. Nanotechnol.* **2010,** *5,* 660.

(6) Patterson, D. M.; Nazarova, L. A.; Xie, B.; Kamber, D. N.; Prescher, J. A. Functionalized cyclopropenes as bioorthogonal chemical reporters. *J. Am. Chem. Soc.* **2012,** *134,* 18638.

(7) Yang, J.; Šeckute, J.; Cole, C. M.; Devaraj, N. K. Live-cell imaging of cyclopropene tags with fluorogenic tetrazine cycloadditions. *Angew. Chem. Int. Ed.* **2012,** *51,* 7476.

(8) Yu, Z.; Pan, Y.; Wang, Z.; Wang, J.; Lin, Q. Genetically encoded cyclopropene directs rapid, photoclick-chemistry-mediated protein labeling in mammalian cells. *Angew. Chem. Int. Ed.* **2012,** *51,* 10600.

(9) Kamber, D. N.; Nazarova, L. A.; Liang, Y.; Lopez, S. A.; Patterson, D. M.; Shih, H.-W.; Houk, K. N.; Prescher, J. A. Isomeric cyclopropenes exhibit unique bioorthogonal reactivities. *J. Am. Chem. Soc.* **2013,** *135,* 13680−13683.

(10) Doss, G. A.; Djerassi, C. J. Sterols in marine invertebrates. 60. Isolation and structure elucidation of four new steroidal cyclopropenes from the sponge *Calyx podatypa. J. Am. Chem. Soc.* **1988**, *110*, 8124-8128.

(11) Li, L. N.; Li, H. T.; Lang, R. W.; Itoh, T.; Sica, D.; Djerassi, C. Minor and trace sterols in marine invertebrates. 31. Isolation and structure elucidation of 23H-isocalysterol, a naturally occurring cyclopropene. Some comparative observations on the course of hydrogenolytic ring opening of steroidal cyclopropenes and cyclopropanes. *J. Am. Chem. Soc.* **1982**, *104*, 6726-6732.

(12) Bao, X.; Katz, S.; Pollard, M.; Ohlrogge, J. Carbocyclic fatty acids in plants: biochemical and molecular genetic characterization of cyclopropane fatty acid synthesis of Sterculiafoetida. *Proc. Natl. Acad. Sci. U.S.A.* **2002**, *99*, 7172-7177.

(13) Hassal, C. H.; Reyle, K. Hypoglycin A, B: biologically active polypeptides from *Blighia sapida*. *Nature* **1954**,*173*, 334-339.

(14) Newman, M. S.; Merrill, S. H. Synthesis of a series of substituted phenylpropiolic acids. *J. Am. Chem. Soc.* **1955**, *77*, 5549–5551.

(15) Ullman, E. F.; Fanshawe, W. J. Unsaturated cyclopropanes. III. Synthesis and properties of alkylidenecyclopropanes and spiropentanes. *J. Am. Chem. Soc.*, **1961**, *83*, 2379–2383.

(16) Qiu, Y. L.; Hempel, A.; Camerman, N.; Camerman, A.; Geiser, F.; Ptak, R. G.; Breitenbach, J. M.; Kira, T.; Li, L.; Gullen, E.; Cheng, Y. C.; Drach, J. C.; Zemlicka, J. (R)-(-)- and (S)-(+)-Synadenol: synthesis, absolute configuration, and enantioselectivity of antiviral effect. *J. Med. Chem.* **1998**, *41*, 5257-5264.

(17) Karver, M. R.; Weissleder, R.; Hilderbrand, S. A. Synthesis and evaluation of a series of 1,2,4,5-tetrazines for bioorthogonal conjugation. *Bioconjugate Chem*. **2011**, *22*, 2263−2270.

APPENDIX A ^{1}H and ^{13}C NMR spectra

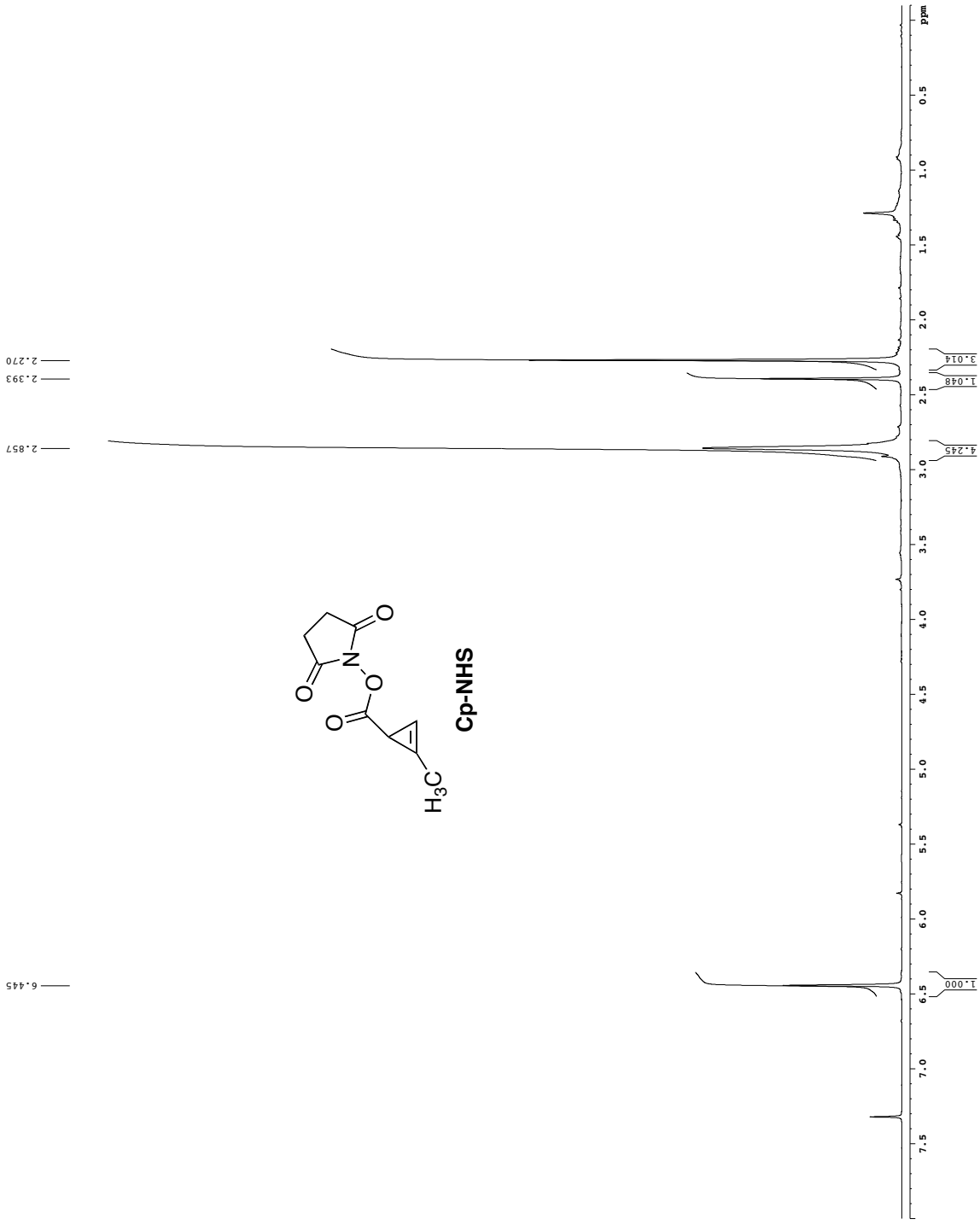

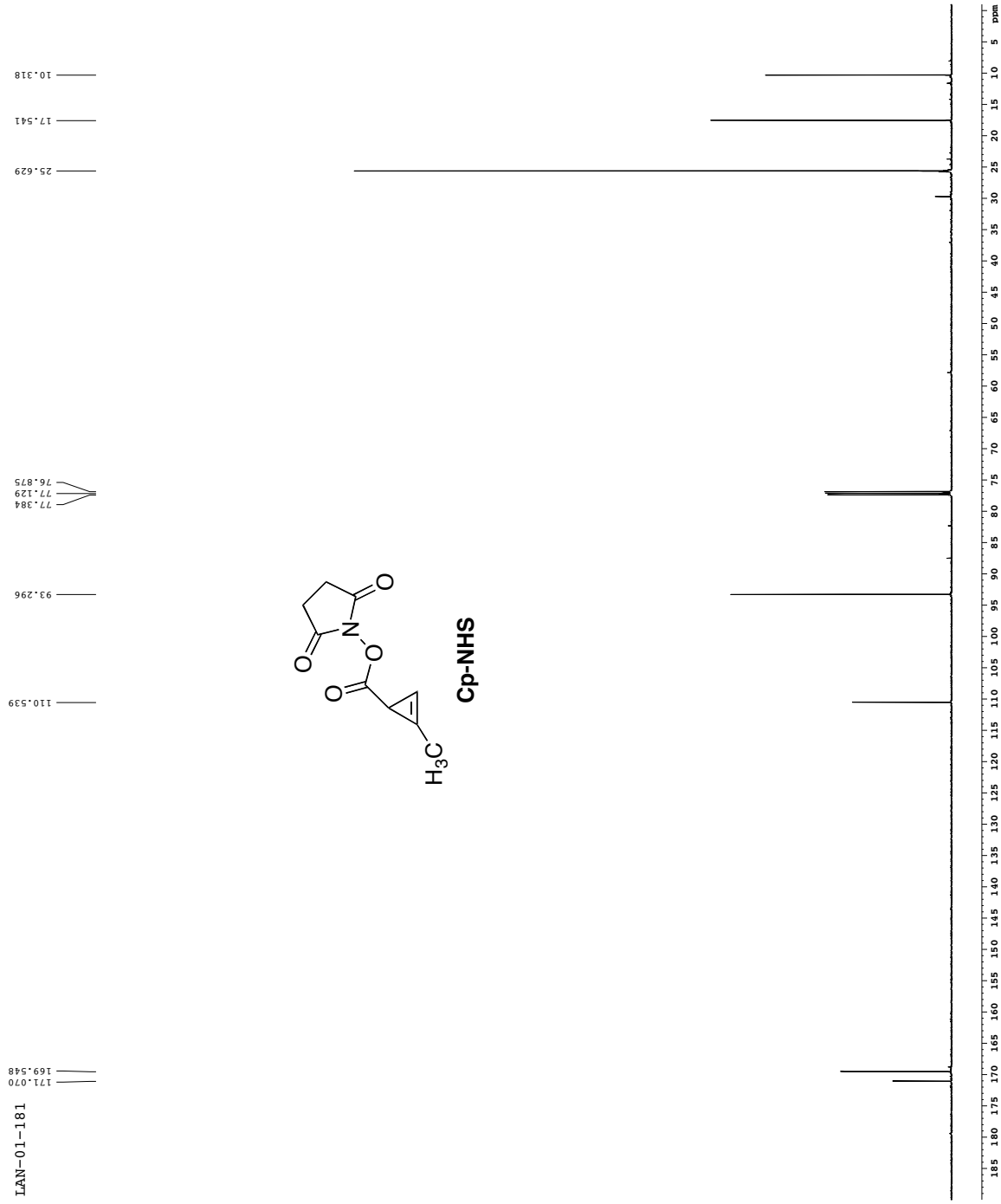
LAN-01-181
169.548
171.070
110.539
93.296
76.875
77.129
77.384
25.629
17.541
10.318
Cp-NHS
ppm

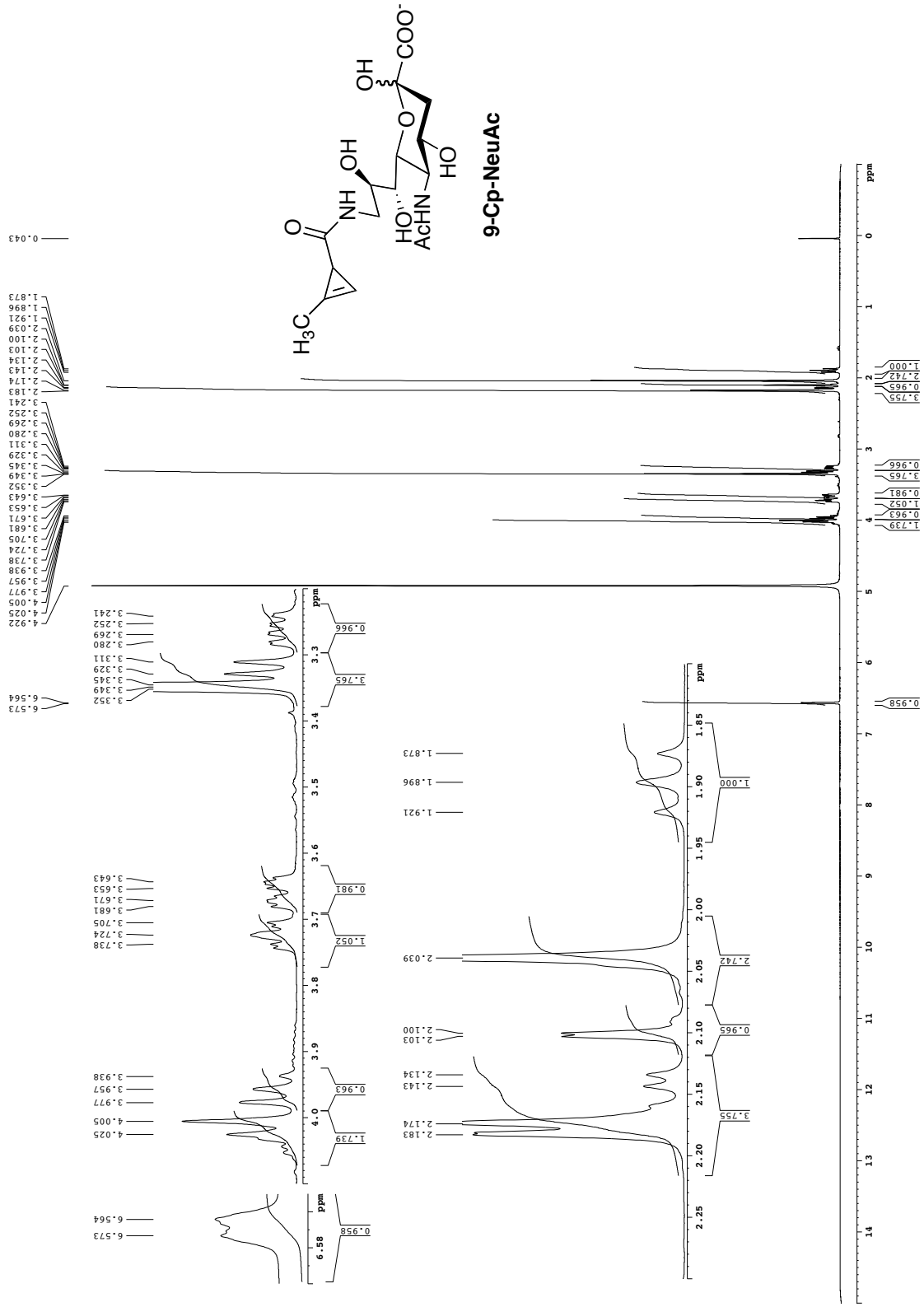
9-Cp-NeuAc

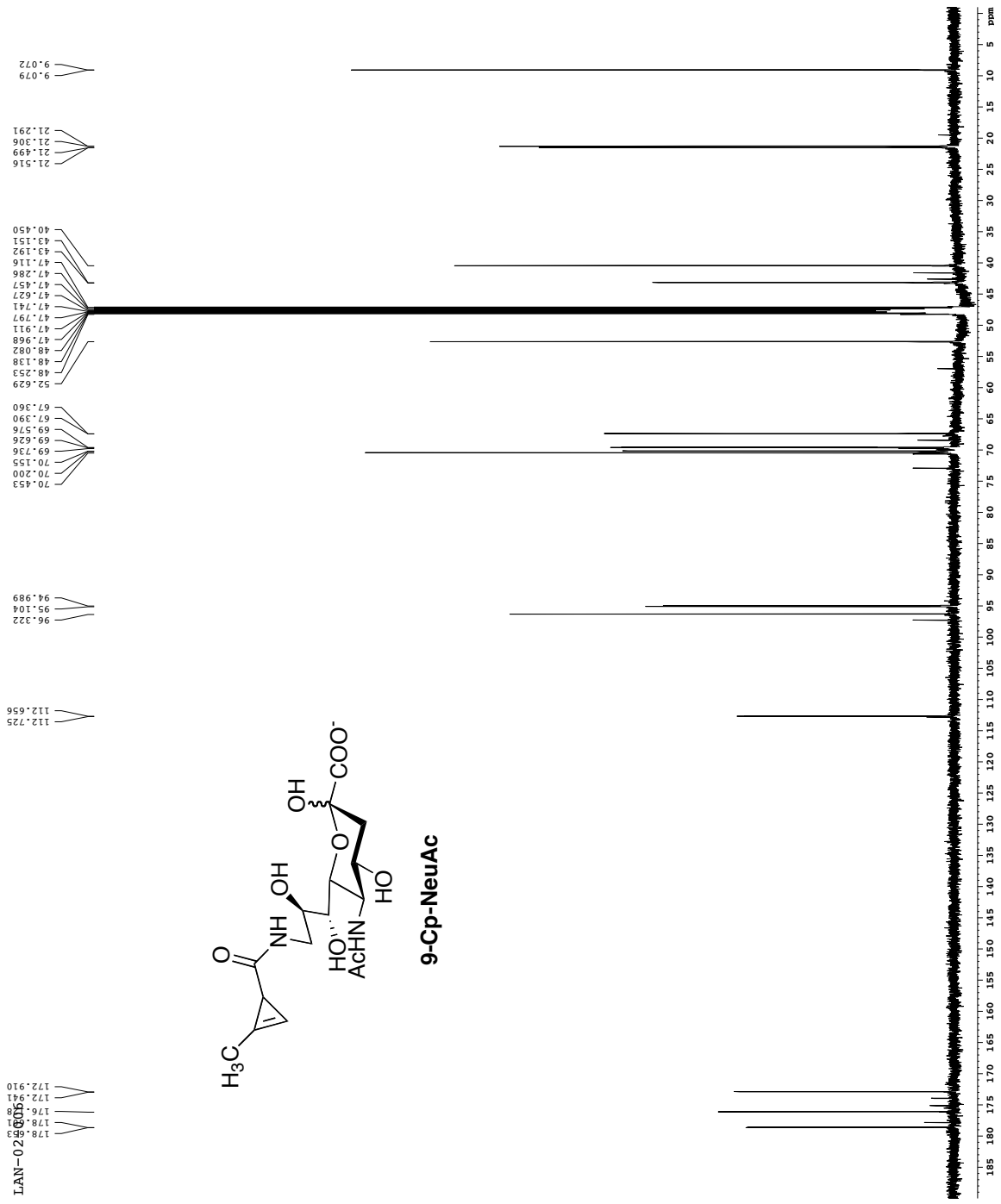
LAN-02-SUC
178.633
178.931
176.578
172.941
172.910
112.656
112.725
96.322
95.104
94.989
70.453
70.200
70.155
69.736
69.626
69.576
67.390
67.360
52.629
48.253
48.138
48.082
47.968
47.911
47.797
47.741
47.627
47.457
47.286
47.116
43.192
43.151
40.450
21.516
21.499
21.306
21.291
9.079
9.072
9-Cp-NeuAc
ppm

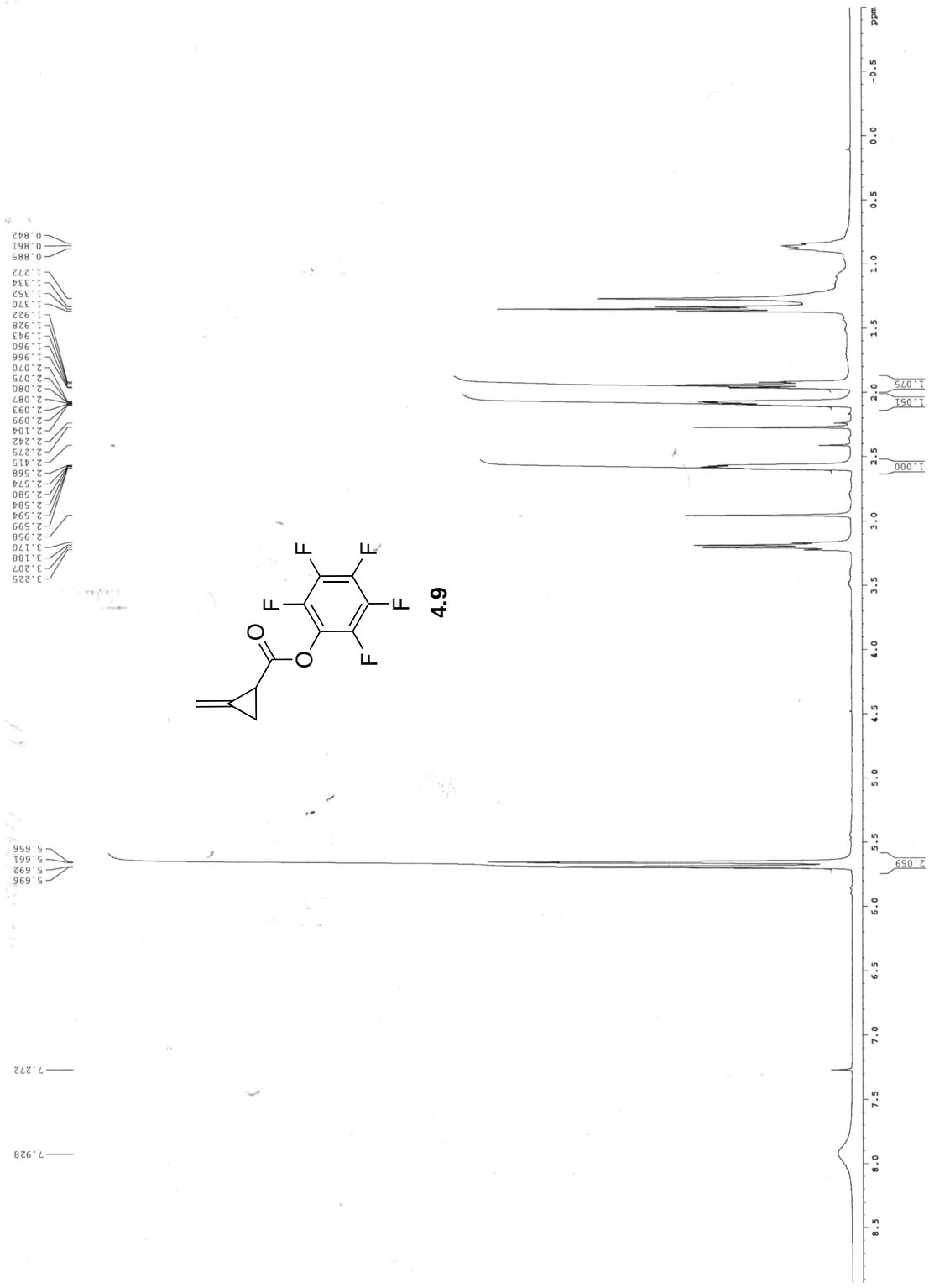
4.9
F
F
F
F
F
O
O
ppm
-0.5
0.0
0.5
1.0
1.5
2.0
2.5
3.0
3.5
4.0
4.5
5.0
5.5
6.0
6.5
7.0
7.5
8.0
8.5
2.059
1.000
1.051
1.075
0.842
0.861
0.885
1.272
1.334
1.352
1.370
1.922
1.928
1.943
1.960
1.966
2.070
2.075
2.080
2.087
2.093
2.099
2.104
2.242
2.275
2.415
2.568
2.574
2.580
2.584
2.594
2.599
2.958
3.170
3.188
3.207
3.225
5.656
5.661
5.692
5.696
7.272
7.928

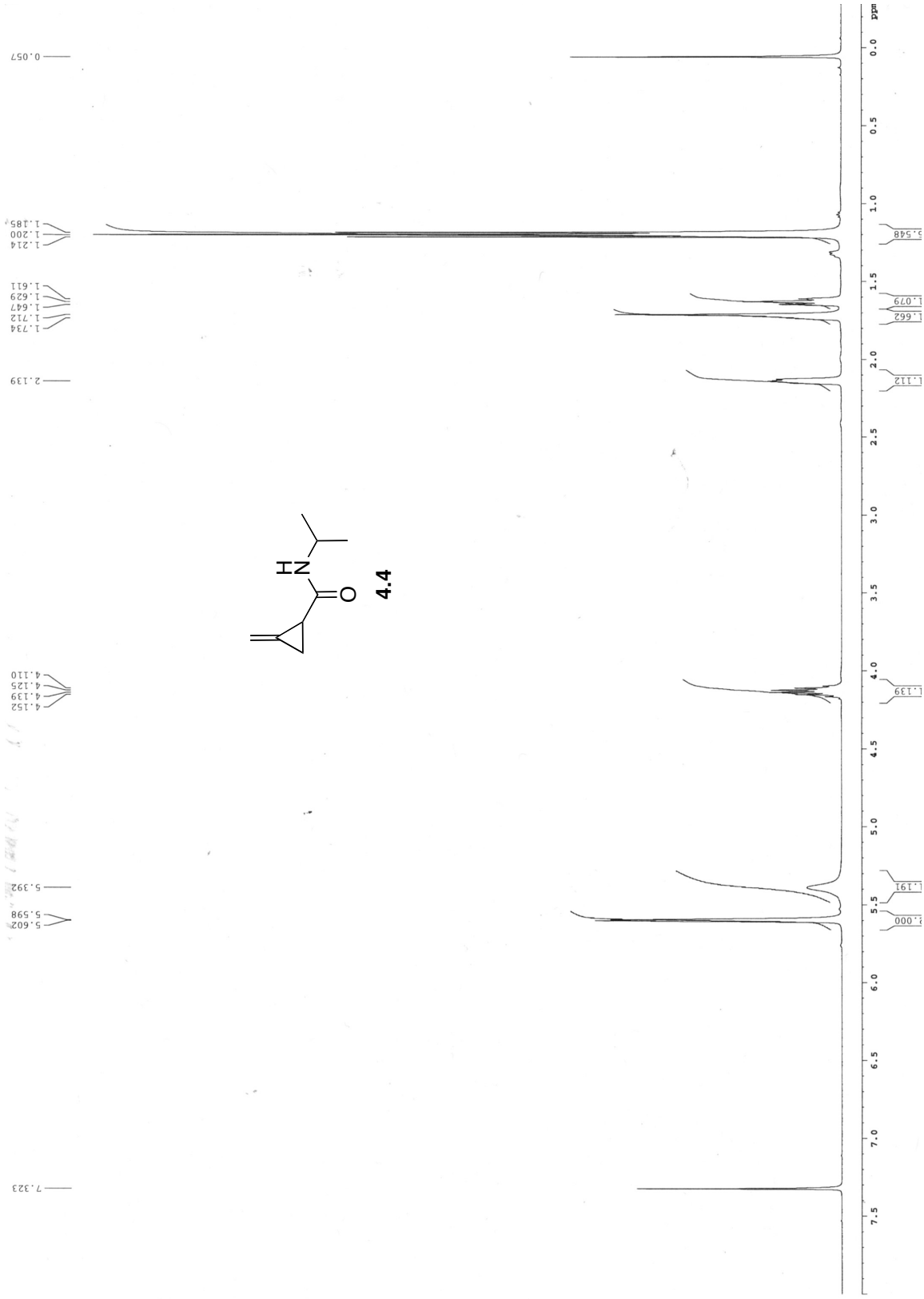
0.057
1.185
1.200
1.214
1.611
1.629
1.647
1.712
1.734
2.139
4.110
4.125
4.139
4.152
5.392
5.598
5.602
7.323
5.548
1.079
1.662
1.112
1.139
1.191
2.000
ppm
0.0
0.5
1.0
1.5
2.0
2.5
3.0
3.5
4.0
4.5
5.0
5.5
6.0
6.5
7.0
7.5
HN
O
4.4

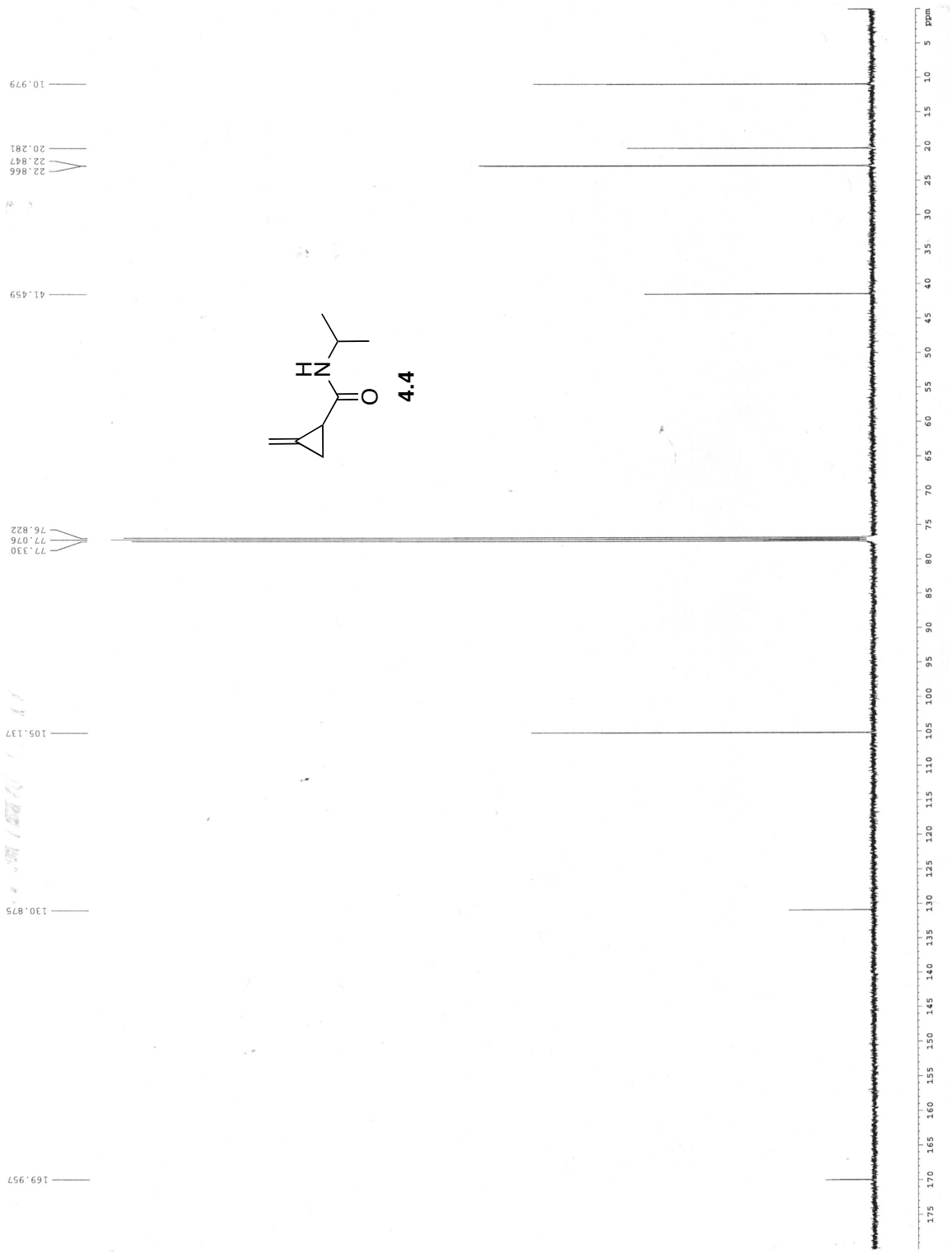
10.979
20.281
22.866
22.847
41.459
77.330
77.076
76.822
105.137
130.875
169.957
ppm
4.4

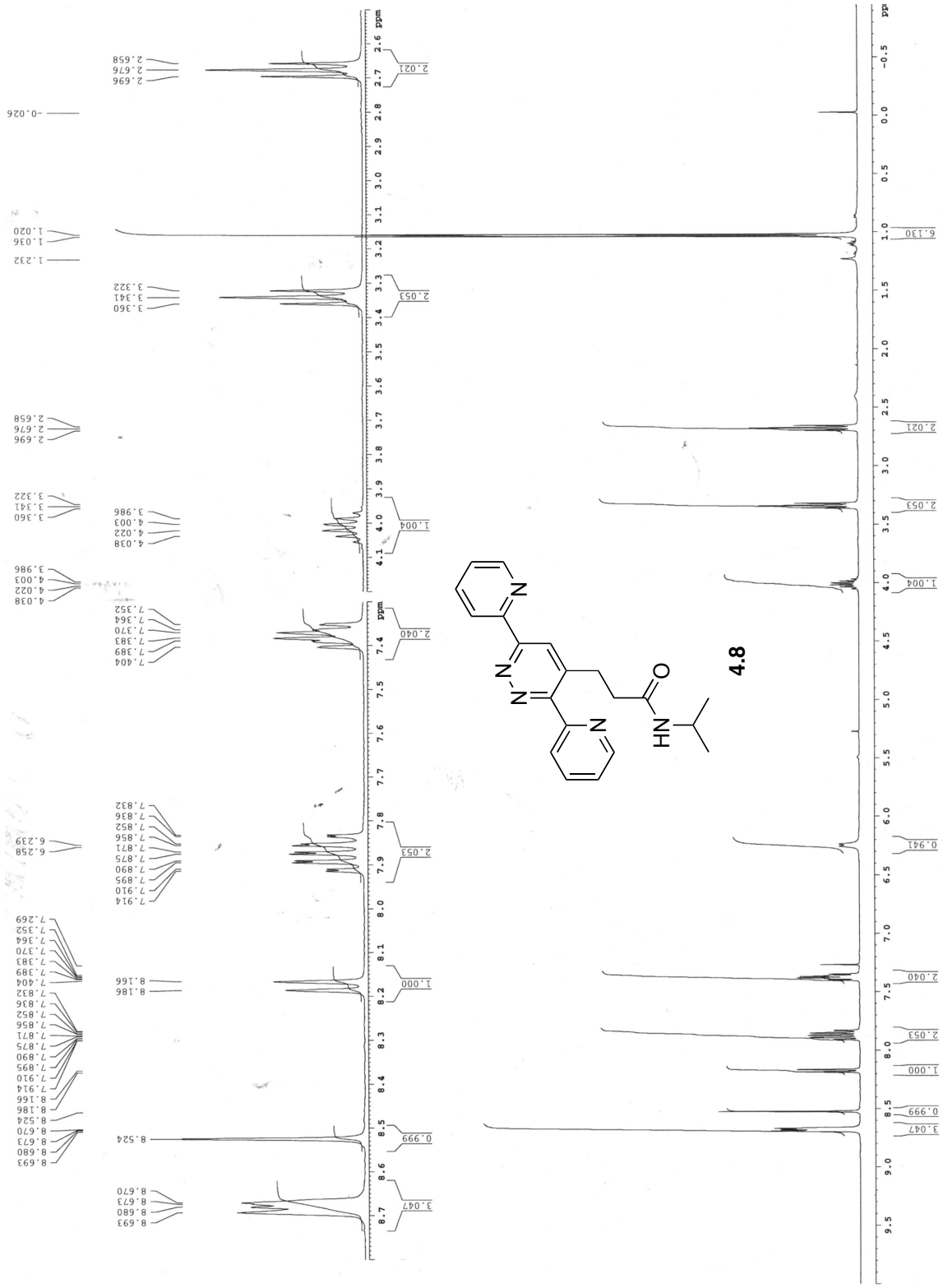
4.8

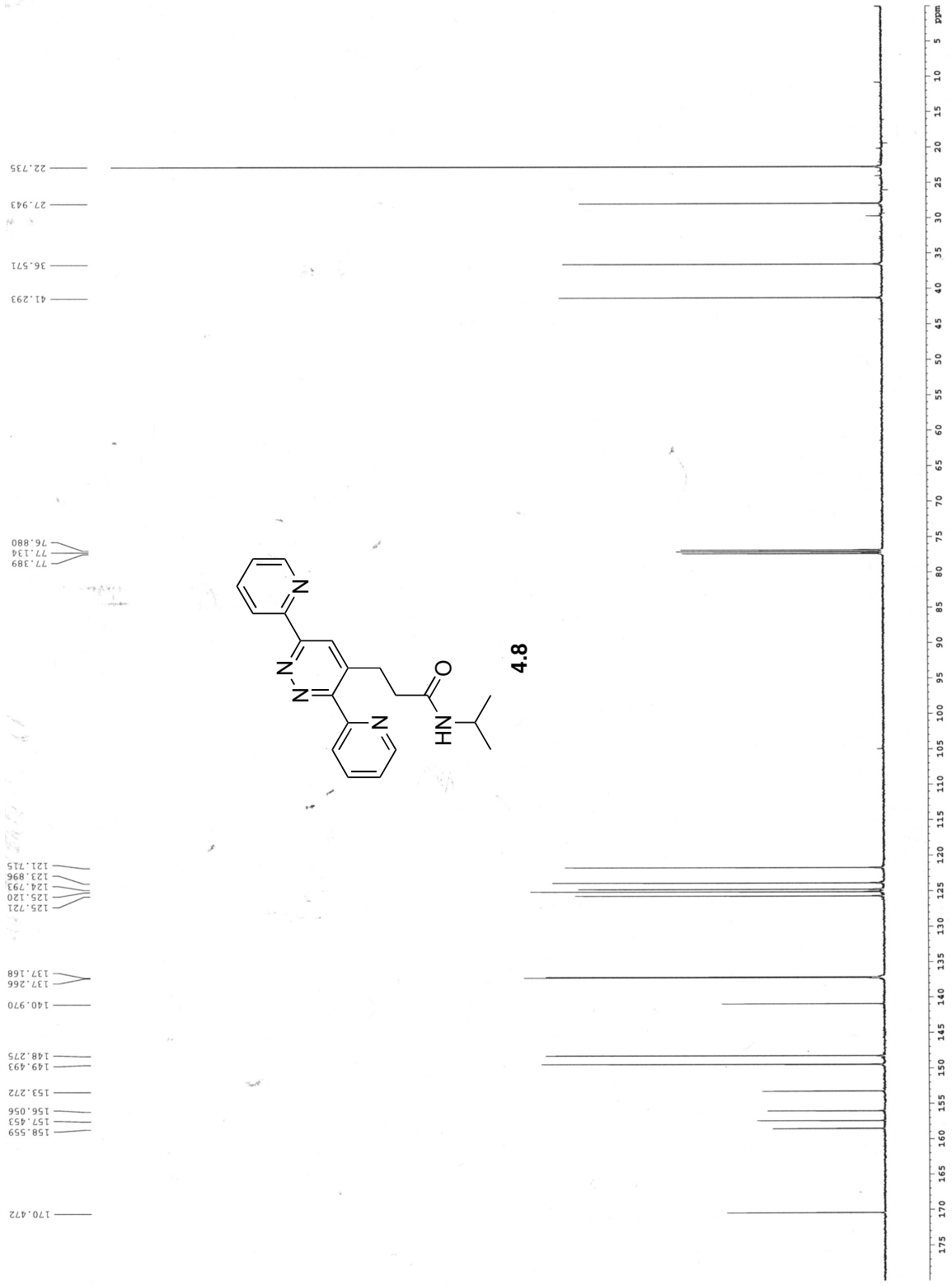
22.735
27.943
36.571
41.293
76.880
77.134
77.389
121.715
123.896
124.793
125.120
125.721
137.168
137.266
140.970
148.275
149.493
153.272
156.056
157.453
158.559
170.472
ppm
4.8

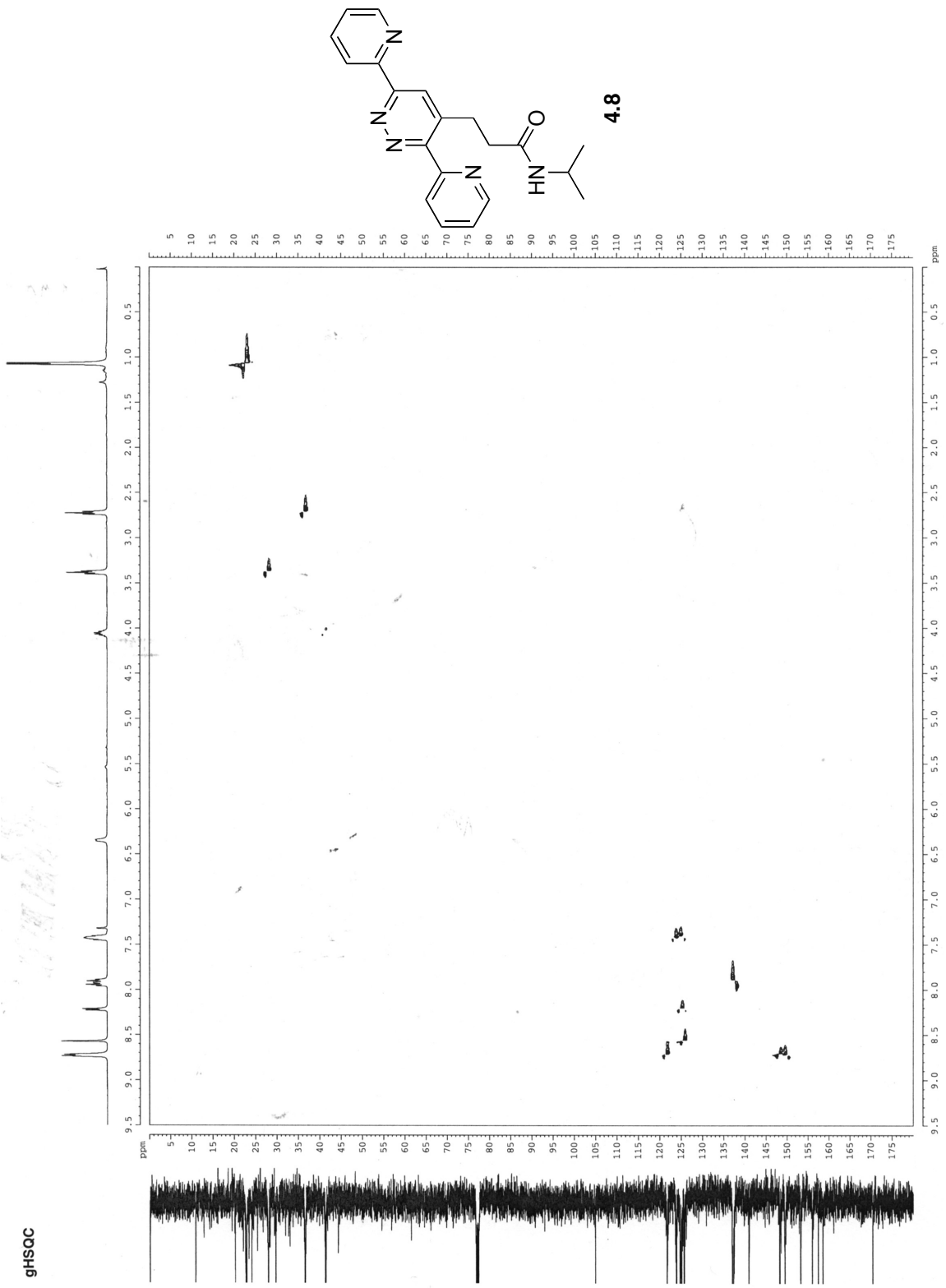
gHSQC
4.8

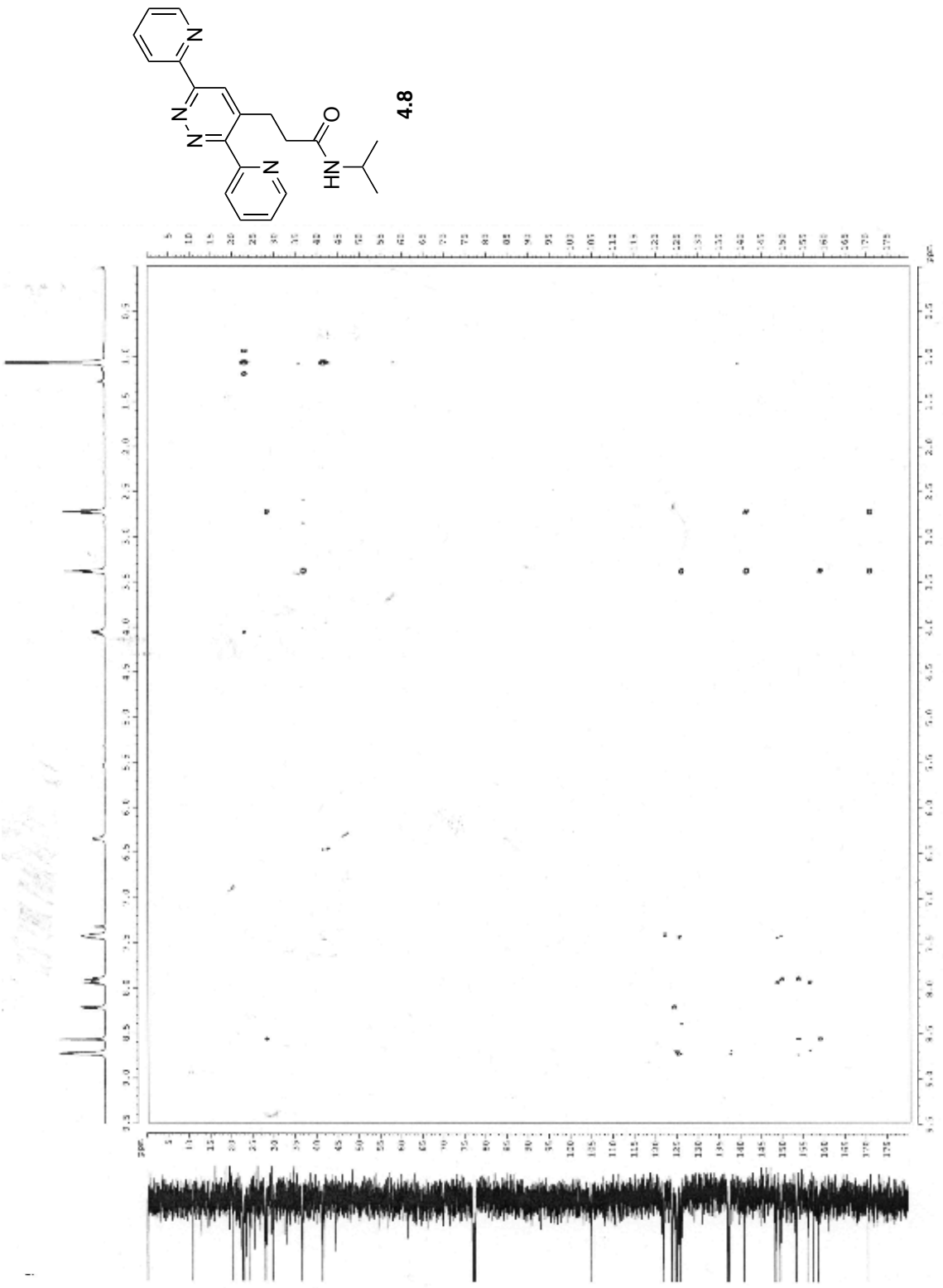
N
N
N
N
O
HN
4.8